UNIVERSITY OF CALIFORNIA, SAN DIEGO

Temporal encoding and homeostatic control in the IKK-IkappaB-NF-kappaB signaling system

A dissertation submitted in partial satisfaction of the requirements for the degree Doctor of Philosophy

in

Bioinformatics

by

Derren Barken

Committee in charge:

Professor Alexander Hoffmann, Chair
Professor Shankar Subramaniam, Co-chair
Professor Jeff Hasty
Professor Tony Hunter
Professor Bernhard Ø. Palsson

2007

The dissertation of Derren Barken is approved, and it is acceptable in quality and form for publication on microfilm:

_____

_____

_____

_____
Co-Chair

_____
Chair

University of California, San Diego

2007

To my family

Table of Contents

List of Figures

List of Tables

Acknowledgements

First and foremost I would like to thank my advisor, Alexander Hoffmann, and my fellow student in the Signaling and Systems lab. I have benefitted greatly from working in the exciting and collegial cross-disciplinary lab that Dr. Hoffmann has established at UCSD. It has been my privilege to learn directly from Dr. Hoffmann, and I would especially like to thank him for his patience in answering my basic experimental questions. Although the great majority of my thesis work has been computational, I appreciate the opportunity I was afforded to work in the lab and receive basic, hands on training, even when it did not directly contribute to near term goals.

I owe a debt of gratitude to my fellow graduate students. Many thanks to Shannon Werner and Ellen O'Dea for being wonderful experimental collaborators; to Jeff Kearns, for many good discussions about computational issues (and for being a fellow computer nerd!); to Oliver Schmah, for teaching me about mice and helping me (tremendously) in the lab; and to Soumen Basak, Hana Kim, Candace Lynch, Christine Cheng, Vincent Shih, Paul Loriaux and James Lee, for making the lab a great place to be scientifically and personally.

I would also like to acknowledge the significant support, encouragement, and intellectual inspiration I have received from Dr. Bernhard Palsson and the members of Systems Biology Research Group (Tim Allen, Iman Famili, Markus Herrgard, Natalie (Duarte) Hurlen, Jason Papin, Nathan Price, and Jennie Reed) during my time there. Although my graduate school career led elsewhere, I learned a tremendous amount from my experience in SBRG, for which I am grateful.

I also appreciate the time and thoughtful guidance provided by my other committee members. My co-chair Dr. Shankar Subramaniam has been an inspirational teacher since before I even started graduate school – without his personal leadership of

the Bioinformatics program, my graduate work would not have been possible. Dr. Jeff Hasty has provided much welcome insight on computational modeling, and my committee has benefitted greatly from Dr. Tony Hunter's deep biological perspective.

Finally, I would like to thank my parents, Israel and Frieda, my brothers Lee and Martin, my sister Randi, my in-laws Scott and Stephanie, my dear friends Carol and Delon, and my sweetie Keren. You are wonderful beyond the reach of words to convey; I hope you know what a difference your love and support have made lo these many years. I do – I know how very lucky I am. Thank you.

Portions of Chapter 2 appear in O'Dea E, Barken D, Peralta RQ, Tran KT, Werner SL, Kearns JD, Levchenko A, Hoffmann A. "A homeostatic model of IκB metabolism to control constitutive NF−κB activity" Molecular Systems Biology, in press. The dissertation author is the second author of this publication.

Portions of Chapter 3 appear in Werner SL[*], Barken D[*], Hoffmann A, "Stimulus specificity of gene expression programs determined by temporal control of IKK activity", Science 309: 1857-61, doi: 10.1126/science.1113319. The dissertation author is the second author of this publication.

Portions of Chapter 4 appear in Barken D[*], Wang CJ[*], Kearns J, Cheong R, Hoffmann A, Levchenko A. "Comment on 'Oscillations in NF-kappaB signaling control the dynamics of gene expression"' Science 308(5718):52, doi: 10.1126/science.1107904. The dissertation author is the first author of this publication.

Vita

1993	B.S.	Stanford University (Palo Alto, CA)
2007	Ph.D.	University of California, San Diego (La Jolla, CA)

Publications

1. Werner SL[*], **Barken D[*]**, Hoffmann A, "Stimulus specificity of gene expression programs determined by temporal control of IKK activity", Science 309: 1857-61

2. **Barken D[*]**, Wang CJ[*], Kearns J, Cheong R, Hoffmann A, Levchenko A. "Comment on 'Oscillations in NF-kappaB signaling control the dynamics of gene expression"' Science 308(5718):52a

3. O'Dea E, **Barken D**, Peralta RQ, Tran KT, Werner SL, Kearns JD, Levchenko A, Hoffmann A. "A homeostatic model of IκB metabolism to control constitutive NF−κB activity" Molecular Systems Biology, in press.

(*) Authors contributed equally to this work.

ABSTRACT OF THE DISSERTATION

Temporal encoding and homeostatic control
in the IKK-IkappaB-NF−kappaB system

by

Derren Barken

Doctor of Philosophy in Bioinformatics
University of California, San Diego, 2007

Professor Alexander Hoffmann, Chair
Professor Shankar Subramaniam, Co-chair

The transcription factor NF−κB is part of a signaling system that interprets a variety of physiological stimuli. NF−κB regulates numerous genes that play important roles in inter- and intracellular signaling, cellular stress responses, cell growth, survival, and apoptosis. This dissertation is an examination of the hypothesis that dynamic control of NF−κB is key to understanding the processing that allows these specific responses. This study investigates the existence, mechanisms, and implications of temporal coding within the IKK-IκB-NF−κB system.

The starting point of this work is a previously published, biochemically detailed ordinary differential equation model of NF−κB signaling whose predictions for dynamic

responses to a single stimuli (TNF) corresponded with experiments. I extend this model in a number of ways.

First, I refine its parameters and reaction list. Doing so allows me to improve the model's equilibrium predictions for resting cells. It also leads me to highlight the importance of a second degradation pathway (IKK independent free IκB degradation) for steady-state regulation, in addition to IKK induced degradation of complexed IκB.

Second, I apply three additional computational techniques to investigate its signal processing characteristics. Clustering allows me to gain insight into the temporal encoding of IKK, such as the lesser importance of early IKK plateaus and greater impact (and fine-grained regulation) of later IKK plateaus. Information theory guides the design and testing of a mutant cell which loses the ability to distinguish stimuli that are distinguished by wild type cells. Principal component analysis allows me to identify common mechanisms whose alterations have stimulus specific effects, altering the responses to some stimuli much more strongly than others.

Third, I test and validate its utility against a much wider range of experiments. Using the experimental work of my collaborators, I am able to link simulations to experiments for multiple stimuli, with genetic and pharmacological interventions, and with multiple doses and timings.

In conclusion, this dissertation breaks new ground in using simulations and experiments to understand temporal control in a cell signaling system of great scientific interest, and develops techniques which have relevance for other efforts to understand cell signaling.

Chapter 1
Introduction

> There is a computer disease that anybody who works with computers knows about. It's a very serious disease and it interferes completely with the work. The trouble with computers is that you 'play' with them!
>
> -- Richard P. Feynman

I first enrolled in the UCSD Bioinformatics program in the fall of 2001. Five and a half years does not seem like an unduly long interval to complete a Ph.D, but during that time, the rate of progress in computational biology has been striking. When I first enrolled in the UCSD Bioinformatics program, in the fall of 2001, the first draft of the human genome had just been published. As I prepare to defend in the spring of 2006, several vendors are racing towards the $1000 genome. The roster of high throughput technologies (genomics, proteomics), which I surveyed in a first year class, has improved and expanded at a healthy pace (metabolomics, automated single cell studies) such that the scientific landscape, like a growing child, is at once familiar and almost unrecognizable. And in my own area of interest, the modeling of biological systems, the initial paucity of specialized books, journals, courses and practitioners has been replaced with a thriving ecosystem of new and exciting work.

In this tremendously fertile and exciting era, I have had the privilege of applying new computational approaches to the study of the NF−κB eukaryotic transcription factor.

This cell signaling pathway, which has been studied for over two decades, is of great practical interest for its important roles in processes of inflammation, development, and human diseases. In this introductory chapter, I broadly survey the necessary background to my work. The first section examines the field of computational modeling. The second section describes the biology of NF−κB and related signaling pathways. The third section describes the previously published Hoffmann-Levchenko model, and surveys other work on computational modeling of NF−κB signaling in particular.

1.1 Computational modeling in biology

Computational modeling has a rich history in modern biology. It is motivated by three goals: curation, prediction, and understanding. Curation is a relatively modest goal – modeling provides a framework to organize the large number of details that inevitably arise from studying biological systems. Prediction may by itself be useful , computation is usually much cheaper than experimental work. However, the ultimate goal of computational modeling in biology is to derive biological insights that were not available by experimental work alone.

In seeking to understand computational modeling, there are many criteria for organizing the large body of existing work. Two of the most useful are by biological process (i.e. what is being modeled?) and by methodology (i.e. how does the model work?)

1.1.1 Models of metabolism, gene regulation, and cell signaling

One obvious way to categorize computational models is by biological process. To simplify a complicated picture, we can identify three subject areas. The oldest, most advanced area is metabolism (Reich 1981; Heinrich and Schuster 1996; Voit 2000), the second is genetic regulation (McAdams and Arkin 1998; Bower and Bolouri 2001; Collado-Vides and Hofestadt 2002), and the most recent is cell signaling (Levchenko 2003; Bhalla 2004; Papin and Subramaniam 2004). This work focuses on cell signaling, but a detailed familiarity with previous approaches is useful.

In particular, the choice of systems to model has been driven by experimental accessibility. Metabolic systems were the first to be amenable to quantitative measurements (Stephanopoulos, Aristidou et al. 1998; Edwards, Ibarra et al. 2001). Models of genetic regulation were developed in tandem with widespread adoption of gene chips and microarrays (DeRisi, Iyer et al. 1997; Ideker, Thorsson et al. 2001). Finally, models of cell signaling have been driven by rapidly expanding knowledge of the protein-protein interactions that make up signaling networks (Gavin, Bosche et al. 2002; Ho, Gruhler et al. 2002).

This simple tripartite categorization, while useful, is not rich enough to be complete. Useful insights and inspiration may also be gleaned from models in areas such as development (von Dassow, Meir et al. 2000), physiology (Fall, Marland et al. 2002), immunology (Smith and Bolouri 2005), and many more.

Finally, within the area of cell signaling models, this work focuses on NF–κB. Many other signaling pathways have been extensively modeled, including JAK-STAT

(Swameye, Muller et al. 2003; Papin and Palsson 2004), WNT (Lee, Salic et al. 2003), and the EGF/MAPK cascade (Bhalla, Ram et al. 2002; Schoeberl, Eichler-Jonsson et al. 2002).

1.1.2 Modeling methodologies

Another useful way to categorize computational models is by methodology. There are many schools of thought, ranging from speculative to well established, as illustrated in Table 1-1. Some approaches are directly inspired by successful techniques from other fields, such as process control from chemical engineering (Yi, Huang et al. 2000), optimization from operations research (Schilling, Edwards et al. 1999), or circuit analysis from electrical engineering (McAdams and Shapiro 1995).

In particular, modeling methodologies may be classified using two traits: they are either discrete or continuous, and either deterministic or stochastic. Enough time has elapsed that the field is now well reviewed (Hasty, McMillen et al. 2001; Gilman and Arkin 2002; Levchenko 2003; Tyson, Chen et al. 2003; Bhalla 2004; Eungdamrong and Iyengar 2004; Sauro and Kholodenko 2004; Vayttaden, Ajay et al. 2004). My work focuses on continuous, deterministic modeling, using systems of ordinary differential equations. I chose to use this approach because it allows modeling which closely corresponds to the biochemical details of the system. I chose deterministic modeling over stochastic modeling because systems like NF−κB, with large numbers of molecules (an estimated 10^5 per cell for NF−κB), are well modeled by deterministic modeling. In such system, deterministic modeling generally will give a similar answer to stochastic modeling, while being less complicated and computationally expensive. For systems

with small numbers of molecules (e.g. bacterial systems), stochastic modeling will give different (better) answers and may be a more appropriate methodology.

1.2 The biology of NF−κB in inflammatory signaling

The eukaryotic transcription factor NF−κB has been extensively studied for almost two decades. It is of interest scientifically and medically, and as a well studied pathway can be taken as a model system for other signaling pathways.

It is notable for being one of the most highly pleiotropic transcription factors yet studied (Chen and Greene 2004). It is involved in a wide variety of biological processes, particularly inflammation, immunity (innate and active), and apoptosis. Again, there are many excellent reviews available (Ghosh and Karin 2002; Chen and Greene 2004; Hayden and Ghosh 2004).

Medically, NF−κB has been implicated in a remarkable number of major diseases, as shown in Table 2.2. As such, it has attracted significant attention as a target for drug development (Garg and Aggarwal 2002; Greten and Karin 2004; Karin, Yamamoto et al. 2004).

In the following sections, we briefly survey the core of the NF−κB pathway (defined as NF−κB, the IκBs, and the IKKs). We then consider upstream signaling events, downstream transcription events, the role of isoforms, control via posttranslational modifications, and the role of crosstalk with other major signaling pathways. For more details, the reviews cited above are a good entry point into the very

extensive literature. (These entry points are necessary, as a recent search of Pubmed using the search term 'nf-kappa-b' returned over 20,000 citations.)

Finally, it should be noted that the details described or alluded to in this section far outstrip the contents of any existing computational model. In many cases, the molecular mechanisms are not yet fully understood, or the descriptions remain non-quantitative. As more information is learned, the biology described below represents an excellent opportunity for expanding the scope and predictive power of previous NF−κB models.

1.2.1 Molecular biology of NF−κB, IκB and IKK

The NF−κB family consists of five related mammalian gene products (RelA/p65, cRel, RelB, p50, p52) which share a REL homology domain. The predominant species in many cell types is a dimer consisting of RelA:p50. Another important dimer is RelB:p50. Signaling through the former dimer is known as the ``classical pathway", and the latter is known as the ``alternative pathway", reflecting the relatively recent interest in the latter.

The activity of NF−κB is regulated and controlled by a family of proteins known as IκB family (inhibitors of kB). This family has seven members, of which three mediate inflammatory signaling: IκBα, IκBβ, and IκBε.

The IκBs are, in turn, controlled by the actions of the IKK family (IκB Kinases). This family has three members (IKK-α, IKK-β, and IKK-γ, also known as IKK1, IKK2, and NEMO, respectively.) All three of these typically form the IKK complex (NEMO is a regulatory subunit, the other two are catalytic.) There is evidence that IKK-β is most

important in inflammatory signaling, while IKK-α is most important for the alternative pathway.

Figure 2-1 is a simplified description of NF−κB activation. Normally, NF−κB is held in the cytoplasm by its association with an IκB, which keeps it inactive. Signals from various stimuli are transduced to the IKK complex, which phosphorylates the IκBs, leading to their ubiquitination and degradation. Freed from IκB, the cytoplasmic NF−κB is able to translocate into the nucleus and initiate transcription. One of the many proteins induced by NF−κB is IκBα, leading to negative feedback.

1.2.2 The NF−κB module in context

NF−κB is induced by a number of stimuli, both on the cell surface (chemokines, cytokines) and internally. Of the many stimuli which have been studied, the most prominent are Tumor Necrosis Factor (TNF-α), Interleukin (IL-1), Lipopolysaccharide (LPS), a cell wall component), Lymphotoxin (LT-β), and UV light. NF−κB is also signalled from T-cell receptors and B-cell receptors. Each of these signals has a cascade of events leading to IKK, and each pathway is under active study. For example, the pathway from the TNF-alpha receptor to IKK is a cascade involving TRADD, TRAF2, RIP, TAB1, TAB2, and TAK1. Similar details are emerging for the other receptors. In general, much has been recently learned, and although the picture is not yet complete, there is clearly rapid progress.

In the nucleus, NF−κB induces hundreds of target genes related to immunity, inflammation, and lymphoid organogenesis. There are temporal differences (early genes

vs late genes, e.g. IP-10 vs RANTES) which are induced by stimulus specific expression of NF−κB, and regulated by mechanisms such as temporal control, combinatorial control of multiple transcription factors, dimer specificity, and post translation modifications. There are also differences based on the exact dimer of NF−κB in the nucleus (e.g. the classical pathway is associated with genes related to the innate immune response, while the alternative pathway has a gene response which is related to the development of adaptive immune system. It is known that histone modifications significantly mediate the effects of NF−κB transcription. The picture is under active study using ChIP-chip and other experimental means.

All of the core constituents of the NF−κB pathway (NF−κB, IκB, IKK) are present in quite a few isoforms, which may interact in various ways. While modeling has begun to account for this (particularly with reference to the IκBs), there is a major opportunity to expand modeling efforts to incorporate the variety of NF−κB dimers which are seen, as well as the reflect the heterodimers, homodimers, and complexes of IKK.

It is increasingly clear that there are myriad opportunities for regulation by post-translation modification (PTMs) within the NF−κB pathway. In particular, NF−κB is modified at multiple sites by phosphorylation, acetylation, and ubiquitination, leading to alterations in its localization, affinity for IκBs, and transcriptional activity (induction or repression).

In addition to the details of NF−κB pathway itself, the transcriptional activities of NF−κB are also linked via combinatorial control to other signaling pathways. One of the

best studied at this point is JNK (c-Jun N-terminal kinase) and AP-1. Several candidate mechanisms have been recently reported, including GADD45-beta, XIAP, and ROS (reactive oxygen species). Both NF−κB and JNK are important in regulating cell death decisions.

Experimental techniques are used both to estimate kinetic parameters for model building, and to measure concentrations of proteins over time, in order to validate the models. For the former, a wide variety of techniques are used, from immunochemistry to mass spectrometry to surface plasmon resonance. For the latter, the mainstay techniques are currently EMSAs (electromobility shift assays), Western blots, and RPAs (RNAse protection assays). These are discussed below in relation to issues of model refinement.

Given the complexity of the system under study, it is inevitable that many aspects of the biology are not neatly incorporated into the big picture. To give a sense of this, several examples are mentioned here. For example, IKK is proposed to enter the nucleus and interact with NF−κB directly. Another issue that was not discusses above is that there are known differences in the NF−κB pathway that depend on tissue (e.g. epithelial cells vs leukocytes) and developmental stage (e.g. early vs late B-cell differentiation.) Overall, the picture is both incredibly complex and incredibly interesting.

1.3 Computational modeling of NF−κB signaling

Having surveyed both modeling and NF−κB biology, we now turn to models of NF−κB signaling, which people have used to understand questions such as the purpose and roles of the IκB isoforms and the bimodal signaling-processing characteristics of the

system. We first consider the seminal Hoffmann-Levchenko model published in Science in 2002 (Hoffmann, Levchenko et al. 2002), followed by a brief survey of other published work.

1.3.1 The Hoffmann-Levchenko 2002 model

The Hoffmann-Levchenko model (HL2002, or model 1.0) consists of 24 metabolites, 35 parameters, and 64 reactions. Some parameters apply to more than one reaction, generally because in the absence of additional data, the simplest assumption is that similar processes have similar rates (e.g. mRNA degradation rates for different IκB transcripts.) It was originally implemented as a Mathematica script, although I have since reimplemented it in Matlab and Visual Basic. On overview of the model is provided in Figure 1-1

1.3.2 Other models

Since the publication of model 1.0, seven additional NF−κB modeling papers from other labs have appeared, some of which directly extend model 1.0. Table 1-4 lists these papers, with comments. None of these papers adjust the parameters or extend the model to allow modeling of the response to different kinds of stimuli – they generally take a different approach from the work described in subsequent chapters. Because they do not address the question of how different stimuli are interpreted by the NF−κB signaling module, they have limited relevance to the questions I address in this thesis.

1.4 Dissertation overview

This introductory chapter provides background information on computational modeling and the biology of NF−κB inflammatory signaling. The following chapters investigate temporal encoding in the IκB-NF−κB signaling system.

In chapter 2, I begin by examining homeostatic control in the system. I improve the previously published Hoffmann-Levchenko model using experimental evidence from genetic tools (produced by my collaborators). These refinements improved the equilibrium predictions of the model, and show the importance of regulation of IκB degradation. In particular, this work reveals that in addition to the well understood importance of IKK induced degradation of IκB from the IκB-NF−κB complex, the degradation rate of free IκB is also an important degradation pathway.

Chapter 3 then focuses on temporal control of IKK activity. In this work, I explore the signaling processing characteristics of the system by modifying it to allow for numerically defined inputs. I then use the same model to predict the response to individual measured stimulus specific IKK profiles, and to shed light on a negative (A20) and positive (TNF) feedback loop.

In chapter 4, I extend this investigation to address whether temporal regulation is functionally important and what the nature of the temporal code may be. I study the relative importance of amplitude vs frequency modulation in NF−κB signaling, and to introduce an information metric which can be used to model the diversity of outputs as a property of the system. The latter is used to design a mutant with a reduction in the stimulus specificity of its responses to stimuli.

Chapter 5 probes the temporal code of NF−κB expression to investigate which mechanisms are important for stimulus specific temporal encoding and how they can be manipulated. I use a broad set of hypothetical alterations to generate a set of simulated responses, which I then analyze using principal component analysis to demonstrate the possibility of stimulus specific alterations to common mechanisms. I then simulate a set of alterations which are modeled on the effects of actual pharmaceutical agents, and am able to compare the simulated responses to a set of experimental results generated by my coworkers. These latter simulations and experiments consider multiple doses and timings (of pharmaceutical treatment relative to stimulus).

Finally, chapter 6 is a broader discussion of current and future directions, in regards to temporal modeling, but also more generally in regards to efforts to gain insight into cell signaling and other biological systems through modeling.

Table 1-1 Modeling Methodologies

GENRE	REFERENCE
Deterministic Boolean Networks	(Kauffmann 1993)
Probabilistic Boolean Networks	(Shmulevich, Dougherty et al. 2002)
Bayesian Networks	(Sachs, Gifford et al. 2002)
Stoichiometric Analysis	(Papin and Palsson 2004)
Flux Balance Analysis	(Schilling, Edwards et al. 1999)
Petri Nets	(Reddy, Liebman et al. 1996)
Piecewise Linear Differential Equations	(De Jong, Gouze et al. 2004)
Det. Nonlin. ODEs: General Mass Action	(Hoffmann, Levchenko et al. 2002)
Deterministic Nonlinear ODEs: S-systems	(Voit 2000)
Stochastic Nonlinear ODEs	(Arkin, Ross et al. 1998)
Compartmental ODE Models	(Schaff, Slepchenko et al. 2001)
Spatial Models	(Shvartsman, Wiley et al. 2001)

Table 1-2 NF−κB in Disease Processes

DISEASE	REFERENCE
Alzheimers	(Mattson and Camandola 2001)
Artherosclerosis	(Collins and Cybulsky 2001)
Arthritis	(Burke 2003)
Asthma	(Levine 2003)
Cancer	(Karin, Cao et al. 2002)
Diabetes	(Arkan, Hevener et al. 2005)
HIV/AIDS	(Hiscott, Kwon et al. 2001)

Table 1-3 Hoffmann-Levchenko model values and units

ASSOCIATION	a1	0.0225	$uM^{-1}s^{-1}$		1.35	$uM^{-1}min^{-1}$
	a2	0.006	$uM^{-1}s^{-1}$		0.36	$uM^{-1}min^{-1}$
	a3	0.009	$uM^{-1}s^{-1}$		0.54	$uM^{-1}min^{-1}$
	a4	0.5	$uM^{-1}s^{-1}$		30	$uM^{-1}min^{-1}$
	a5	0.5	$uM^{-1}s^{-1}$		30	$uM^{-1}min^{-1}$
	a6	0.5	$uM^{-1}s^{-1}$		30	$uM^{-1}min^{-1}$
	a7	0.185	$uM^{-1}s^{-1}$		11.1	$uM^{-1}min^{-1}$
	a8	0.048	$uM^{-1}s^{-1}$		2.88	$uM^{-1}min^{-1}$
	a9	0.07	$uM^{-1}s^{-1}$		4.2	$uM^{-1}min^{-1}$
DISSOCIATION	d1	0.00125	s^{-1}		0.075	min^{-1}
	d2	0.00175	s^{-1}		0.105	min^{-1}
	d3	0.00175	s^{-1}		0.105	min^{-1}
	d4	0.0005	s^{-1}		0.03	min^{-1}
	d5	0.0005	s^{-1}		0.03	min^{-1}
	d6	0.0005	s^{-1}		0.03	min^{-1}
IMPORT/EXPORT	tp1	0.0003	s^{-1}		0.018	min^{-1}
	tp2	0.0002	s^{-1}		0.012	min^{-1}
	k1	0.09	s^{-1}		5.4	min^{-1}
	k01	0.00008	s^{-1}		0.0048	min^{-1}
	k2	0.0138	s^{-1}		0.828	min^{-1}
	k2h	0.0069	s^{-1}		0.414	min^{-1}
SYNTHESIS	tr1	0.00408	s^{-1}		0.2448	min^{-1}
	tr2	0.0165	$uM^{-1}s^{-1}$		0.99	$uM^{-1}min^{-1}$
	tr2a	0.00000154	uMs^{-1}		0.0000924	$uMmin^{-1}$
	tr2b	0.000000178	uMs^{-1}		0.00001068	$uMmin^{-1}$
	tr2e	0.000000127	uMs^{-1}		0.00000762	$uMmin^{-1}$
DEGRADATION	deg1	0.000113	s^{-1}		0.00678	min^{-1}
	deg4	0.0000225	s^{-1}		0.00135	min^{-1}
	r1	0.00407	s^{-1}		0.2442	min^{-1}
	r2	0.0015	s^{-1}		0.09	min^{-1}
	r3	0.0022	s^{-1}		0.132	min^{-1}
	r4	0.0204	s^{-1}		1.224	min^{-1}
	r5	0.0075	s^{-1}		0.45	min^{-1}
	r6	0.011	s^{-1}		0.66	min^{-1}
	k02on	0.00012	s^{-1}		0.0072	min^{-1}
	k02off	0.18	s^{-1}		10.8	min^{-1}
	tr3	0.00028	s^{-1}		0.0168	min^{-1}

(Also see Figure 1-2; data from (Hoffmann, Levchenko et al. 2002))

Table 1-4 Other NF−κB Modeling Efforts

Investigations into the analysis and modeling of the TNF−α-mediated NF−κB signaling pathway (Cho, Shin et al. 2003) [Genome Research] Comment: Adds upstream components (TNF receptor, TRADD, RIP, etc); removes IκB isoforms
Experimental design in systems biology, based on parameter sensitivity analysis using a monte carlo method: a case study for the TNF−α-mediated NF−κB signal transduction family (Cho, Shin et al. 2003) [Simulation] Comment: Only model to do multiple parameter sensitivity
Oscillations in NF−κB signaling control the dynamics of gene expression (Nelson, Ihekwaba et al. 2004) [Science] Comment: Extensive single-cell GFP experiments; issues with NF−κB levels (see section 3.5)
Mathematical model of NF−κB regulatory module (Lipniacki, Paszek et al. 2004) [Journal of Theoretical Biology] Comment: Adds A20 feedback, removes IκB isoforms
Stochastic effects of multiple regulators on expression profiles in eukaryotes (Paszek, Lipniacki et al. 2005) [Journal of Theoretical Biology] Comment: First stochastic model
Sensitivity analysis of parameters controlling oscillatory signaling in the NF−κB pathway: the roles of IKK and IκBα (Ihekwaba, Broomhead et al. 2004) [Syst. Biol.] Comment: Phase plane plot analysis; different sensitivity analysis results, emphasizing IκBα.
In silico simulation of inhibitor drug effects on nuclear factor kB pathway dynamics (Sung and Simon 2004) [Molecular Pharmacology] Comment: Models effect of real chemotherapy drug: bortezomib, a proteosome inhibitor.
Achieving stability of lipopolysaccharide-induced NF-kappaB activation (Covert, Leung et al. 2005) [Science] Comment: Modeling of LPS/TLR4 pathway using first order transfer functions

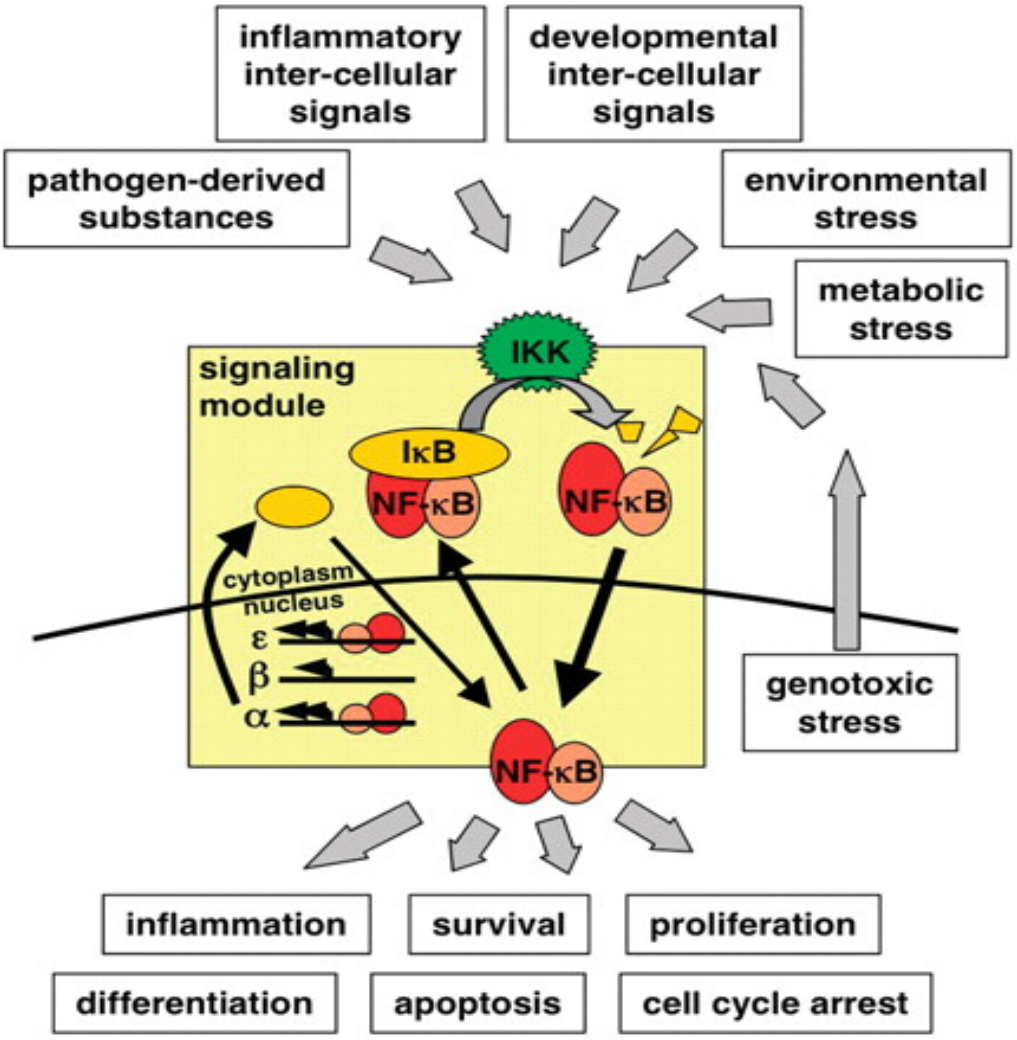

Figure 1-1 Overview of IκB-NF-κB Signaling Module

Schematic of the NF-κB signaling module and its physiological importance in the transduction of diverse inflammatory, developmental and stress signals. Negative feedback is indicated via NF-κB induced expression of IκBα and IκBε.

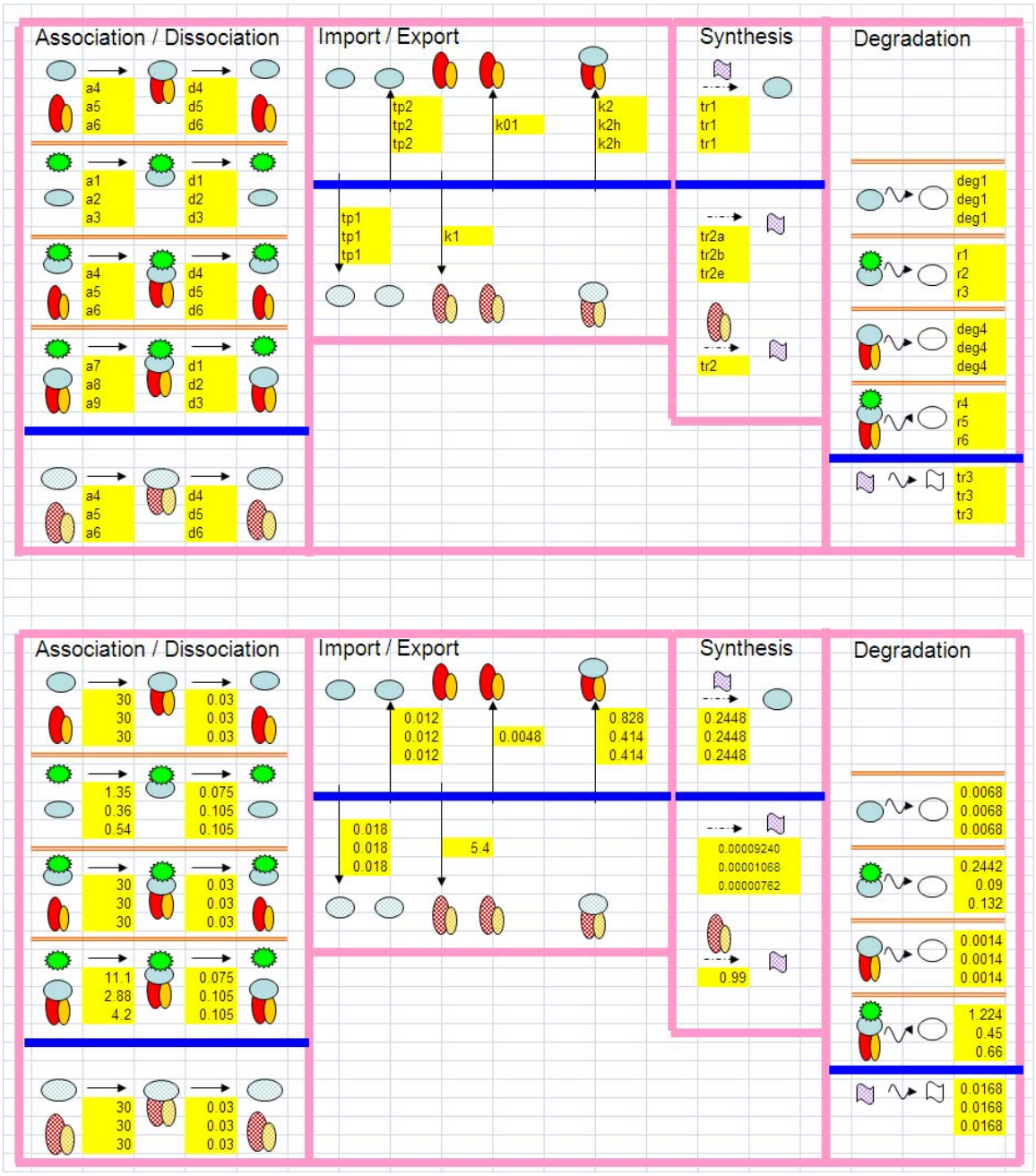

Figure 1-2 Hoffmann-Levchenko model: reactions, parameters names and values

Four categories of reactions are shown: association/dissociation, import/export, synthesis, and degradation. The heavy blue line indicates the cytoplasm/nucleus boundary (cytoplasm is always above, nucleus below). For individual proteins, solid fills indicate cytoplasm, hatched fills indicate nucleus, empty fills (outlines) indicate degradation. For each yellow box, triplet indicates IκBα, IκBβ, IκBε (top to bottom). For units, see Table 1-3. Values from (Hoffmann, Levchenko et al. 2002).

Chapter 2
Homeostatic Control of IκB-NF–κB: regulation of protein degradation

In this chapter, I use computational modeling to study homeostatic control in the IκB-NF–κB signaling system. Specifically, I focus on the regulation of the equilibrium state. As explained below, I focus on and elucidate protein degradation processes, in addition to the obvious effects of protein synthesis.

This chapter contains four sections. The first section examines NF–κB in resting cells, in contrast to previous work which focused on its response to stimuli. It points out the shortcomings of the previous (Hoffmann-Levchenko) model. The second section details the methods I used to refine the Hoffmann-Levchenko model. The third section illustrates the improved model predictions in the equilibrium state. The fourth section elaborates on the biological implications of this modeling work: emphasizing the importance of degradation processes and the presence of IκB functional compensation.

2.1 The NF–κB signaling module as a homeostatic system

Cellular signal transduction pathways are usually studied following administration of an external stimulus. However, disease-associated aberrant activity of the pathway is often due to misregulation of the equilibrium state. In the NF–κB system, while inflammatory signaling leads to transient NF-κB activity that is dynamically regulated by feedback mechanisms, elevated constitutive levels of active NF-κB are associated with chronic inflammatory diseases and many types of cancer (Karin 2006).

Despite the importance of this homeostasis, previous computational models had not recapitulated it. In particular, the Hoffmann-Levchenko model, in the unstimulated state, was found to predict unexpectedly high IκB levels (Lipniacki, Paszek et al. 2004). In fact, the vast majority of IκB molecules were calculated to be in the free form, contradictory to experimental studies showing that free IκBα accounts for less than 15% of the total cellular IκB (Rice and Ernst 1993).

In this chapter, I present my computational work which sheds light on these issues. This computational work focuses on four degradation parameters, and their effects on equilibrium. As shown in Figure 2-1, these correspond to four IκB degradation pathways within the NF−κB signaling system which govern the in-vivo half life of IκB proteins. An IκB molecule can exist in either the free or NF−κB bound form. Both forms may be degraded in an IKK-dependent manner (parameters r1,r4), but are also subject to constitutive degradation in an IKK independent manner (parameters deg1, deg4).

To explore the functional significance of each IκB degradation rate constant in NF−κB signal transduction, I simulate TNF signaling after altering one of the four rate constants (simultaneously for the IκBα, IκBβ, IκBε isoforms) with a parameter multiplier ranging from 0.01 to 100. For each parameter multiplier, I calculated the average nuclear NF−κB level in response to TNF during the early phase (during the 1st hour of stimulation) and the later attenuation phase (during the 2nd hour of a 4 hour stimulation) (Figure 2-2). By plotting the calculated NF−κB activity against its parameter

multiplier (Figure 2-3), I can interpret the sensitivity of the system to each rate constant for two critical features of the NF−κB response to transient TNF stimulus: activation and attenuation of NF−κB activity.

I first examine the impact of changes in IKK-dependent IκB degradation rate constants on NF−κB activation. During the first hour of TNF stimulation, the amount of nuclear NF−κB calculated by the model is fairly insensitive to even drastic changes in the IKK-dependent degradation rate of free IκB (Figure 2-3A, blue line). In contrast, slowing down the IKK-induced degradation of NF−κB-bound IκB severely dampens NF−κB activity (Figure 2-3A, red line). During the attenuation phase, the amount of nuclear NF−κB predicted by the model was similarly found to be insensitive to changes in IKK-dependent degradation of free IκB (Figure 2-3B, blue line), but slowing the IKK-dependent degradation rate of bound IκB results in a loss of attenuation (Figure 2-3B, red line).

The IKK-independent IκB degradation rates control the stimulus-independent turnover of IκB proteins, and thus maintain a resting state equilibrium of IκB levels. Examining whether these IKK-independent degradation rates play a role in determining the cellular responsiveness to inflammatory stimuli revealed that during the first hour of TNF stimulation the signaling module is dramatically more sensitive to the basal turnover rate of free IκB (Figure 2-3C, blue line) than of bound IκB (Figure 2-3C, red line). Furthermore, our simulations predicted that a more stable free IκB results in a loss of

attenuation, whereas the basal turnover rate of the bound IκBs had no effect (Figure 2-3D).

In sum, my computational simulations revealed that two of the four possible degradation pathways play a particularly important role in controlling NF–κB signaling. Whereas much is known about the stimulus-responsive IKK mediated degradation pathway, the IKK-independent degradation mechanism of free IκB has received surprisingly little experimental attention.

Given the importance of these degradation rate constants in my computational analysis, I set out to refine their parameters. I update these parameters by directly or indirectly calculating them from new experimental evidence, as described below. This evidence comes from genetic tools, a panel of mouse knockout cell lines, to cleanly isolate the endogenous free and bound IκB protein pools and probe their degradation with kinase knockouts and pharmacological inhibitors. The experimental work which underlies these calculations was done by my collaborators, with one exception - I measured one important parameter, the inhibitory effectiveness of cycloheximide.

2.2 Refining the Hoffmann-Levchenko model

In order to refine the Hoffmann-Levchenko model and arrive at model 1.1, I update degradation parameters (deg1, deg4, r1, r4) a dissociation parameter (d4) and synthesis parameters (tr1, tr2, tr2a). Some parameters are updated directly from experimental estimates of half-lives, while others are estimated indirectly, as explained

below. A summary of parameter changes appears in Table 2-1. A full picture of the parameters in model 1.1 appears in Figure 2-4.

2.2.1 Parameter values from newly measured half life data

The Hoffmann-Levchenko model value for deg1, the rate constant for degradation of free IκBα, corresponded to a half life of 102 minutes (Pando and Verma 2000; Hoffmann, Levchenko et al. 2002). The model 1.1 value corresponds to a half life of approximately 6 minutes. This new estimate comes from a CHX/EMSA experiment in NF−κB knockout cells and immunoblotting for IκBα, as shown in Figure 2-5.

The rate constants for degradation of free IκBβ and IκBε are set relative to that for IκBα. They are both set to be less stable (faster degradation), in accordance with the evidence shown in Figure 2-6 (for example, subfigure A, columns 2 and 4)

The Hoffmann-Levchenko value for r4, the rate constant for IKK induced degradation of IκBα bound to NF−κB, corresponded to a half life of approximately half a minute (Hoffmann, Levchenko et al. 2002). The model 1.1 value corresponds to a half life of 2 minutes. This is consistent with experimental evidence shown in Figure 2-7. The Hoffmann-Levchenko value for r1 was set relative to r4 – according to previous work (Zandi, Chen et al. 1998) the catalytic rate constant for IKK phosphorylation of IκB proteins is 5-fold higher in the presence of NF-κB. With an updated r4 value in model 1.1, the r1 value is adjusted as well, maintaining this ratio.

2.2.2 Parameters values from simulation and indirect experimental evidence

The Hoffmann-Levchenko value of deg4, the rate constant for degradation of (IKK independent) IκBα bound to NF−κB corresponds to a half life of 513 minutes. The model 1.1 value corresponds to an extremely long half life of approximately 200 hours.

This value is estimated indirectly, using experiments in which wild type and mutant cells are treated with cycloheximide in order to block protein synthesis. In wild type cells, the half life of the appearance of active NF−κB, as assayed by EMSA, is estimated to be 24-60 hours. However, in IKK knockout cells, there is a sustained absence of NF−κB over 60 hours. This experiment is shown in Figure 2-8.

I adjust the Hoffmann-Levchenko model value for deg4 in order to have the simulation recapitulate this behavior. A panel of deg4 values (as a percentage of the Hoffmann-Levchenko value) and their predicted levels of NF−κB at 60 hours are shown in Table 2-2. The new deg4 value is 1.5% of the Hoffmann-Levchenko value, in order to have active NF−κB at 60 hours (in simulation) at less than 2 nM. In these simulations, the effect of cycloheximide is simulated by multiplying tr1, the mRNA translation rate constant, by 0.15. This corresponds to my experimental measurements indicating that cycloheximide is approximately 85% effective, discussed below.

The Hoffmann-Levchenko value of d4, the dissociation rate constant for the IκBαNF−κB complex, was approximately 20 minutes. The new dissociation rate constant corresponds to an extremely long half life of approximately 200 hours.

I adjust the Hoffmann-Levchenko model value for d4 (and d5 and d6, the corresponding parameters for other IκB isoforms) in order to have the simulation

recapitulate the behavior shown in Figure 2-8. A panel of d4 values (as a percentage of the Hoffmann-Levchenko value) and their predicted levels of active NF−κB at 60 hours are shown in Table 2-3. The new deg4 value is 0.2% of the Hoffmann-Levchenko value, in order to have active NF−κB at 60 hours (in simulation) at 2 nM.

2.2.3 Estimating equilibrium IKK activity in unstimulated cells

The Hoffmann-Levchenko model included zero IKK in equilibrium. I update this value to reflect evidence of IKK in resting cells, as shown in Figure 2-11. After simulating baseline IKK at multiple level, I estimate 1 nM baseline IKK to recapitulate the delayed appearance of active NF−κB in CHX treated single IκB expressing cells.

2.2.4 Parameters estimated from semiquantitative fitting

Following adjustment of the above parameters, several synthesis parameters are also adjusted (by smaller factors of 2-4) in order to improve the equilibrium predictions (in the following section). These smaller adjustments are within the range of uncertainty for the original parameter estimates.

2.2.5 Estimating the inhibitory efficacy of CHX

In refining the above parameters, and in order to calculate the improved equilibrium concentrations described below, my simulations were not compatible with the assumption that CHX is 100% effective. To reconsider this assumption, I used I found it difficult to

2.3 Improved predictions in the equilibrium state

In Figure 2-12, I compare the steady state levels of IκB predicted for unstimulated cells by the Hoffmann-Levchenko model and the new version of the model that incorporates the new rate constants. The new degradation rate constants result in predictions of a much smaller pool of free IκB protein, as well as less total cellular IκB protein. The simulation results produced with the new model (1.1) are therefore in much better agreement with experimental observations (Rice and Ernst 1993) than those with the previous model.

Next, I examine the consequences of the new degradation parameters on constitutive NF−κB activity in a series of IκB knockout cell lines. The previous model predicts that the removal of IκB isoforms results in high levels of nuclear NF−κB activity in unstimulated cells (Figure 2-13), which does not match with experimental observations. The differential degradation rates of bound and unbound IκB protein results in molecular compensation among the IκB isoforms; upon deletion of a single IκB isoform, the newly available NF−κB may act to stabilize the remaining IκB isoforms, resulting in the cytoplasmic retention of NF−κB. Indeed, model 1.1 predicts a lower level of NF−κB activity in unstimulated knockout cells than version 1.0 (Figure 2-13, compare white and gray bars). EMSA results confirm the new predictions, indicating that functional IκB compensation via differential half-life control does indeed exist.

2.4 Biological implications

My analysis of the NF-κB signaling module in unstimulated cells reveals a highly dynamic homeostatic state that is controlled by multiple synthesis and degradation mechanisms of the regulatory IκB proteins. Computational simulations allow us to calculate the flux or rates of degrading IκBs (Figure 2-14). Based on my estimates in growing fibroblasts, the model predicts that >90% of all newly synthesized IκB is degraded in the unbound form in an IKK-independent pathway, while about 5% is degraded via an IKK-dependent pathway from the NF-κB-bound state. (In contrast, fluxes for IKK-dependent free IκB degradation or IKK-independent bound degradation are predicted to be exceedingly low, correlating with the lack of NF-κB signaling sensitivity to these rates.) As such we find that NF-κB itself has two roles in regulating its own basal activity. NF-κB binding to IκB proteins removes them from this rapid degradation pathway, and sensitizes them to a slow degradation mechanism that is dependent on basal IKK activity. Secondly, constitutive NF-κB activity also impacts transcription rates of IκBα and IκBε, thus providing for negative feedback even in the absence of an external stimulus.

My studies identify the free IκB protein degradation pathway as a major determinant of constitutive NF-κB and of stimulus-responsiveness of the NF-κB signaling module. Given this hitherto unappreciated importance, determining the enzymatic and potentially regulatory mechanisms of the free IκB degradation pathway is critical to understanding the regulation of NF-κB in diverse physiological and

pathological settings. Due to the dynamic nature of the IκB-NF-κB equilibrium, the majority of newly synthesized IκB is likely degraded before ever binding NF-κB. However, this is not unlike other signal transduction pathways that consume significant cellular resources for the maintenance of a dynamic homeostatic state. For example, the transcription factors p53 and HIF-1α are continually synthesized and degraded. Upon signaling, the respective degradation pathways are inhibited to allow for their nuclear accumulation and function (Ivan, Kondo et al. 2001; Jaakkola, Mole et al. 2001; Moon 2005).

(This chapter, in part, is a reprint of material in press as "A homeostatic model of IκB metabolism to control constitutive NF−κB activity" O'Dea E, Barken D, Peralta RQ, Tran KT, Werner SL, Kearns JD, Levchenko A, Hoffmann A. *Molecular Systems Biology*. The dissertation author is the primary investigator of all computational work and an author of the materials used from this paper.)

Table 2-1 Parameter changes in Model 1.1

		Model H-L	Model 1.1		
DISSOCIATION	d4	0.03	0.00006		IkBaNFkB => IkBa + NFkB
	d5	0.03	0.00006		IkBbNFkB => IkBb + NFkB
	d6	0.03	0.00006		IkBeNFkB => IkBe + NFkB
DEGRADATION	deg1	0.00678	0.12		IkBa =>
	deg2	0.00678	0.18		IkBb =>
	deg3	0.00678	0.18		IkBe =>
	deg4	0.00135	0.00006		IkBaNFkB => NFkB
	deg5	0.00135	0.00006		IkBbNFkB => NFkB
	deg6	0.00135	0.00006		IkBeNFkB => NFkB
	r1	0.2442	0.072		IKKIkBa => IKK
	r2	0.09	0.024		IKKIkBb => IKK
	r3	0.132	0.036		IKKIkBe => IKK
	r4	1.224	0.36		IKKIkBaNFkB => IKK + NFkB
	r5	0.45	0.12		IKKIkBbNFkB => IKK + NFkB
	r6	0.66	0.18		IKKIkBeNFkB => IKK + NFkB
SYNTHESIS	tr2	0.99	1.98		2 NFkB => 2 NFkB + IkBat
	tr2a	0.00009240	0.0001848		=> IkBat
	tr2b	0.00001068	0.00004272		=> IkBbt
	tr2e	0.00000762	0.00003048		=> IkBet

Table 2-2 deg4 fitting to experimental evidence

deg4 factor	NF−κB at 60 hours
5.0 %	8.95 nM
3.0 %	5.01 nM
2.0 %	2.90 nM
1.5 %	1.98 nM
1.0 %	1.13 nM
0.5 %	0.42 nM

Table 2-3 d4/d5/d6 fitting to experimental evidence

d4/d5/d6 factor	NF−κB at 60 hours
1.0 %	13.11 nM
0.5 %	5.92 nM
0.2 %	2.16 nM
0.1 %	1.01 nM

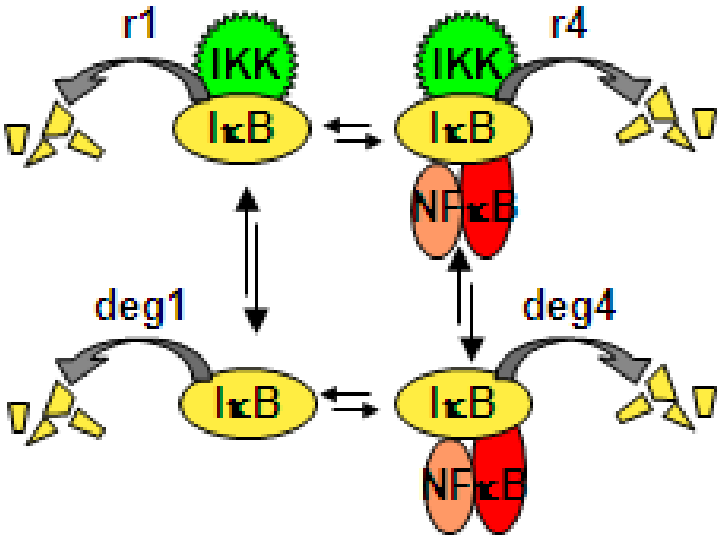

Figure 2-1 Illustration of the four IκB degradation pathways

Deg1 and deg4 are IKK-independent degradation rate constants for free and bound IκBα
R1 and r4 are IKK-dependent degradation rate constants for free and bound IκBα.

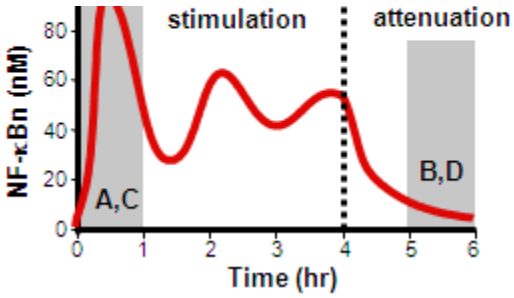

Figure 2-2 Stimulation and attenuation in Hoffmann-Levchenko model

Computational simulation of NF-κB activation over a 6-hour time course using the Hoffmann-Levchenko model. TNF stimulation begins at time 0, and is removed at 4 hours. Mean activity in the first hour of stimulation, and the second hour after removal of the stimulus (both shaded in gray) are shown (as labeled) in Figure 2-3.

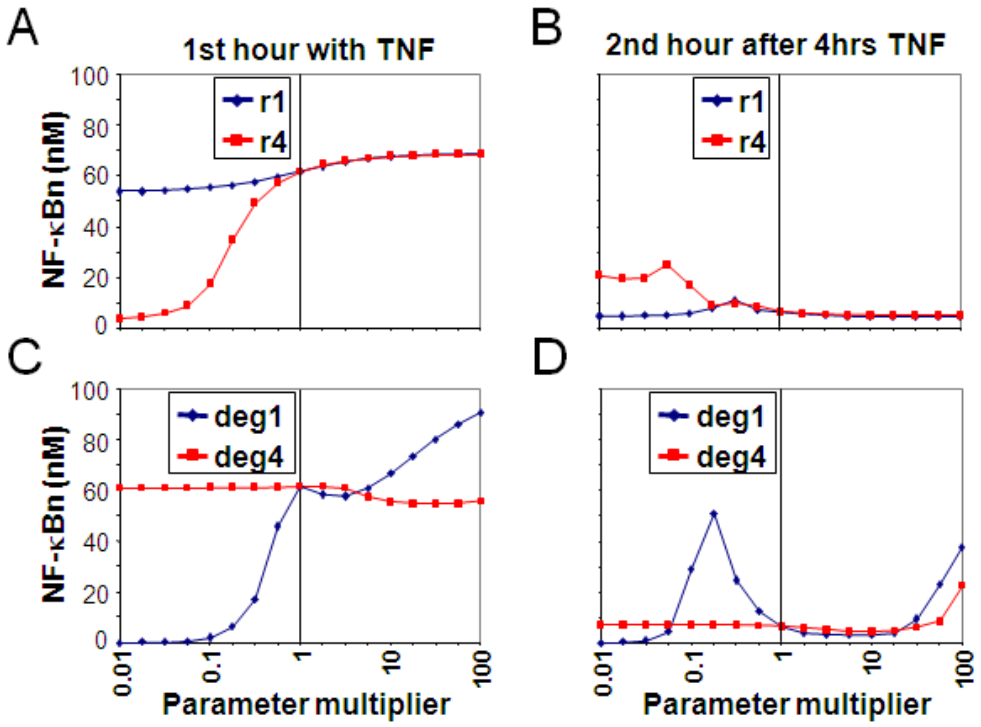

Figure 2-3 Sensitivities of IκB degradation pathway parameters

Graphs showing the average nuclear NF-κB (y-axis) during the first hour (A,C) or during the second hour after 4 hours (B,D) of TNF stimulation for different values (x-axis) of the IKK dependent (A,B) or independent (C,D) degradation rate constants of free (blue line) or bound (red line) IκB.

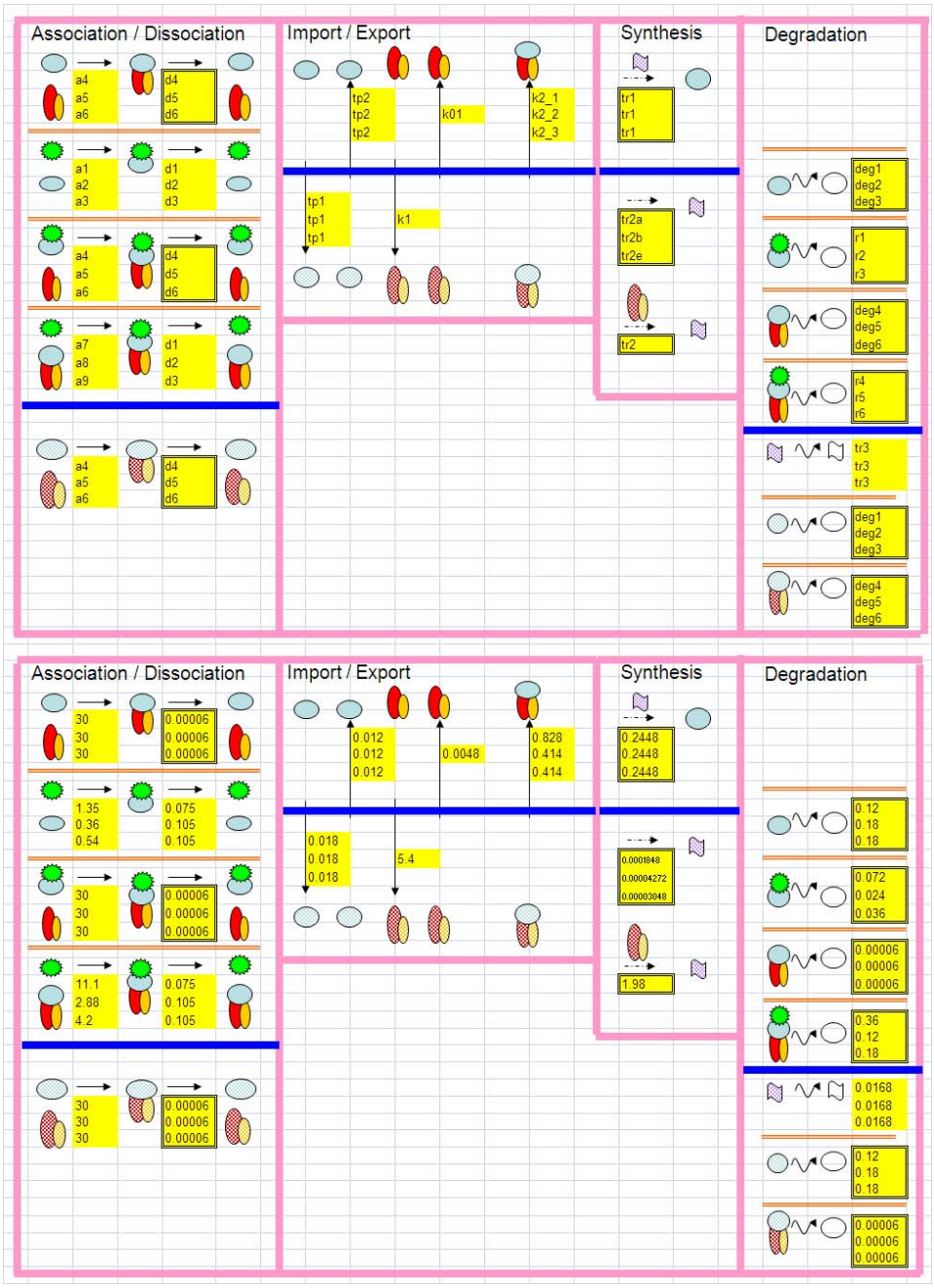

Figure 2-4 Model 1.1 parameter names and values

Four categories of reactions are shown: association/dissociation, import/export, synthesis, and degradation A double border indicates changed values from the Hoffmann-Levchenko model. The heavy blue line indicates the cytoplasm/nucleus boundary (cytoplasm is always above, nucleus below). For individual proteins, solid fills indicate cytoplasm, hatched fills indicate nucleus, empty fills (outlines) indicate degradation. For each yellow box, triplet indicates IκBα, IκBβ, IκBε (top to bottom). For units, see Table 1-3.

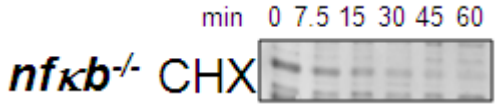

Figure 2-5 Experimental studies of degradation pathway of free IκBα protein

Western blots for IκBα of protein extracts from NF-κB$^{-/-}$ cells treated with 10 μg/mL CHX. Work from (O'Dea E, Barken D et al. 2007).

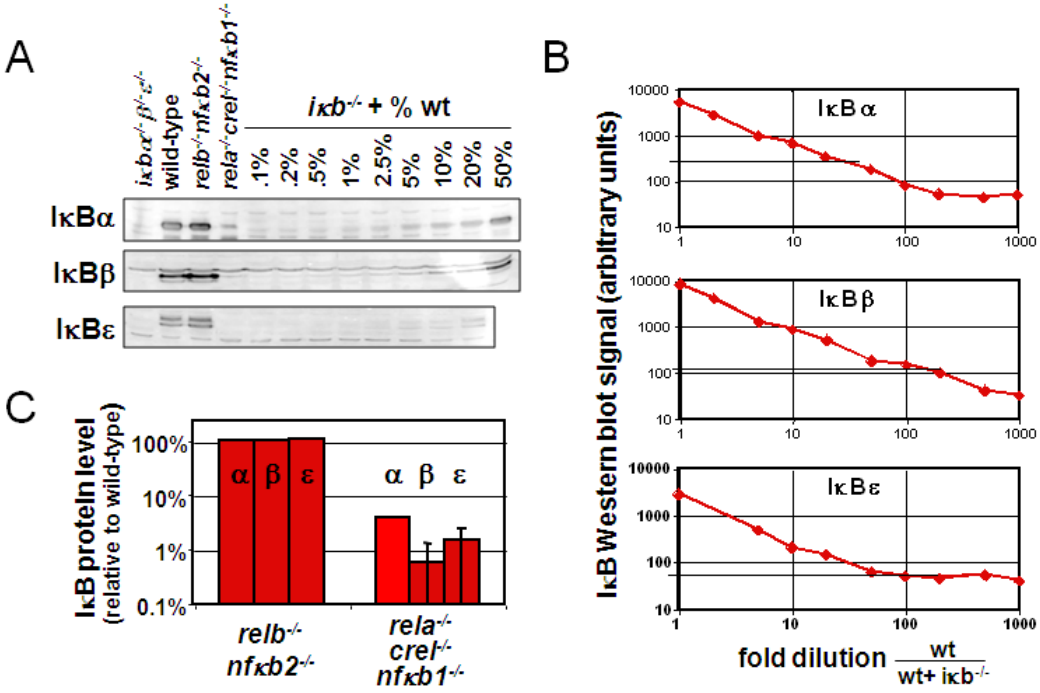

Figure 2-6 Experimental studies of relative stability of free IκB proteins

(A) Western blots for IκBα, IκBβ, and IκBε in different cell genotypes (labeled above each lane). The percentage of IκB protein in the NF-κB-/- cells compared to the amount in wild-type cells was approximated by a dilution series of IκBα-/-b-/-e-/- extract with wild-type extract.

(B) Standard curve of Western blot signals for each IκB isoform based on the dilution series in (A). Loss of linearity at the low end indicates background and limits the sensitivity of detection. The line indicates the signal measured for samples derived from NF-κB-/- cells.

(C) Graph of quantitated IκB protein levels in non-canonical and canonical NF-κB protein knockouts (relb-/-NF-κB2-/- and rela-/-crel-/-NF-κB1-/- MEFs) relative to wild type cells as determined in (A) and (B).

Work from (O'Dea E, Barken D et al. 2007).

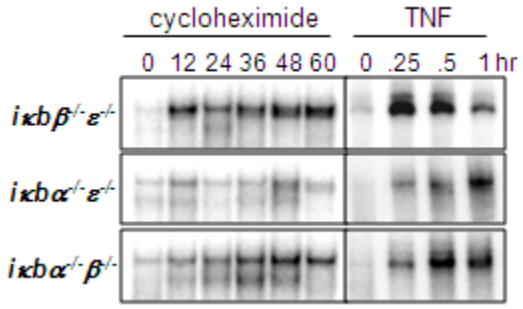

Figure 2-7 Experimental studies of IKK induced degradation of free IκB proteins

NF-κB activity as measured by EMSA of nuclear extracts from *IκBβ*$^{-/-}$*ε*$^{-/-}$, *IκBα*$^{-/-}$*ε*$^{-/-}$, or *IκBα*$^{-/-}$*β*$^{-/-}$ cells treated with 10 μg/mL CHX or 1 ng/mL TNF. Work from (O'Dea E, Barken D et al. 2007).

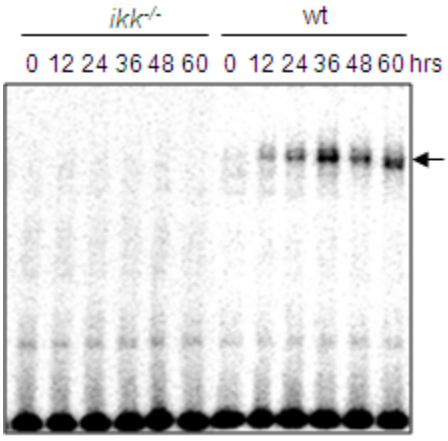

Figure 2-8 Experimental studies of degradation pathways

NF-κB activity as measured by EMSA of nuclear extracts from ikkα$^{-/-}$ β$^{-/-}$ or wild-type MEFs treated with 10 μg/mL CHX.
Work from (O'Dea E, Barken D et al. 2007)

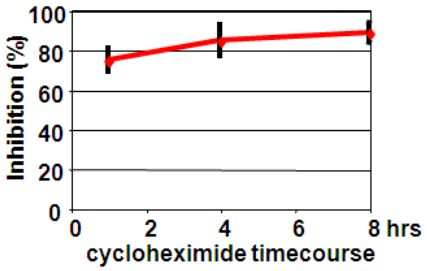

Figure 2-9 Cycloheximide inhibition efficacy

Graph showing the percentage of bulk protein synthesis inhibition in cells treated with 10μg/mL CHX as compared to cells without CHX. Cells treated with or without CHX were metabolically labeled with 200 μCi/mL ^{35}S-Methionine and protein extracts were measured by scintillation count at indicated time points. Experiments conducted in

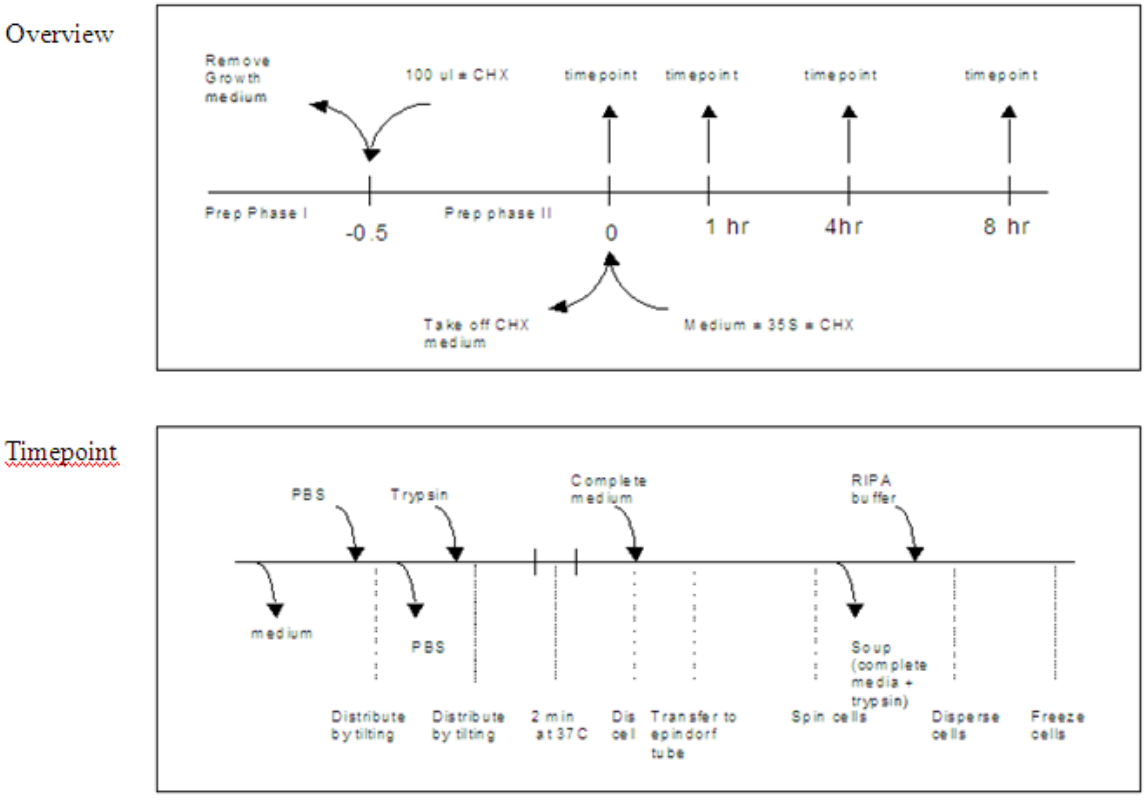

Figure 2-10 Experimental procedure for cycloheximide efficacy experiment

A flowchart for the experimental procedure described in the text. Above: timepoints Below: detailed procedure at a timepoint.

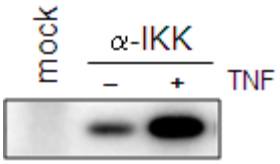

Figure 2-11 Experimental evidence of IKK in resting cells

Cytoplasmic extracts of wild-type cells were immunoprecipitated with IKKγ antibody and subject to an in vitro kinase assay. In the "mock" lane, no antibody was added during the IP. Work from (O'Dea E, Barken D et al. 2007).

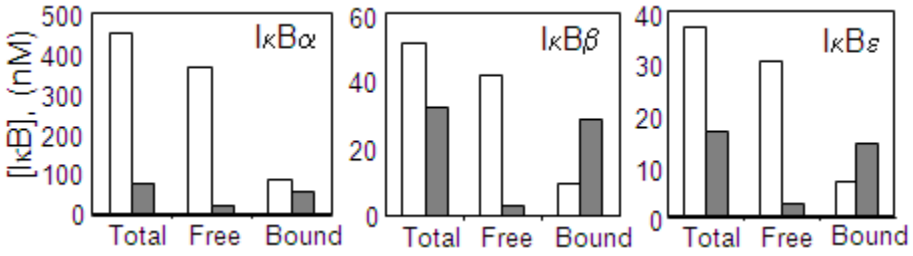

Figure 2-12 Equilibrium IκB levels

Model calculations of IκBα, b, and e protein levels (nM) in unstimulated cells for total IκB, free IκB, or NF-κB-bound IκB. Hoffmann-Levchenko predictions are white bars, model 1.1 predictions are gray bars.

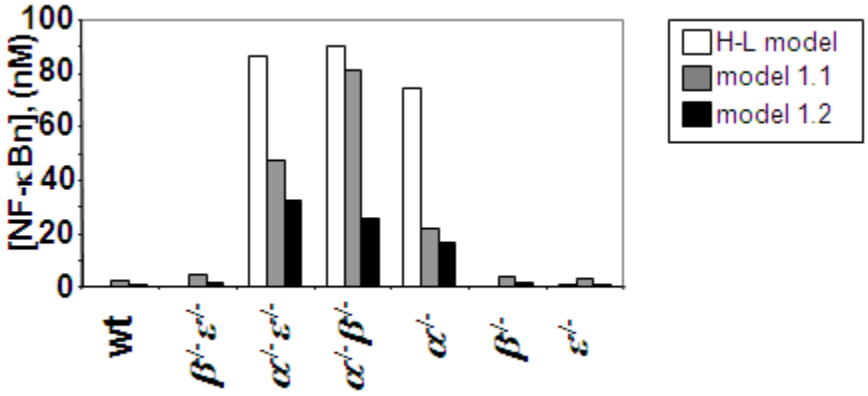

Figure 2-13 An improved model of the homeostatic NF–κB signaling module.

Model calculations of NF-κB activity (nM) in unstimulated wild-type and *IκB*$^{-/-}$ cells predicted by the Hoffmann-Levchenko model (white bars), and version 1.1 (gray bars). Model 1.2 (black) is an update to version 1.1 with NF-κB induced expression of IκBε.

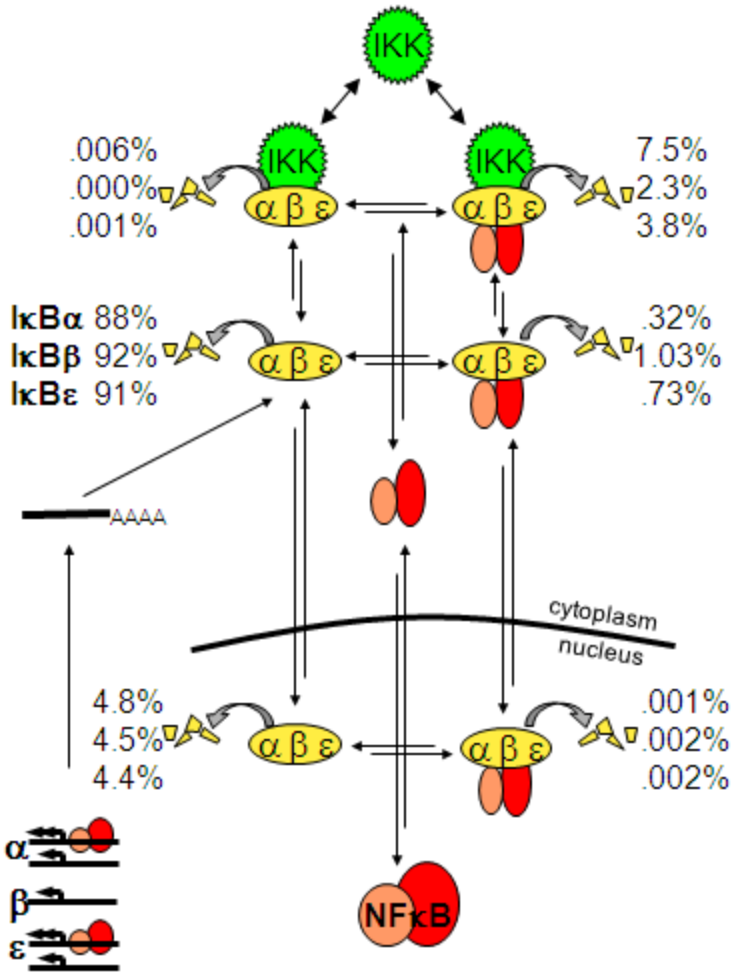

Figure 2-14 Flux Calculations of IκB Degradation Rates

Rates calculated with model version 1.1. In resting cells new IκB protein is continuously synthesized, which is balanced by equal IκB protein degradation in the cytoplasm and nucleus. The shown percentages indicate the fraction of the total degradation rate/flux through each degradation pathway. These calculations indicate that in resting cells more than 90% of all newly synthesized IκB protein is degraded before binding to NF-κB.

Chapter 3
Temporal Control of IKK activity

This chapter develops the thesis that different inflammatory stimuli induce distinct IKK temporal profiles of IKK activity, and that temporal control of IKK can ultimately allow for selective gene activation by producing stimulus specific temporal profiles of NF-κB. The computational work in this chapter is enabled by a key alteration to previous models – allowing the IKK input to be numerically specified. This opens the door to a systematic exploration of the system's characteristics, and simulation of experimentally measured IKK profiles.

Correspondingly, this chapter contains two sections. In the first, I consider the capabilities of the system, by analyzing a library of hypothetical IKK timecourses. In the second, I simulate the response to several experimentally measured stimulus specific IKK profiles. In both sections, I relate the computational results to to biological conclusions, leading to new insights about signaling pathway-specific mechanisms.

3.1 Exploring the signal processing characteristics of the IKK-NF-κB module

In this section, I generate a library of hypothetical IKK timecourses. Treating each member of the library as an input, I run a simulation and generate a corresponding timecourse of active NF−κB. I cluster and analyze this set of output timecourses, which allows me to draw generalized biological conclusions about the relative importance of early vs. late levels of IKK, as explained in detail below.

3.1.1 Specifying the IKK timecourse

As reviewed in Chapter 1, dynamic models are simplified representations of a real world biological entity or system. In producing such a model, one implicitly or explicitly chooses a structure, which in turn may limit the range of problems to which the model may be applied.

The first published NF−κB model (Hoffmann, Levchenko et al. 2002) was structured as a set of differential equations. The "input signal" consisted of IKK concentration, which varied over time. In the ODE formulation, this input signal was specified analytically. Specifically, the concentration of IKK was set to zero during an equilibration phase, then raised to a positive value at "time zero", and its decay was governed by the rate constant of a decay reaction, which translated into a term in a linear, first order ordinary differential equation.

This approach has successfully applied to questions of biological interest. (Hoffmann, Levchenko et al. 2002; Cheong, Bergmann et al. 2006). However, it imposes a limitation – any desired input profile of IKK must be expressed analytically. In fact, in order to be used in the system of differential equations, it must be expressed indirectly, as the formula for the first derivative of the desired function. Furthermore, it is inherently unsuited for simulating an input which is expressed as a combination of metabolites (e.g. total IKK). For these reasons, I developed two additional methods for specifying the IKK profile numerically.

The first method (Werner, Barken et al. 2005) directly calculates the reaction rates of a subset of reactions involving active IKK. There are eight reactions that add or

remove active IKK from free or complexed pools in the system, as shown in Table 3-1. The rates of these reactions are calculated proportionally for each pool to produce the total IKK profile specified at one-minute intervals as the input. This method allows the total IKK to change over time.

The second method (Barken, Werner et al. 2007) does not adjust the levels of IKK. Instead, it adds a pseudo-parameter to each reaction which involves IκB degradation from a complex which involves IKK (Table 3-2). That pseudo-parameter scales the rate of degradation from 0-100%. In this formulation, the input profile of IKK is re-evaluated as the percentage of IKK which is active, and the input profile is thus used as the pseudo-parameter. Consequently, in this formulation, the total amount of IKK is a constant, but the activity is altered over time. This method generally gives similar results, but is preferable for being biologically more intuitive.

3.1.2 Generating a library of dynamic IKK input signals

If one has a library of IKK input profiles, it is possible to generate the set of corresponding nuclear NF−κB timecourses. If the input library has reasonable coverage of the possible input space, and if it represents a reasonable sample of the set of IKK profiles of interest, then it is possible to analyze the input/output pairs to gain understanding of the system's overall processing characteristics.

To generate a library of inputs, I used a simple algorithm, as shown in Figure 3-1. Five parameters were varied over a set of discrete values, as detailed in the figure legend; with duplicate timecourses removed, the resulting set of IKK timecourses, as shown in Figure 3-2. Specifically, a set of diverse IKK profiles was computationally generated by

the following algorithm: each input had a rising phase (parameter a), a first plateau (parameter b) a falling phase (parameter c) and a second plateau, each with varying time values of 0, 60, 120 or 240 minutes (parameter a), or 0, 5, 15, 30, 60 or 120 minutes (parameter b) or 0, 60, 120 or 240 minutes (parameter c). The heights of the first (parameter x) and second (parameter y) plateaus were also varied to 4, 12, 34, or 101 nM IKK (parameter x) or 1, 4, 12, 34 or 101 nM IKK (parameter y), with $y \leq x$, and with duplicate signals removed. Finally, for each input, the corresponding output was calculated. Representative input / output pairs (IKK/active NF–κB) are shown in Figure 3-3. The full set of outputs is shown in Figure 3-4.

These simulations were done using "model 2.0", which has the same parameter values as model 1.1, with the following two alterations. First, NF-κB induced expression of IκBε is added, based on work of my colleague Jeff Kearns (Kearns, Basak et al. 2006) showing that IκBε provides negative feedback. Second, the rates for the two NF-κB induced transcription reactions (IκBα and IκBε) are adjusted to accurately model the responses to TNF and LPS pulses, as detailed in (Werner, Barken et al. 2005).

3.1.3 Clustering dynamic NF–κB output signals

I next grouped the full set of outputs using standard k-means clustering, in order to investigate which IKK activity profiles are distinguished by the signaling module and which profiles, although seemingly different, are likely to have similar biological effects. Specifically, I clustered the set of NF–κB timecourses (the outputs), then examined the

sets of IKK profiles (the inputs) that corresponded to each cluster. A number of biological insights were revealed.

3.1.4 Biological discussion

Examination of the clusters (Figure 3-13) allows me to draw a large number of biological inferences. These include the following:

1. The amplitude of the first peak of IKK activity is not a major determinant of the NF−κB activity profile (Figure 3-5).
2. Different rates of IKK activation (immediate vs one hour) result in different NF−κB activity profiles (Figure 3-6)
3. Different durations of the first peak in the IKK profile result in different NF−κB activity profiles (Figure 3-7)
4. The signaling module does not distinguish very much between different decay rates of IKK activity at late times (Figure 3-8)
5. The level of IKK activity in the second plateau is very important to determining the active NF−κB profile (Figure 3-9)
6. Transient aberrations in IKK activity do not result in much active NF−κB response (Figure 3-10)
7. Large but very transient IKK activities have similar signaling effects as sustained smaller increases – both provoke NF−κB responses that are much longer that the duration of the transient pulse. (Figure 3-11).

8. The signaling module is particularly sensitive to sustained low IKK activity but robust to transient perturbations. (Figure 3-12).

It is worth pointing out that other models of cell signaling systems may similarly be analyzed by generating a diverse library of inputs, simulating a set of outputs, clustering the outputs, and examining the inputs and their corresponding outputs in order to draw conclusions about the system's behavior.

3.2 Simulating the response to measured stimulus specific IKK profiles

In the previous section, I modified the model to incorporate a numerical IKK input, and then simulated a library of hypothetical inputs. In addition, thanks to the IKK IP-kinase affinity measurements by my colleague Shannon Werner, I am able to present the computational model with inputs derived from experimental measurements. In the following section, I present work following this strategy.

3.2.1 Biological measurements and computational simulations

One prediction of the cluster analysis described above is that long-lasting NF−κB activity may be mediated by unexpectedly low amplitudes of IKK activity, whereas transient NF−κB activity requires a much higher increase in IKK activity. Examining the actual kinase activity profiles in cells exposed to either brief (45 minute) or prolonged stimulation with TNF−α reveals that IKK is highly active at early time points but that activity drops to low levels after about 30 minutes (Figure 3-14). Consistent with the computational investigation described above, IKK activity profiles were similar, with

only a slightly increased late plateau of activity elicited by persistent stimulation. However, these simulation conditions have distinct biological effects mediated by a late phase of NF−κB activity. The importance of small changes in late or prolonged IKK activity suggests that mechanisms may have evolved to modulate it with remarkable precision.

3.2.1.1 TNF & LPS induced IKK activity

Actual cellular IKK activity profiles are determined by signaling pathways emanating from receptors that allow for stimulus-specific signal processing. My colleague Shannon Werner therefore measured the IKK activity profiles in response to the inflammatory stimuli TNF and bacterial lipopolysaccharide (LPS), which engage TNF receptor TNFR and toll-like receptor 4 (TLR4), respectively. Transient administration of these stimuli (45 minutes) resulted in different IKK activity profiles (Figure 3-15). LPS elicited a small increase in IKK activity within the first 30 minutes, a larger increase between 45 and 90 minutes, and a slowly attenuating late phase. In contrast, TNF elicited a sharp peak of IKK activity within the first 15 minutes, with a return to baseline within 60 minutes.

Computational simulations with those experimentally determined IKK activity profiles predicted temporally distinct NF−κB activity profiles, as shown in Figure 3-16. Experimental measurements revealed temporal NF−κB activity profiles similar to those predicted (Figure 3-17). Thus, my computational model recapitulates NF−κB activation events in response to multiple inflammatory stimuli. The successful in-silico

reconstitution of LPS and TNF signaling may mean that no further biochemical factors and mechanisms need be invoked to explain the regulation of nuclear NF−κB translocation by IKK.

3.2.1.2 Negative feedback as a determinant of the TNF induced IKK profile

In the TNFR signaling pathway, the NF−κB response gene A20 has been proposed to function in postinduction attenuation of NF−κB activity by modulating the signaling mechanisms that regulate IKK activation (Lee, Boone et al. 2000; Wertz, O'Rourke et al. 2004). Using my computational model, I examine whether misregulation of IKK in A-20 deficient cells is sufficient to explain the increased activation of NF−κB and the consequent inflammatory phenotype seen in A20-deficient mice. I used quantitative measurements of the TNF-induced IKK activity profile in wild-type and A20 knockout cells, as measured by my colleague Shannon Werner (Figure 3-18), as inputs to my computational model to predict NF−κB activation profiles (Figure 3-19). Biochemical analyses of nuclear NF−κB activity (Figure 3-20) match the computational predictions. Thus, A20 appears to function in fibroblasts in attenuating NF−κB signaling by modulating the temporal profile of IKK activity in the TNF signaling pathway but less so in the LPS signaling pathway.

3.2.1.3 Positive feedback as a determinant of the LPS induced IKK profile

For the TLR4 signaling pathway, the molecular mechanisms that regulate IKK are less well understood (Akira, Takeda et al. 2001). LPS induced IKK has a biphasic profile (Figure 3-15). By using the ribosome inhibitor cycloheximide, my colleague Shannon

Werner found that the LPS-specific second phase was dependent on new protein synthesis (Figure 3-21). She also found that IKK activity varied with the density of the primary cells in culture (Figure 3-22). Consequently, we hypothesized that LPS-specific primary response genes may function to potentiate late IKK activity through an autocrine mechanism. LPS rapidly increased expression of genes encoding 10 secreted cytokines and chemokines, many of which were also expressed in response to TNF stimulation (Figure 3-23). However, the interleukin-10 (IL-10), IL-1, and TNF genes were specifically expressed in response to LPS. TNF functions in endotoxin toxicity by a proinflammatory paracrine mechanism (Beutler, Milsark et al. 1985; Beutler and Kruys 1995). When my co-author Shannon Werner stimulated TNF-deficient cells at high density with LPS, the late phase of IKK activity was lost, whereas TNFR-responsive IKK activation remained intact (Figure 3-24).

When I calculate simulations using these measured IKK profiles, our computational model predicts a defect in NF−κB activation by LPS in TNF-deficient cells (Figure 3-25), which my colleague confirmed experimentally (Figure 3-26).

By employing MEFs deficient in canonical NF−κB proteins, we revealed that LPS-induced expression of TNF requires NF−κB. Furthermore, LPS-induced IKK activity was lower in NF−κB deficient cells than in controls, whereas TNF-induced IKK activity was largely unaffected by NF−κB deficiency. Together, these results indicate that TNF involvement in TLR4 signaling constitutes a positive feedback mechanism. TLR4 signaling to IKK was previously shown to be mediated by the adaptor protein MyD88 and, with delayed kinetics, by TRIF through an unknown signaling pathway

(Akira, Takeda et al. 2001; Barton and Medzhitov 2003). Our data suggests that the proposed signaling pathway is mediated by de-novo synthesis of TNF (Figure 3-27). Secondary IKK activation mediated by TNF autocrine feedback may thus depend not only on the first phase of NF–κB activity, but also possibly on TRIF-dependent IRF-3.

3.2.2 Biological discussion

These finding indicate that TNF (and possibly other cytokines) mediate feedforward mechanisms in response to endotoxin challenges that produce positive feedback on IKK activity (and likely also regulate other signal transduction events) and are critical for the induction of a stimulus-specific gene expression program. The particular sensitivity of the biological response to the temporal profile of IKK activity suggests that the underlying molecular mechanisms, including negative and positive feedback mechanisms (Figure 3-27), may provide sensitive signaling nodes that cells may use for signaling crosstalk.

In this chapter, I examined the temporal control of IKK activity and its relation to the concentration of NF–κB over time. I discussed how feedback regulates late IKK, and how modeling supports the idea that late IKK is important. In the next chapter, I extend this analysis, characterizing the connection between the temporal code and stimulus specific gene expression.

(This chapter, in part, is a reprint of material published as "Stimulus specificity of gene expression programs determined by temporal control of IKK activity", Werner SL*, Barken D*, Hoffmann A, Science 309(5742): 1857-61. The dissertation author is the

primary investigator of all computational work and an author of the materials used from this paper.)

Table 3-1 Reactions Creating or Destroying IKK

	=> IKK
IKK	=>
IKKIκBα	=> IκBα
IKKIκBβ	=> IκBβ
IKKIκBε	=> IκBε
IKKIκBαNF–κB	=> IκBα + NF–κB
IKKIκBβNF–κB	=> IκBβ + NF–κB
IKKIκBεNF–κB	=> IκBε + NF–κB

Table 3-2 Reactions Involving IKK Dependent Degradation of IκB

IKKIκBα => IKK
IKKIκBβ => IKK
IKKIκBε => IKK
IKKIκBαNF–κB => IKK + NF–κB
IKKIκBβNF–κB => IKK + NF–κB
IKKIκBεNF–κB => IKK + NF–κB

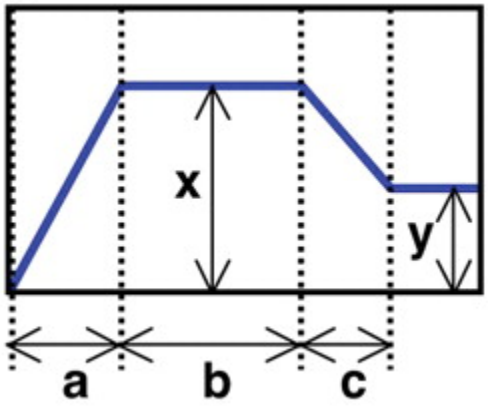

Figure 3-1 Parameters for Generating IKK Library

A set of diverse IKK profiles was computationally generated by the following algorithm: each input had a rising phase (parameter a) a first plateau (parameter b), a falling phase (parameter c) and a second plateau, each with varying time values of 0, 60, 120 or 240 min (parameter a) or 0, 5, 15, 30, 60, 120 min (parameter b) or 0, 60, 120 or 240 min (parameter c). The heights of the first (parameter x) and second (parameter y) plateaus were also varied to 4, 12, 34 or 101 nM IKK (parameter x) or 1, 4, 12,34 or 101 nM IKK (parameter y), where $y \leq x$.

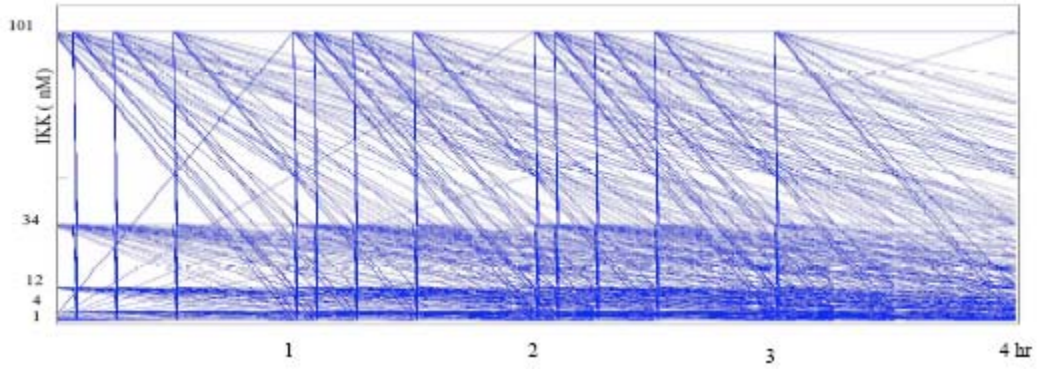

Figure 3-2 Library of IKK timecourses

Graphical representation of a set of 687 IKK timecourses generated according to methodology described in Figure 3-1

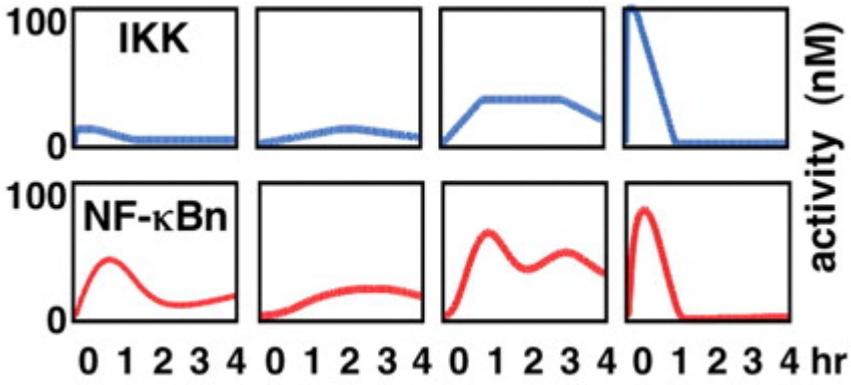

Figure 3-3 Examples of IKK and corresponding active NF–κB timecourses

Four examples from a library of 687 distinct IKK activity profiles (blue), generated as shown in Figure 3-1. Corresponding simulated active NF-κB levels are shown in red.

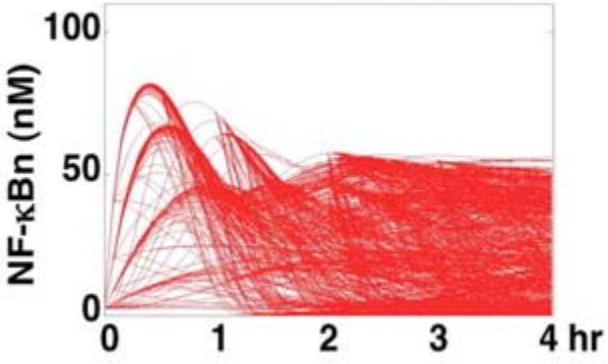

Figure 3-4 Active NF–κB timecourses corresponding to IKK library

Set of 687 NF-κB timecourses generated as shown in figures Figure 3-1, Figure 3-2, and Figure 3-3

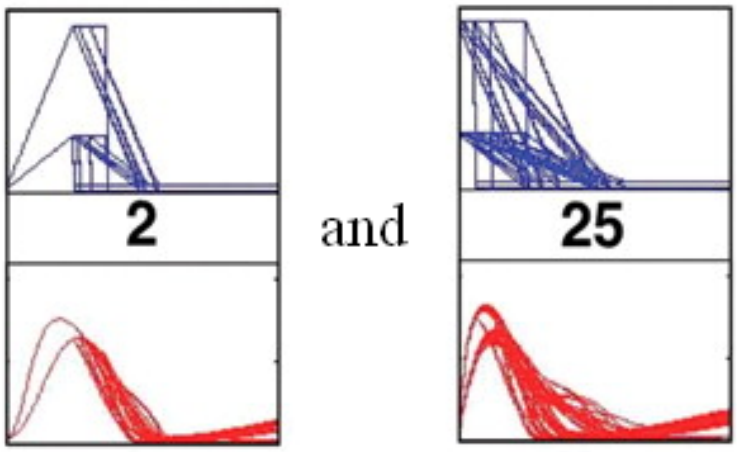

Figure 3-5 Clusters illustrating minimal effect of early plateau level

Two clusters of NF-κB outputs (red; subsets of Figure 3-4), shown with their corresponding IKK inputs (blue; subsets of Figure 3-2). Both clusters have different early plateaus, but not much variation in the outputs (resulting in the outputs being clustered together.)

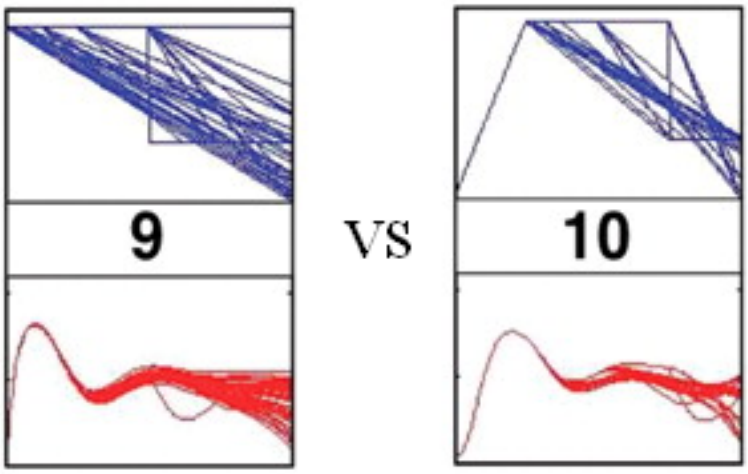

Figure 3-6 Different Clusters from Different Rates of IKK Activation

Two clusters of NF-κB outputs (red; subsets of Figure 3-4), shown with their corresponding IKK inputs (blue; subsets of Figure 3-2). The IKK profiles (blue) on the left have a very fast (first hour) rise, while the IKK profiles on the right have a more gradual rise. The resulting clusters of NF-κB (red) show distinct differences in the early rise (first hour), leading to distinct clusters.

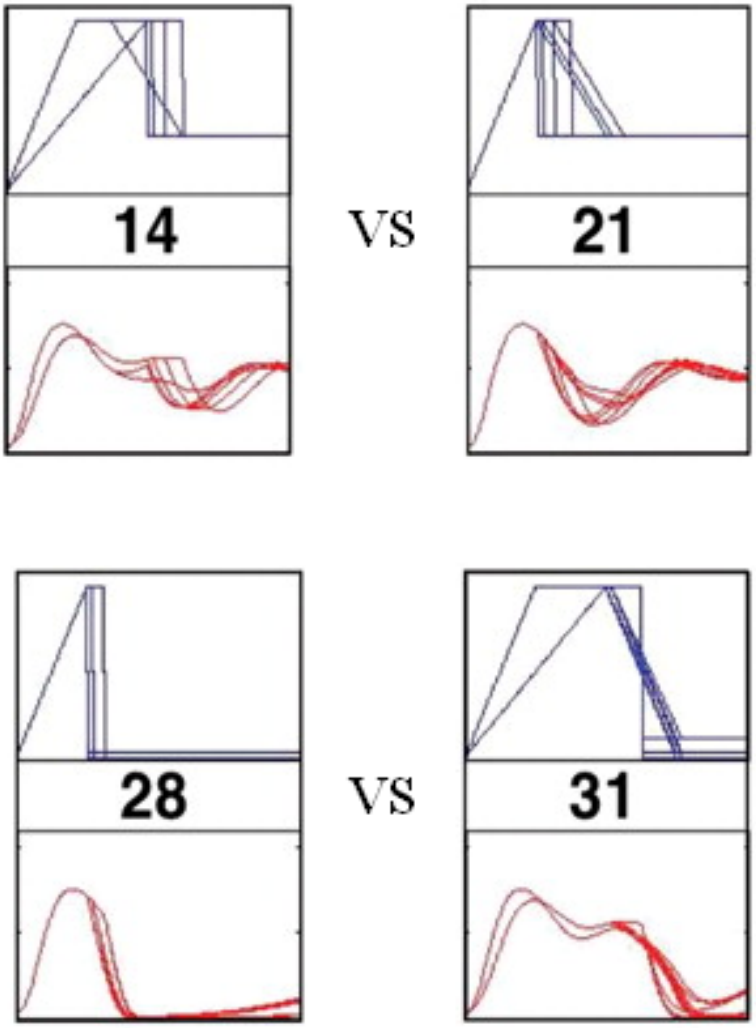

Figure 3-7 Different Clusters from Different Duration of First Plateau

Two clusters of NF-κB outputs (red; subsets of Figure 3-4), shown with their corresponding IKK inputs (blue; subsets of Figure 3-2). The IKK inputs (blue) in the cluster on the left have a relatively long first plateau, compared to the short first plateaus on the right. The resulting NF-κB output curves (red) are sufficiently different to cluster separately.

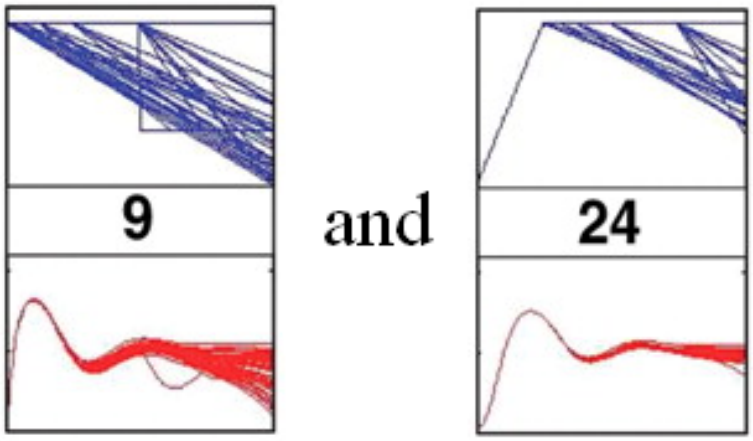

Figure 3-8 Clusters Illustrating Minimal Effect of Different IKK Decay Rates

Two clusters of NF-κB outputs (red; subsets of Figure 3-4), shown with their corresponding IKK inputs (blue; subsets of Figure 3-2). Both clusters illustrate the minimal effects of different IKK decay rates – in both clusters, some IKK inputs decay and some do not, yet the NF-κB outputs are similar and cluster together.

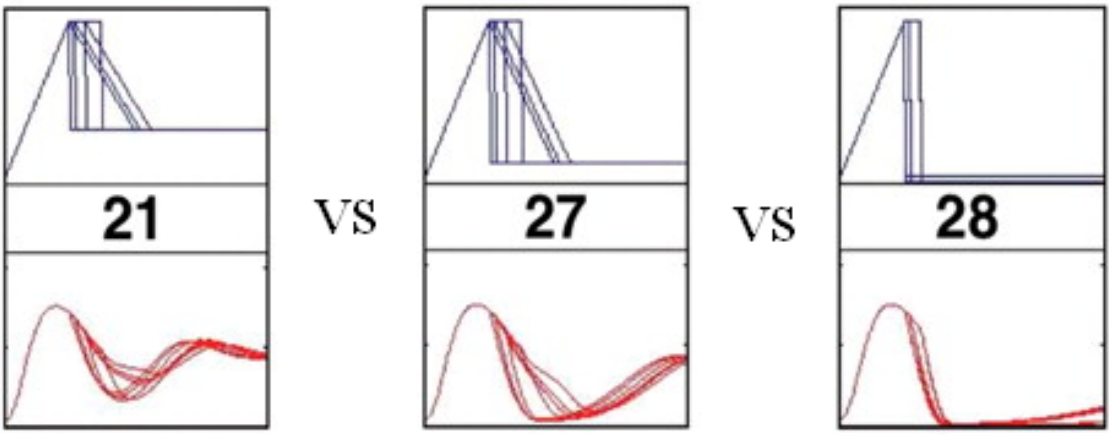

Figure 3-9 Clusters Illustrating the Importance of IKK Levels in the Second Plateau

Three clusters of NF-κB outputs (red; subsets of Figure 3-4), shown with their corresponding IKK inputs (blue; subsets of Figure 3-2). These clusters illustrate the importance of the level of IKK in the second plateau.

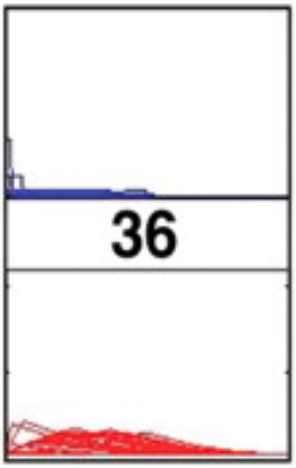

Figure 3-10 Cluster Illustrating Minimal Importance of Early Transient IKK

This cluster illustrates that for early, transient IKK signals that are relatively small, the response is similar to (and clustered with) responses to transient or sustained low IKK. The signaling module does not make a strong distinction the two types of input IKK profiles.

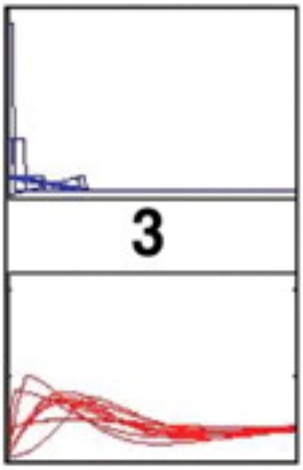

Figure 3-11 Illustration of Response Similarity to Transient and Low Sustained IKK

This cluster illustrates that for early, transient IKK signals that are somewhat larger, the response is similar to sustained IKK at a slightly higher level.

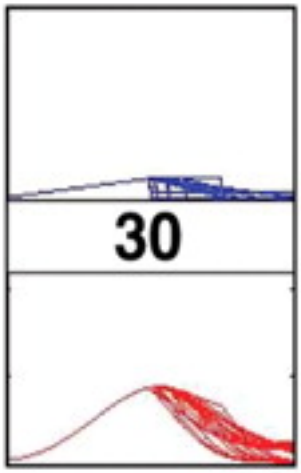

Figure 3-12 Cluster Illustrating Sensitivity to Sustained Low IKK

This cluster illustrates that the system is sensitive to sustained low IKK activity but robust to transient perturbations.

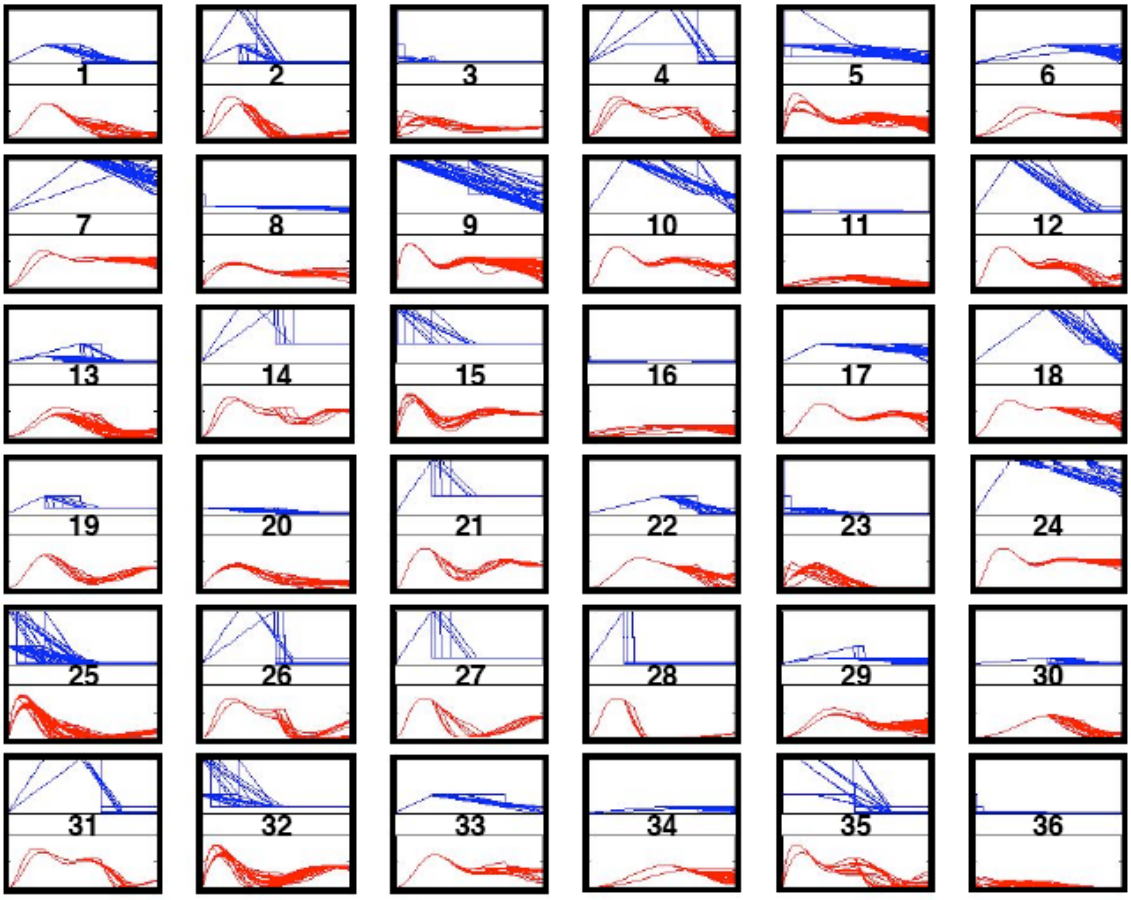

Figure 3-13 Complete Set of K-Means Clusters on Active NF–κB

Clusters of NF-κB outputs (red; subsets of Figure 3-4), shown with their corresponding IKK inputs (blue; subsets of Figure 3-2).

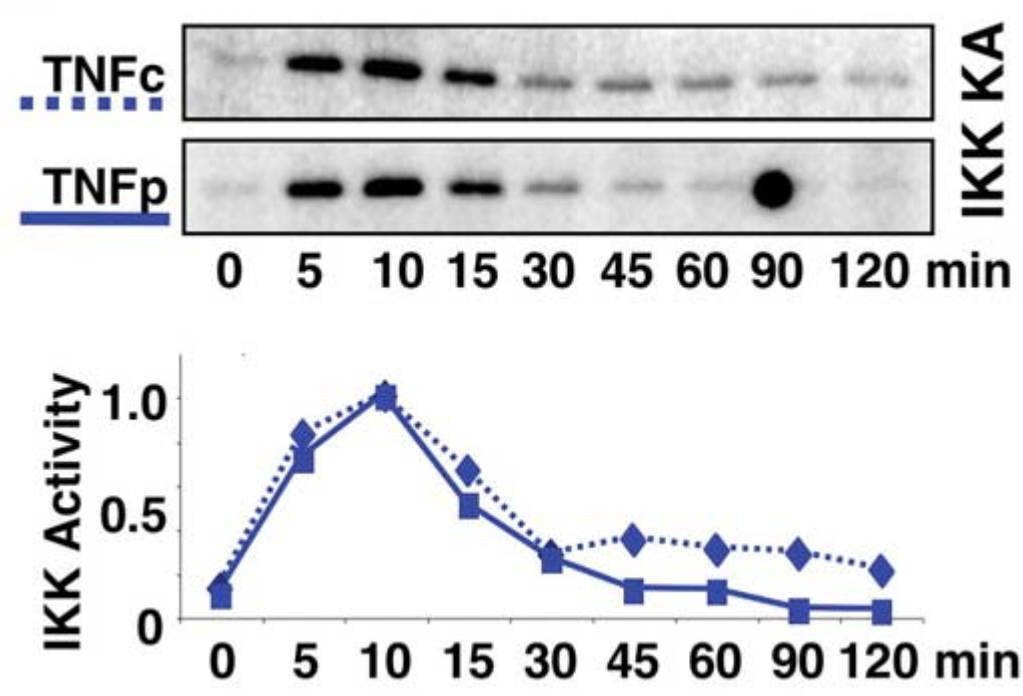

Figure 3-14 IKK Activity after TNF Stimulation

IKK activity was measured in mouse embryonic fibroblasts (MEFs) after chronic (TNFc) or 45-minute pulse (TNFp) TNF stimulation (1ng/ml) by IP-kinase assay (IKK KA). GST-IκBα(1-54) served as a substrate in the assay, and its phosphorylation of IKK was quantitated, normalized, and graphed. Work by colleague Shannon Werner.

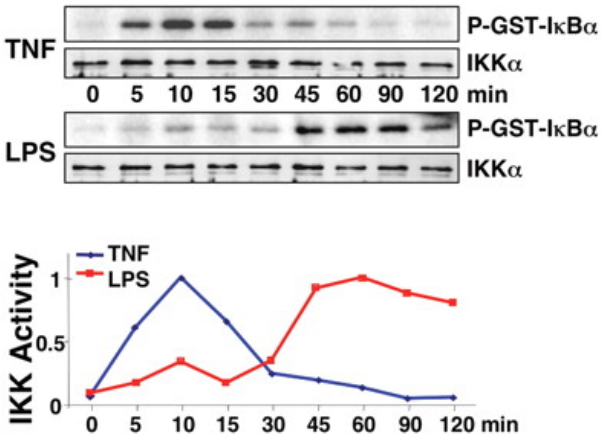

Figure 3-15 Measured IKK Profiles for TNF and LPS Pulses

IKK profiles were measured by IKK IP-kinase assay in MEFs stimulated with a 45-min pulse of either TNF (1 ng/ml) or LPS (0.1 μg/ml). Equal protein loading was confirmed with an immunoblot against IKKa. Quantitated and normalized results were graphed as shown. Work by colleague Shannon Werner.

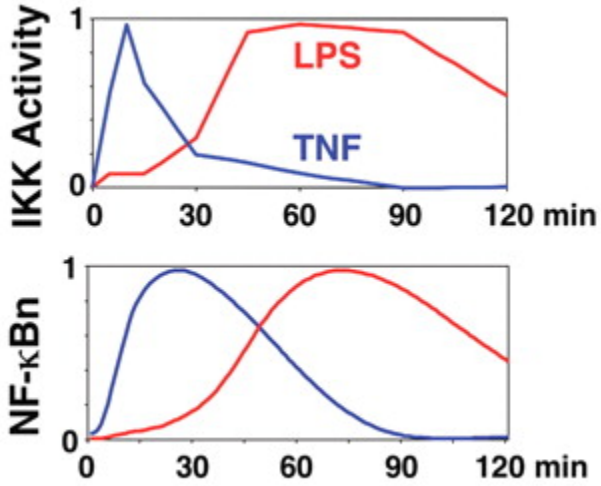

Figure 3-16 Simulated Response to Measured IKK Profiles

IKK profiles measured in Figure 3-15 were graphed on a linear time scale (top) and used as inputs in computational simulations to predict normalized NF-κB activity profiles (bottom) in response to TNF (blue) or LPS (red).

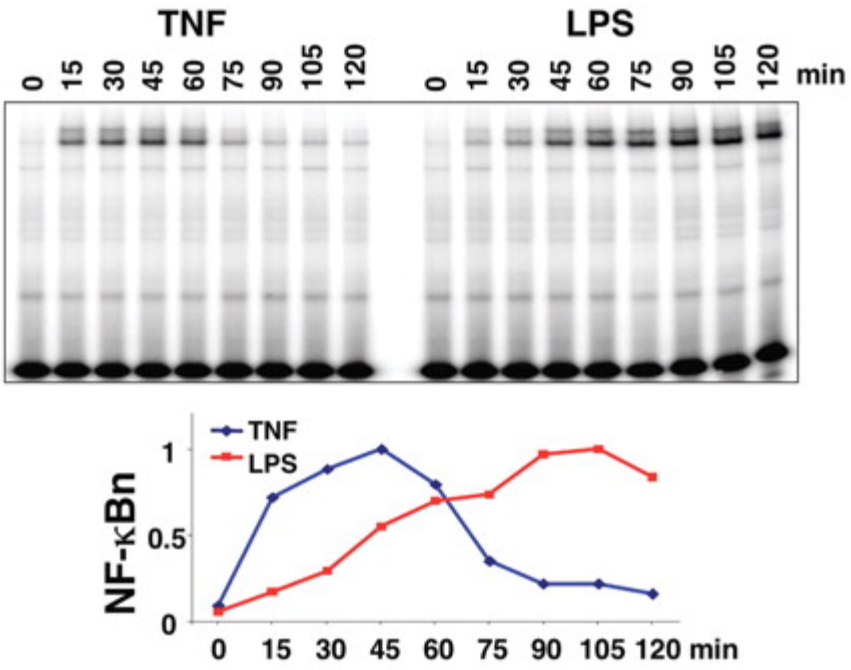

Figure 3-17 EMSAs of NF−κB profiles in Response to TNF/LPS Pulses

NF-κB activity profiles were measured by electrophoretic mobility shift assay (EMSA) in response to a 45-min pulse of TNF (1 ng/ml) or LPS (0.1 μg/ml). Results from the EMSA were normalized and graphed. Work by colleague Shannon Werner.

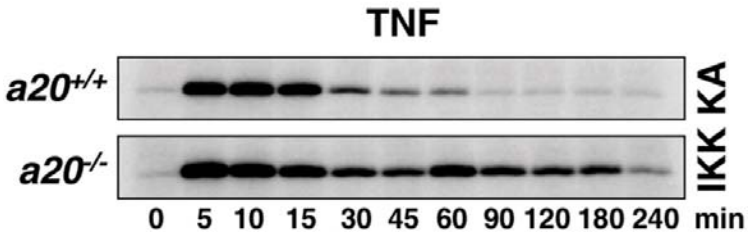

Figure 3-18 IKK Activity Profiles in A20$^{+/+}$, A20$^{-/-}$

IKK activity profiles were measured by IKK IP-kinase assays from A20$^{+/+}$ and A20$^{-/-}$ cells in response to 45-min pulse TNF stimulation over a 4 hour time course. Work by colleague Shannon Werner.

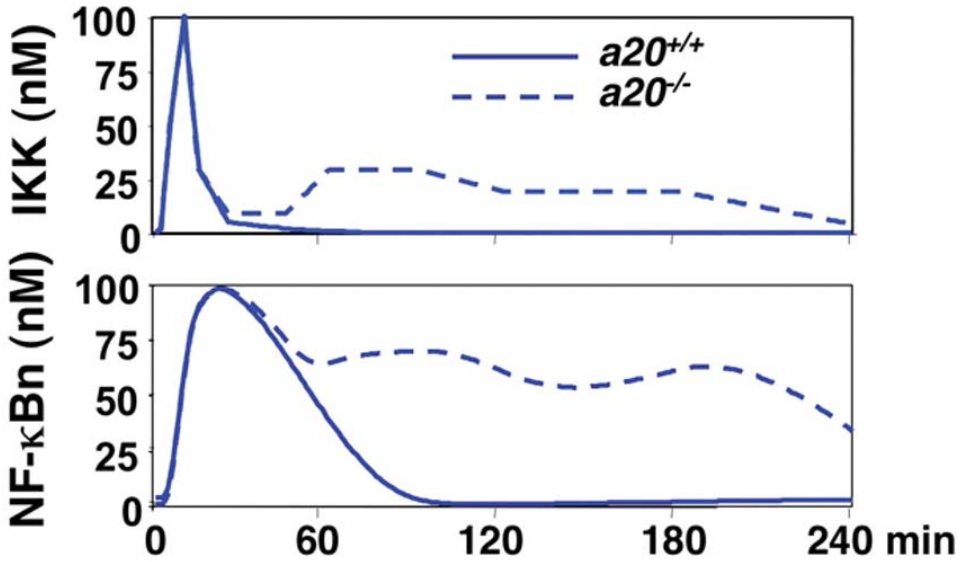

Figure 3-19 Simulations of A20$^{+/+}$, A20$^{-/-}$ Responses

Quantitated experimental IKK data (Figure 3-18) was used as an input for computational simulations that predict NF-κB activity profiles in A20$^{+/+}$ and A20$^{-/-}$ cells.

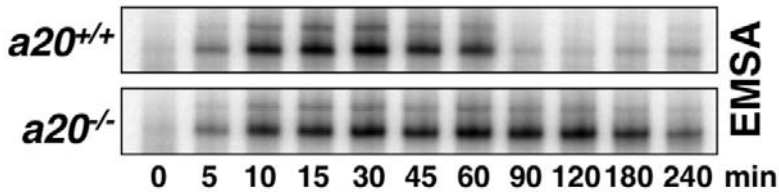

Figure 3-20 NF–κB Activity Profiles in A20$^{+/+}$, A20$^{-/-}$ cells

NF-κB activity profiles were measured by EMSA in response to 45-minute pulse TNF in A20$^{+/+}$ and A20$^{-/-}$ cells over a 4-hour time period. Work by colleague Shannon Werner.

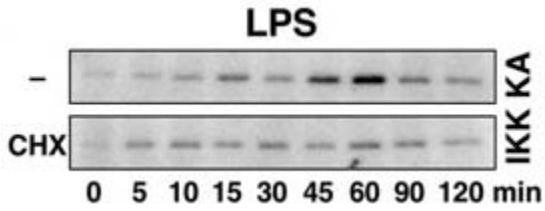

Figure 3-21 Effect of CHX on IKK Activity in Response to LPS Pulse

IKK activity was monitored by IP-kinase assay in MEFs stimulated with a 45-minute pulse of LPS in the presence or absence of 10 ug/ml cycloheximide (CHX). Work by colleague Shannon Werner.

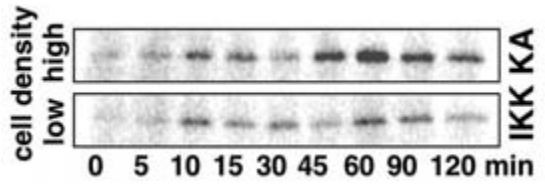

Figure 3-22 Effect of Cell Density on IKK Activity in Response to LPS Pulse

Cell density affects the IKK activity profile in response to LPS. IP-IKK activity assays were performed with extracts prepared from MEFs stimulated with LPS at low and high cell density. Work by coauthor Shannon Werner.

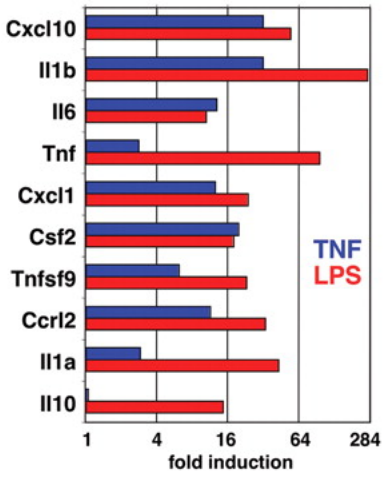

Figure 3-23 Microarray Expression Measurements in Response to TNF/LPS Pulses

Stimulus-induced increases in expression of cytokines and chemokines induced by a a factor of >10 over baseline in the firs hour of LPS stimulation. Results are extracted from microarray expression profiling in MEFs stimulated with a 45-min pulse of TNF or LPS. Work by colleague Shannon Werner.

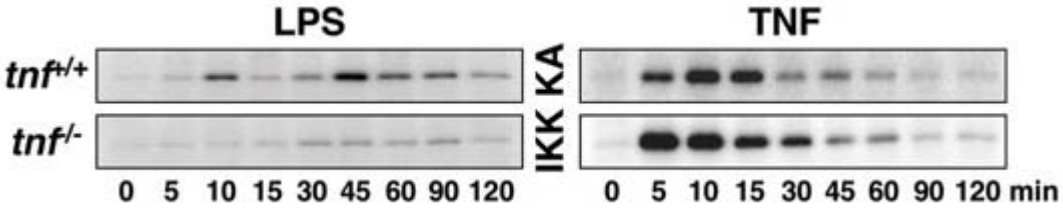

Figure 3-24 IKK Activity Profiles in WT and TNF Knockout Cells

Profiles measured by IP-kinase assay in response to a 45-minute pulse of TNF or LPS. Work of coauthor Shannon Werner.

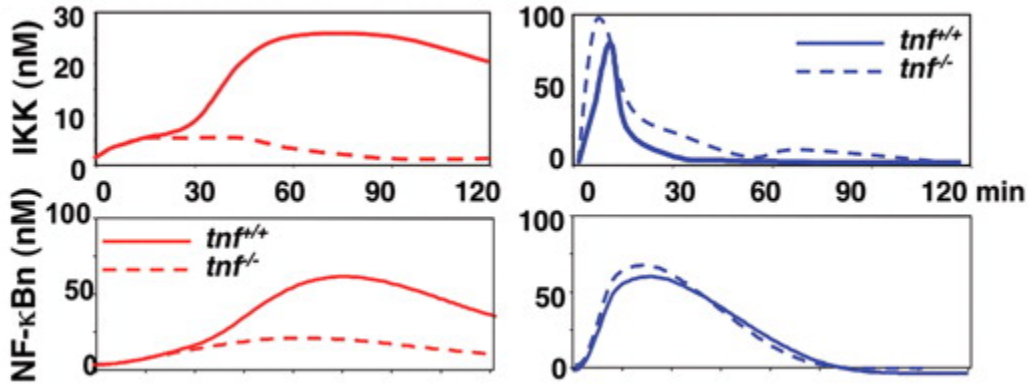

Figure 3-25 Computational Simulations of Responses in Wildtype, TNF Knockouts

Quantitated experimental IKK data were used as an input for computational simulations to predict NF-κB activity profiles in LPS-stimulated wild-type and TNF deficient MEFs.

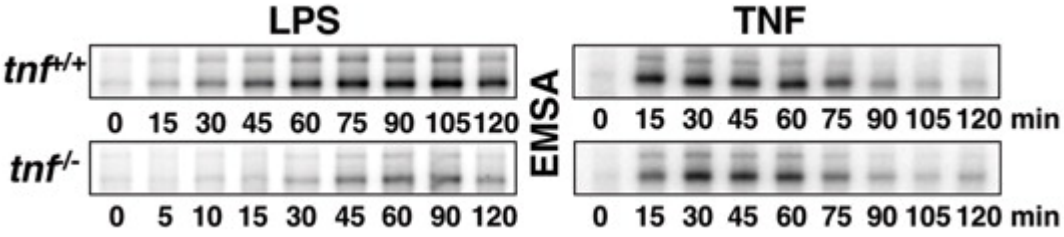

Figure 3-26 EMSA Measurements of Responses in Wildtype, TNF Knockouts

Nuclear NF-κB activity profiles were measured in response transient TNF or LPS stimulation of wild type or TNF deficient cells. Work of coauthor Shannon Werner.

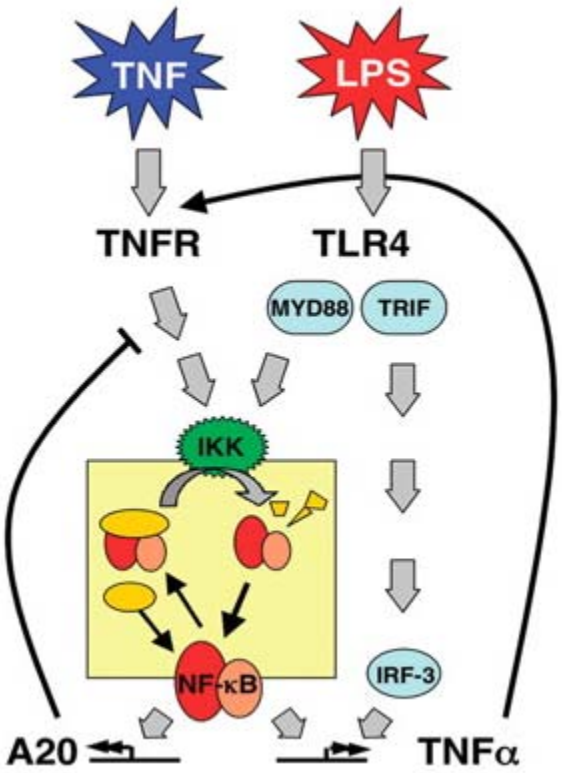

Figure 3-27 A Schematic of A20 and TNF Feedback

IKK activity is regulated by signaling pathway specific negative and positive feedback loops. The schematic shows the A20-mediated negative feedback loop in the TNFR signaling pathway and a positive feedback/feedforward loop in the LPS signaling pathway that is controlled by NF-κB and possibly IRF-3, resulting in the expression of TNF−α. Both feedback mechanisms allow for stimulus specific temporal profiles of IKK activity, which result in stimulus-specific NF-κB and gene expression patterns.

Chapter 4
Characterizing the temporal code of NF–κB Signaling

In previous chapter, I have introduced the thesis that different inflammatory stimuli induce distinct IKK profiles (timecourses), and suggested that temporal control of IKK can ultimately allow for selective gene activation. In this chapter, I characterize the effects of the temporal code of NF–κB signaling, in order expand on the latter suggestion.

This chapter contains two subsections. In the first, I address the question about the relative importance of amplitude modulation (the focus of previous chapters) compared to frequency modulation (i.e. oscillations). In the second section, I demonstrate the computational modeling, using an information metric approach which is original to this context, can successfully guide the design of mutants with altered temporal decoding and altered stimulus specific gene expression.

4.1 AM vs FM modulation

Oscillations and waves are extremely well studied across science and engineering (Semmlow 2005). They have also been productively studied in biological contexts(Edelstein-Keshet 1988; Goldbeter 1996), from the physiological (Fall, Marland et al. 2002) to the molecular (Field 1999). Naturally, with the observed oscillatory behavior (Hoffmann, Levchenko et al. 2002), many observers have been interested in understanding the importance and/or regulation of oscillations in the NF–κB signaling module.

In particular, one high profile recent publication (Nelson, Ihekwaba et al. 2004) studied the NF−κB signaling module by using fluorescent moieties fused to NF−κB and IκBα to follow signaling dynamics in vivo, on a single-cell basis, and in real time. As such, this work addressed itself to the question of whether population measurements such as EMSAs were masking significant cell-to-cell variations of biological significance. This work was a tour de force of experimental technique. However, the experimental work was combined with simulations to suggest that, to quote the title, "Oscillations in NF−κB Signaling Control the Dynamics of Gene Expression". In other words, this paper suggested that frequency modulation (rather than amplitude modulation) was key in understanding gene regulation.

In this section, I present my work which, to the contrary, suggests that amplitude modulation, rather than frequency modulation, is the key to explaining gene regulation by the NF−κB signaling module (Barken, Wang et al. 2005).

4.1.1 Studying oscillations – experimental considerations

To study the regulation of NF−κB activity in real time in single cells, Nelson at al. used ectopic expression of IκBα and NF−κB-p65 fused to fluorescent protein moieties. They transiently transfected HeLa (human cervical carcinoma) cells and SK-N-AS cells (human S-type neuroblastoma cells) with p65-DsRed (red fluorescent protein) and NF−κB-inducible IκBα-EGFP (enhanced green fluorescent protein) expression plasmids. Nelson et. al. estimate that NF−κB-p65 is overexpressed 3- to 5-fold in successfully transfected cells and suggest that this has a negligible effect on the

fundamental characteristics of NF−κB nuclear-cytoplasmic oscillations in response to stimulation by tumor necrosis factor alpha (TNF−α).

However, my modeling work, presented in section 4.1.2 below, strongly contradicts this assertion, and predicts that even 1.5- or 2-fold overexpression of either of the two components forming the negative feedback loop (NF−κB-p65 and IκBα, separately or in combination) can significantly alter the dynamics of NF−κB activity in response to TNF−α.

This suggests that caution is necessary in interpreting the dynamic recordings of cells genetically manipulated with GFP fusion proteins. Oscillations recorded in overexpressed feedback systems do not allow us to conclude that oscillations of the same persistence, amplitude, and period occur in normal, genetically unaltered cells. GFP experiments may be more conclusive when clonal cell lines are established in which individual cells are genetically identical and expression levels of the exogenous fusion proteins and functionally relevant endogenous signaling proteins can be quantitated to inform computational simulations.

4.1.2 Modeling overexpression of NF−κB, IκBα, or both

In order to simulate the effects of plasmid driven overexpression, I modified the Hoffmann-Levchenko model (Hoffmann, Levchenko et al. 2002), with the tr2 and tr2a parameters, accounting for the rates of constitutive and NF−κB induced transcription, increased by up to a factor of four, both individually (Figure 4-1, Figure 4-3) and in combination (Figure 4-2).

A number of differences are dramatically apparent in these simulations. First, oscillations are more persistent because the damping effects mediated by IκBβ and IκBε are diminished relative to the negative feedback effects mediated by both overexpressed NF−κB and inducible IκBα. This situation is analogous to the relative strengthening of the negative feedback by knocking out nonfeedback IκB isoforms. Second, the oscillation frequency may dramatically change, which suggests that cells with different degrees of overexpression may have oscillatory responses with drastically different periods. This suggests that as a result of inevitable cell-to-cell variations in the amount of plasmid DNA, transfected cells are likely to be much less synchronous in their NF−κB response than are untransfected cells.

4.1.3 Synchrony in cell population measurements

Using fluorescent moieties fused to NF−κB and IκBα allowed Nelson et al. to follow signaling dynamics in vivo, on a single-cell basis, and in real time. This is in contrast to EMSA (Electrophoretic Mobility Shift Assay) measurements, which are derived experimentally from a population of cells. Nelson et al. suggest that these populations are heterogeneous and unsynchronized, emphasizing the importance of single-cell measurements. The question of synchrony and cell variability has also been considered in other systems, such as p53/Mdm2 (Geva-Zatorsky, Rosenfeld et al. 2006).

In the NF−κB signaling system, an alternative way to experimentally address the response in single cells is to perform immunohistochemical analysis of individual, but genetically unmodified, cells (Figure 4-4). This approach does not allow tracking of

individual cells over time, but can reveal the variance of responses across the cell population at different time points. Variance in measured data may be the result of technical variation (error in measurement) or biological variation (e.g. due to asynchrony). If the responses of individual cells are asynchronous and show undamped oscillations (Figure 4-5), my simulations suggest that one would expect higher variance at late times than at early times and lower averages due to prolonged phases between peaks (Figure 4-6). However, immunohistochemical experimental evidence consistently shows that the variance of the responses is lower at late times than at early times and that averages remain high (Figure 4-7). Such a variance distribution is more consistent with a simulation in which the observed variance is derived from technical measurement errors that may be assumed to be proportional to the measured value itself (Figure 4-8). These data and simulations suggest that NF−κB activation in genetically unmodified fibroblasts is synchronous and highly damped.

4.2 Engineering temporal coding mutants

In this section, I turn to the question of whether simulations can guide the design of temporal coding mutants, testing the hypothesis that temporal control of NF-κB is critical for gene expression specificity. I use an information metric as a measure of diversity, an original approach in this context. Using this metric, I predict that a particular combination of mutations should lead to loss of stimulus specificity, a prediction that is confirmed by experiments.

4.2.1 Information metric

In section 3.1 of this thesis, I presented a procedure for generating a library of IKK profiles, which were used as inputs. By carrying out a set of simulations, I generated a library of NF–κB timecourses, which were the outputs. This procedure is illustrated in Figure 4-9. It would be helpful to be able to characterize the set of outputs with a single metric that summarized the diversity of the set at any given moment – intuitively, there is more diversity to at later times (to the right) in the bottom of Figure 4-9.

One obvious measure of diversity is root mean squared, or RMS, which is related to the variance of a set of numbers. However, for diversity, this turns out to be a poor choice, as illustrated in Figure 4-11. In that figure, in the rightmost column (two clusters), there is intuitively a low amount of diversity (only two clusters). The RMS value for these points would be high, while an entropy value would be low, illustrating why an entropy metric is a better choice. Thus, I use an information metric, a measure of entropy that is well established in physics and the theory of communication ((Shannon 1948; Shannon 1948; Cover and Thomas 1991; MacKay 2003)). In this formulation, for a set of discrete numbers, the information is given by the formula

$$H(X) = -\sum_{i=1}^{n} p_i log_2(p_i)$$

Using this information metric, I am able to graph diversity as a function of time in the set of responses of the wild-type system, as shown in Figure 4-11. The diversity has

an early rise and then continues to increase, approaching the maximum possible diversity for this set.

4.2.2 Applying an information metric to design a mutant

I next seek to apply my information metric to the design of a mutant cell in which the NF−κB system has lost its ability to generate diverse responses to different stimuli, and as a consequence produces undifferentiated gene expression patterns in the mutated cells compared to stimulus specific gene expression patterns in the wild type cell. A schematic illustrating this approach appears in figure Figure 4-12.

Revisiting the diversity metric for the wild type (as shown in Figure 4-11), I repeat the diversity calculation (using a set of IKK inputs as shown in Figure 4-9) for six additional systems: the single and double knockouts of IκBα, IκBβ, and IκBε. The resulting information metric plots are shown in Figure 4-13. Of the six mutant systems I examine, one system (the IκBα/IκBε double knockout) has significantly lower NF−κB signal diversity.

For this particular double knockout, using individual IKK timecourses measured in response to TNF and LPS pulses, I am able to examine the resulting NF−κB timecourses both computational (Figure 4-14, top, middle) and experimentally (Figure 4-14, bottom). The results indicate that there is a reduction in stimulus specific NF−κB diversity in the IκBα/IκBε double knockout as compared to the wildtype system. Furthermore, when my colleagues experimentally measure the expression patterns of NF−κB target genes (Figure 4-15), the results indicate that there is a dramatic loss of

stimulus specific gene expression patterns, inline with the predicted loss of stimulus specific diversity.

In this chapter I characterized the temporal code of NF−κB signaling using two approaches. First, I discussed the relative importance of amplitude versus frequency in understanding the effects of NF−κB timecourses on NF−κB target genes. Next, I used an information metric to guide the design of an NF−κB mutant with the predicted effects on the timecourses of NF−κB target genes. In the next chapter, I probe the temporal code, predicting the effects of a larger set of alterations, include ones that are experimentally testable via pharmacological rather than genetic alterations.

(This chapter, in part, is a reprint of material published as "Comment on 'Oscillations in NF-kappaB signaling control the dynamics of gene expression"' Barken D[*], Wang CJ[*], Kearns J, Cheong R, Hoffmann A, Levchenko A. Science 308(5718):52. The dissertation author is the primary investigator of all computational work and an author of the materials used from this paper.)

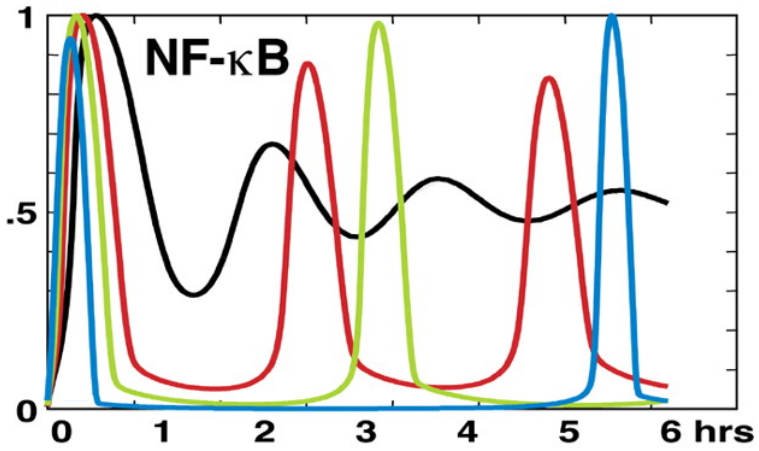

Figure 4-1 NF–κB Activation Profiles as a Function of Increased NF–κB Levels

Relative (peak normalized) nuclear NF-κB activity graphed as a function of time in response to TNF–α stimulation. Levels of NF-kB are normal (black) or increased 1.5-fold (red), 2 fold (green) or 4-fold (blue).

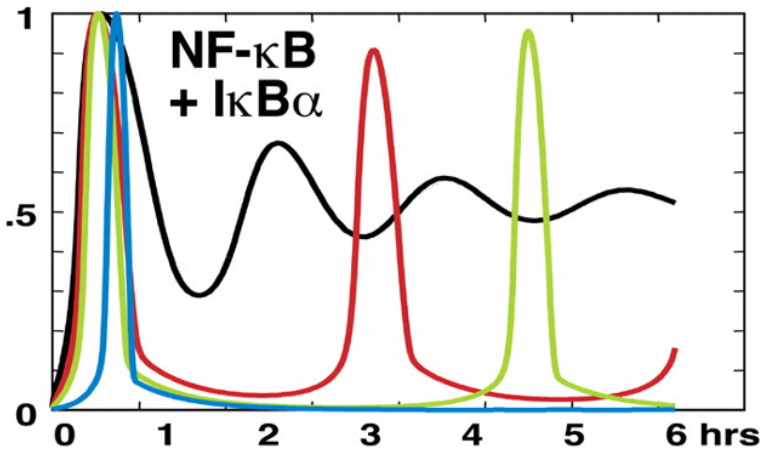

Figure 4-2 NF–κB Activation Profiles as a Function of Increased NF–κB and IκBα

Relative (peak normalized) nuclear NF-κB activity graphed as a function of time in response to TNF–α stimulation. Levels of NF-κB and IκBα transcription are normal (black) or increased 1.5-fold (red), 2 fold (green) or 4-fold (blue).

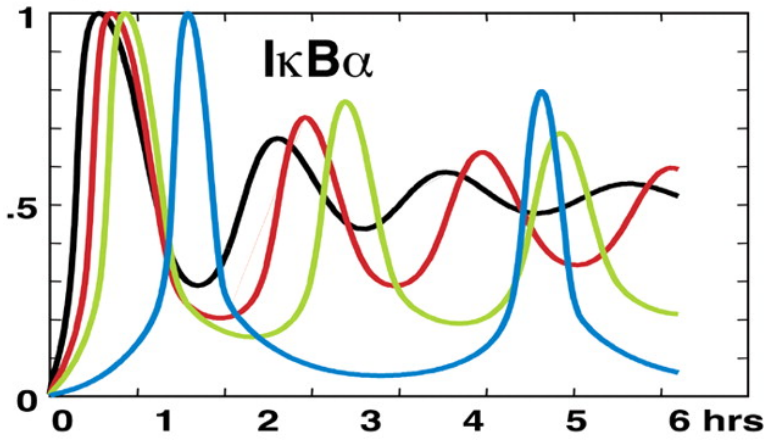

Figure 4-3 NF–κB Activation Profiles as a Function of Increased IκBα

Relative (peak normalized) nuclear NF-κB activity graphed as a function of time in response to TNF–α stimulation. IκBα transcription rates are normal (black) or increased 1.5-fold (red), 2 fold (green) or 4-fold (blue).

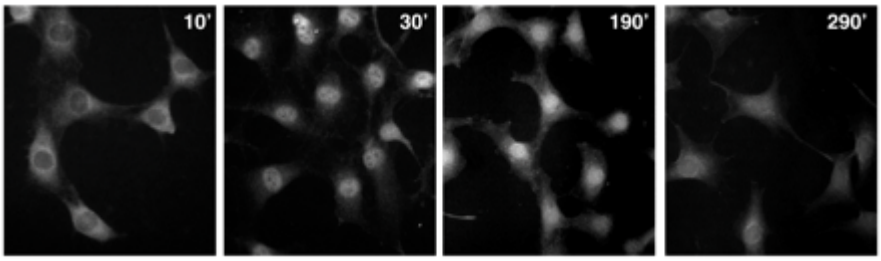

Figure 4-4 NF–κB Activation In Single Cells - Images

Immunohistochemistry for endogenous NF-κB in NIH 3T3 cells (mouse fibroblasts) stimulated with TNF–α. Cells were fixed and stained at 10 min, 30 min, 190 min, and 290 min after administration of TNF–α and stained with an antibody to p65. Work of Andre Levchenko.

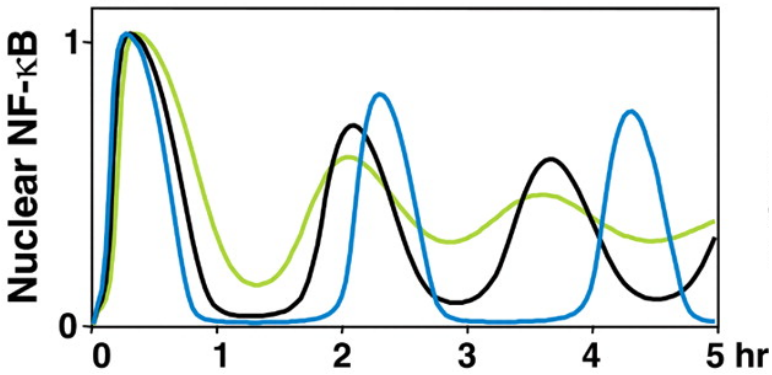

Figure 4-5 Simulations of Varying NF–κB Levels in IκBβ/IκBε Knockout Cells

Computational simulations of oscillatory NF-κB in IκBβ/IκBε deficient cells that contain NF-κB protein levels that are wild type (black), 1.2x (blue) or 0.8x (green)

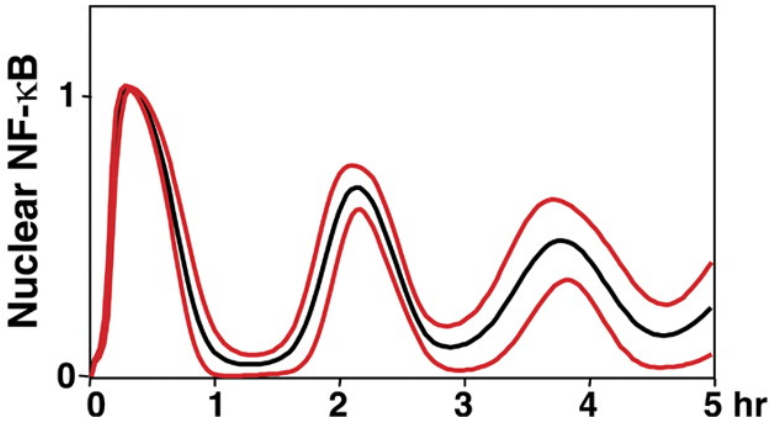

Figure 4-6 Simulation Conditions Leading to Higher Variance at Later Times

The mean NF-κB activity (black line) produced by computational simulations of IκBβ/IκBε deficient cells containing a distribution of NF-κB protein levels with a standard deviation of 10%. Red lines indicate the mean +/- 1 SD

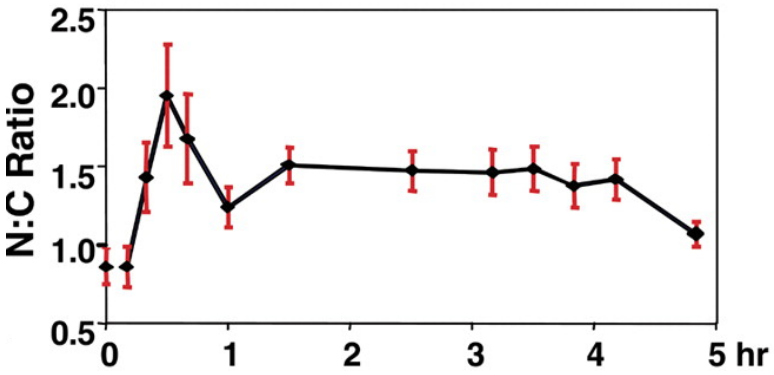

Figure 4-7 NF–κB Activation In Single Cells - Quantitation

NF-κB localization data derived from immunohistological analysis graphed as nucleus:cytoplasm (N:C) ratio as a function of time in response to TNF–α stimulation. Vertical bars indicate the standard deviation in the data for each time point. Work of Andre Levchenko.

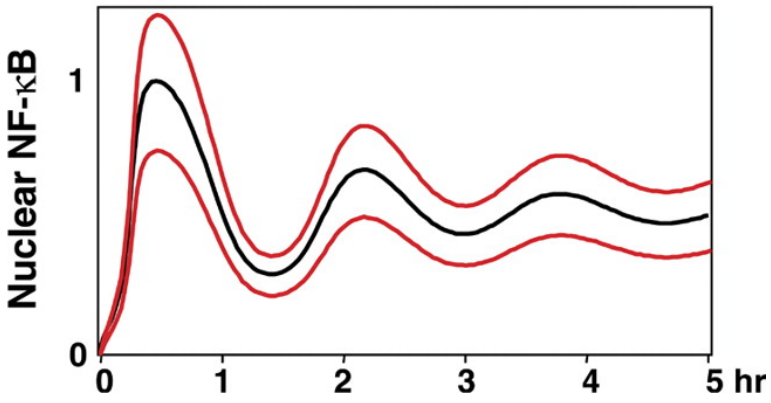

Figure 4-8 Simulation Conditions Leading to Higher Variance at Earlier Times

Computational simulation of NF-κB activity in wild-type cells in response to TNF–α stimulation. Red lines indicate 1.2x and 0.8x NF-κB activity.

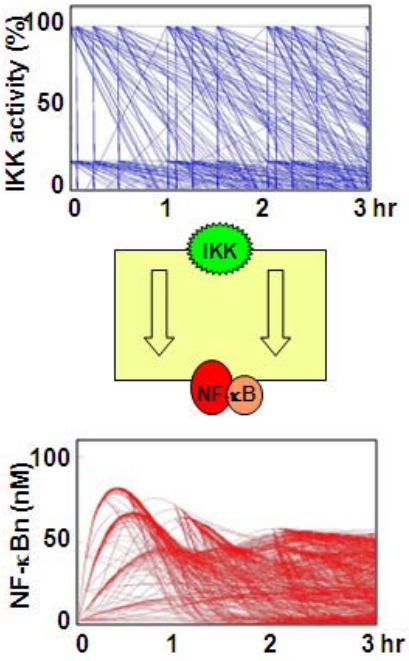

Figure 4-9 Illustration of Diverse Inputs and Outputs in the Wildtype System

Top: set of IKK timecourses, generated as explained in section 3.1. Bottom: diverse set of corresponding calculated NF-κB timecourses.

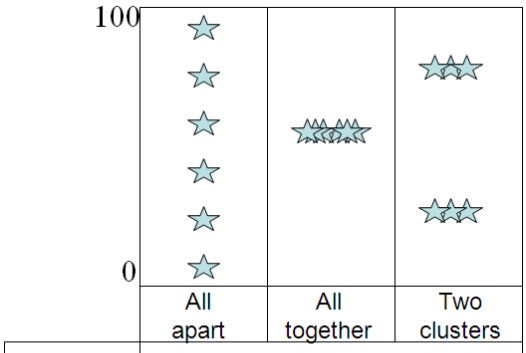

Figure 4-10 Comparison of RMS and Entropy/Information as Measure of Diversity

When a set of values are well separated (left), both root mean squared and entropy are high. When the values are very close (middle), both RMS and entropy are low. When the values are grouped into a small number of clusters (intuitively having low diversity), RMS is high but entropy is low, illustrating why entropy is a preferable as a metric for diversity.

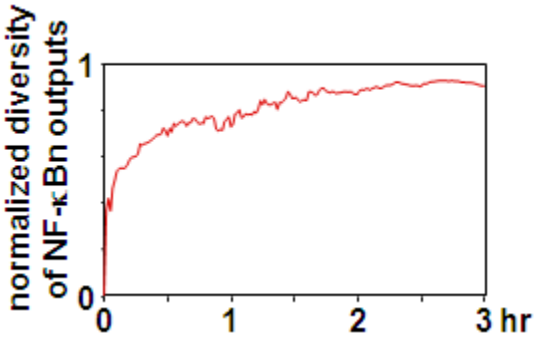

Figure 4-11 Measure of Diversity of Simulated NF–κB Profiles over Time

Calculated information/entropy in a set of 687 simulated NF-κB timecourses at one minute intervals. Values were grouped into 1 nM "buckets" (n=100) in order to use the Shannon's discrete formula for information. Values are normalized to the maximum possible entropy for 687 values in 100 buckets (uniform distribution).

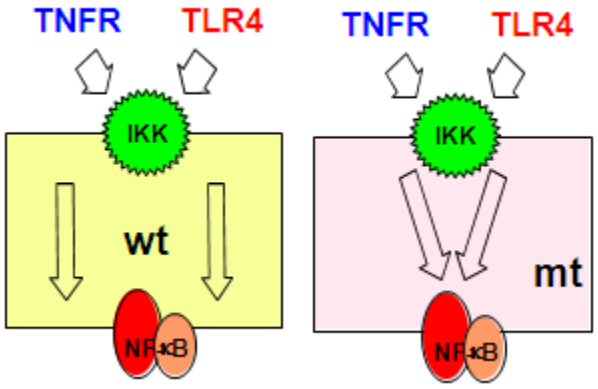

Figure 4-12 Strategy for Experimental Validation of Loss of Signaling Diversity

In the wild type, diverse inputs lead to diverse outputs. Simulations can predict which mutations lead to a loss of response diversity the NF-κB signaling system. These predictions are then testable experimentally.

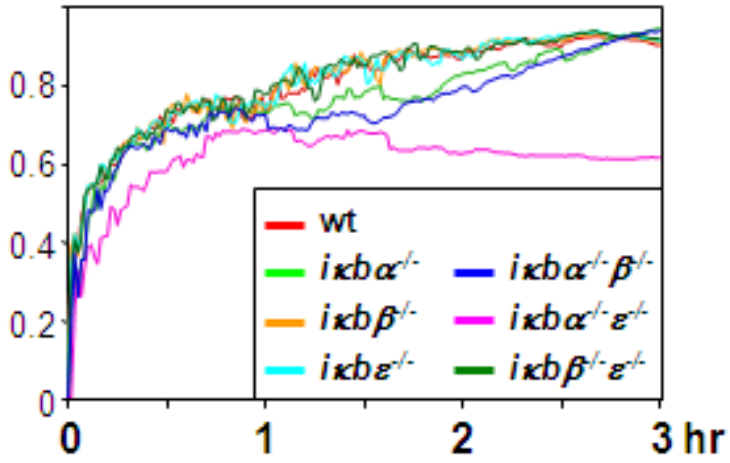

Figure 4-13 Diversity of Simulated NF–κB Profiles in Wildtype and Mutants

For wildtype , and IκB single and double knockouts, an information metric was calculated over time as described in Figure 4-11. The IκBα/IκBε double knockout showed significantly reduced diversity.

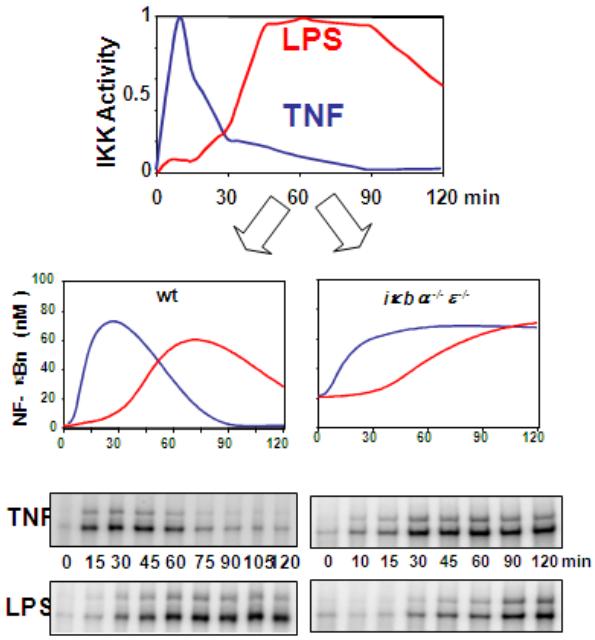

Figure 4-14 TNF/LPS NF–κB Response Similarity in Knockout System

TNF and LPS pulse timecourses from IKK kinase assay measurements (top) were simulated in both wildtype (middle, left) and IκBα/IκBε knockout (middle, right) systems. The knockout system had reduced diversity in the resulting NF-κB profiles, a prediction confirmed by EMSA measurements (bottom). Experimental work by colleague Shannon Werner.

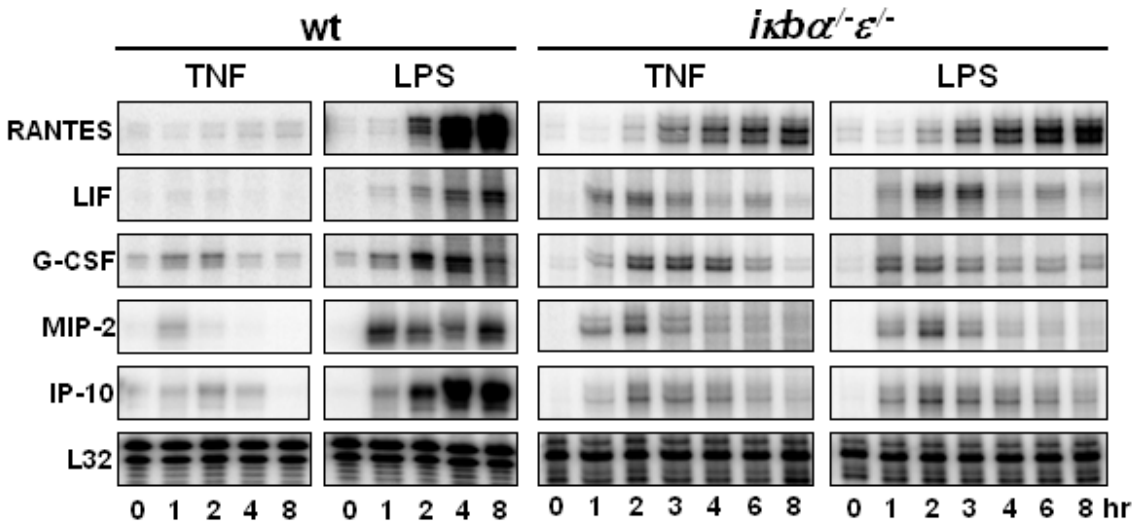

Figure 4-15 TNF/LPS NF–κB Target Gene Expression Similarity in K.O. System

RNAse protection assay (RPA) analysis of indicated NF-kB target genes induced by TNF and LPS stimulation in wild type and IκBα/IκBε knockout cells. Work by colleague Shannon Werner.

Chapter 5
Probing the temporal code of NF−κB signaling

In this chapter I extend my investigation into dynamic coding of NF−κB activity. To manipulate the temporal code that produces gene expression specificity, I use a number of computational approaches to identify biochemical mechanisms within the common NF−κB signaling module that are essential for the transduction of one but not another inflammatory signal. By perturbing the parameter space with pharmacological agents, I am able to predict stimulus specific alterations that are experimentally supported, and show that drugs targeting common mechanisms within the NF−κB signaling module can indeed have stimulus specific effects on gene expression. My results suggest that a biochemical understanding of stimulus specific dynamic coding mechanisms within cellular signaling modules may prove valuable in the evaluation and targeting of pharmacological agents.

5.1 Identifying important biochemical mechanisms

In this section, I computationally explore the mechanisms that give rise to stimulus specific gene expression within the NF−κB signaling system. This work is motivated by the possibility of finding strategies that allow for the modulation of NF−κB-dependent gene expression in response to one NF−κB inducing stimulus, but not another.

5.1.1 Parameter groupings – exploring system behavior via clustering

My initial set is to group the 73 model parameters into 25 biochemical groupings, as shown in Figure 5-1 and Table 5-1. In the following set of simulations, the parameters in each of the 25 biochemical groupings were simultaneously altered on a logarithmic scale by factors of 100, 10, 1 (wt), 0.1 and 0.01. For each of the 25 groups of parameters, under each alteration condition, I stimulated NF–κB activation in response to three stimulation regimes (TNF-chronic, TNF-pulse, and LPS-pulse).

To identify which features of the temporal profile can be manipulated, I cluster the resulting 101 curves (25 parameter groupings times 4 factors + 1 wildtype) for each stimulus into groups of similar profiles. The resulting clusters are shown in Figure 5-2 (TNFc), Figure 5-3 (TNFp), and Figure 5-4 (LPSp).

For each stimulus, I identify one cluster of profiles that is close to wild type (A). Other clusters contain profiles that are generally depressed or elevated (E,F, respectively). In addition, I found clusters that contain shortened (C) or extended (D) activation profiles, as well as a large group (B) of mildly depressed or delayed profiles that are less oscillatory (for TNF-chronic stimulation in particular). This analysis reveals that particular features or stimulus specific NF–κB activity are modulated specifically by controlling particular biochemical mechanisms. It does not, however, give insight into which parameters do or do not control which responses.

5.1.2 Identifying stimulus-specific parameter sensitivities by PCA

To identify which biochemical rate constants play critical roles in the dynamic control of NF–κB and whether any may have stimulus specific effects, I decompose the

entire set of curves by principal component analysis. The curves are generated by the same procedure discussed previously, except that I use twice the number of parameter alterations on the same logarithmic scale (in other words, my multipliers are 10^{-2}, $10^{-1.5}$, 10^{-1}, $10^{-0.5}$, 10^{0} (wt), $10^{0.5}$, $10^{1.0}$, $10^{1.5}$, 10^{2}). By using two components / dimensions, I capture 92.4% of the variance in the data, as shown in Figure 5-5. This allows me to represent each curve as a single point on a two dimensional plot.

The resulting PCA values are plotted in Figure 5-7. Each of the 25 boxes represents a different group of parameters. Within each box, each point represents a timecourse – the corresponding / underlying timecourses can be seen in . Within each box of Figure 5-7, there are three lines, representing TNFc, TNFp, and LPSp, as explained in the caption. Within each line, the central, black dot represents the wild type curve. There are four connected dots in each direction, corresponding to the simulations run using the multipliers enumerated above.

Thus, by using PCA, I am able to simultaneously visualize the effects of all 600 simulations. In particular, in Figure 5-7, linking the points denoting related curves allows me to determine the relative sensitivity of each parameter for the dynamic signal transduction of each of the three stimuli. The following are some of the conclusions I can draw from this representation.

5.1.3 Results: important rate constants

All but three (b2, b12, b13) of the 25 biochemical groupings play important roles in the signal processing characteristics of the signaling module, and seven (b1, b10, b11, b14, b15, b18, b24) show great sensitivity when the relevant parameters are increased or

decreased.. Interestingly, I find that the well-studied dissociation rate of the IκB-NF−κB complex (Malek, Huxford et al. 1998) is not nearly as sensitive as the corresponding association rate (b2 vs b1). Similarly, the nuclear import of IκB is revealed as a critical parameter, whereas the converse export rate is not (b10 vs b9). Intriguingly, while IKK catalyzed degradation of NF−κB bound IκB (b14) is critically important for signaling, the IKK independent degradation of free IκB (b11) plays a much more important role than the analogous degradation of NF−κB bound IκB (b12). The IKK-dependent degradation pathway of NF−κB bound IκB is well understood (Karin and Ben-Neriah 2000), while the mechanism of free IκB degradation (Pando and Verma 2000) deserves further study, as discussed in section 2.2.

5.1.4 Results: stimulus specific rate constants

By comparing the relative sensitivities of a particular parameter in the signal transduction of the three model stimuli, I am able to identify biochemical mechanisms that are predicted to be rate limiting for signaling in response to one stimulus but not another. The computational analysis suggests that the NF−κB responsive IκBε transcription rate (b25), for example, plays a greater role in regulating TNFc signaling than TNF and LPSp, as it primarily affects late NF−κB activity via a negative feedback mechanism. Conversely, increased IκB-NF−κB association (b1) affects LPS signaling to a greater degree than TNF signaling. Interestingly, decreases in the IKK-independent free IκB degradation rate (b11) is detrimental to LPS signaling and early TNF responses, but does still allow for late phase activity characteristic of TNFc stimulation. Post-

induction attenuation of NF−κB responses is controlled by a variety of parameters, including the half-life of IκBα mRNA (b18) or its translation (b15), and is particularly important for the faithful transmission of transient cytokine signals as opposed to pathogen-triggered TLR signaling.

5.2 Towards rational drug targeting

In the previous section, I carried out a comprehensive set of simulations to simulate altered signaling in-silico. In this section, I focus on a smaller set of simulations which are designed to be experimentally testable. As experimental work by my collaborator Shannon Werner confirmed, these simulations correctly model stimulus specific pharmacological modifications to the NF−κB system via alteration of the temporal code.

5.2.1 Modeling the effects of drugs

The drugs I and my collaborators use to model and test are detailed in Table 5-3. Briefly, CHX inhibits translation, LMB inhibits nuclear export, MG132 inhibits protein degradation, PDTC inhibits NF-κB binding to DNA, and TSA, which usually promotes transcription, inhibits transcription in this system (Adam, Quivy et al. 2003). As each drug affects multiple biochemical mechanisms described in the model, I classify the parameters into pharmacological groupings (Table 5-1). Computationally, I simulate the effect of each drug on TNFc, TNFp, and LPSp signaling by varying both the dose and time of administration. The dose is simulated by varying the multiplier by which the parameters are altered – for inhibitors, I use a logarithmic scale in which the parameters listed in Table 5-1 were multiplied by 10^{-2}, $10^{-1.5}$, 10^{-1}, $10^{-0.5}$, or 10^{0}=1 (wt). The timing

can be simulated by applying the changes to the parameters before, simultaneously to, or after the change in the IKK signal (time zero) in the simulations. In this case, I simulate pre-treatment as 60 minutes prior to the introduction of the IKK signal, and post-treatment as treatment 60 minutes after the introduction of the IKK signal.

For modeling the effects of pharmacological inhibitors on the response to LPS stimulation, a simplified model of TNF feedback was used. One additional metabolite (TNF) and two additional reactions (TNF synthesis and degradation) were introduced (with rate constants of 0.4 min^{-1} and 0.3 min^{-1}, respectively). TNF synthesis was modeled as NF-κB dependent with a hill coefficient of 1. The external IKK profile used was that measured in response to LPS stimulation in TNF knockout cells, as previously published in (Werner, Barken et al. 2005). The total IKK profile including the TNF feedback component resembles the IKK activity profile measured in wildtype cells.

5.2.2 Simulation Results

From a large dataset, I am able to identify treatment conditions that were predicted to result in stimulus-specific effects (Figure 5-10). Interestingly, the proteasome inhibitor MG132 is predicted to inhibit late phase TNFc and LPSp-induced NF-κB activity but to have little effect on early responses. Whereas TNFc-induced late phase NF-κB activity is preferentially inhibited by the nuclear export inhibitor leptomycin B (LMB) (Tam, Lee et al. 2000), postinduction attenuation of nuclear NF-κB - a hallmark of transient TNFp stimulation – is predicted to be impaired by treatment with the HDAC inhibitor trichostatin A (TSA) (Adam, Quivy et al. 2003). In addition, specific effects were found

to be dependent on the dose and timing of drug administration. For example, low doses of the antioxidant pyrrolidine dithiocarbamate (PDTC) (Brennan and O'Neill 1996) were predicted to preferentially inhibit LPS-induced NF-κB activity as well as post-induction repression following TNFp stimulation, whereas high doses would be inhibitory to all stimuli. Similarly, administration of the ribosome inhibitor cycloheximide (CHX) with the onset of inflammatory stimulation would have severe effects on post-induction attenuation during TNF signaling, but extensive pretreatment with CHX would block all signaling dynamics because of severely elevated constitutive NF-κB activity.

With the experimental work of my colleagues (Figure 5-11), I am interested in addressing predictions of stimulus-specific inhibition. As the available pharmacological agents have very broad cellular effects, such specificity would indeed be surprising. While high doses of proteasome inhibitor generally abrogate NF-κB signaling (and are toxic to cells), we find that an intermediate dose of MG132 attenuated late phase NF-κB activity while early activity remained intact, as predicted. As predicted, TSA inhibited postinduction repression of NF-κB in response to TNFp although NF-κB activation in response to TNFc and LPS remained intact. Similarly, low doses (0.01 mM) of the antioxidant PDTC impaired postinduction repression of both nuclear NF-κB activity and MIP-2 expression in response to transient TNF stimulation; however, high doses (1 mM) blocked NF-κB activation and target gene expression for all stimuli by inhibiting mechanisms that allow for IKK activation. Similarly, co-treatment with CHX inhibited attenuation of NF-κB in response to transient TNF treatment, whereas a CHX pretreatment regimen led to elevated basal NF-κB activity that impaired the stimulus-

responsive NF-κB in response to all stimuli. Although the available drugs are highly pleiotropic, computational simulations helped identify pharmacological treatment conditions that resulted in modulation of NF-κB activation in response to one inflammatory stimulus, and not another.

In this chapter, I have presented evidence suggesting that mammalian tissue cells are capable of distinct stimulus specific gene expression programs, and that stimulus specific dynamic amplitude modulation of NF−κB, a ubiquitiuos and functionally pleiotropic transcription factor, specifies a temporal code that plays a critical role in stimulus-specific gene expression. I identified biochemical mechanisms that are required for the generation of specific features of the dynamic NF−κB activation profile, and that are rate-limiting for the signal transduction of one stimulus but not another. Even with a limited pharmacological tool set, I was able to identify conditions in which modulation of the dynamic control of signaling resulted in stimulus specific alteration of NF−κB activity and target gene expression. The present study suggests that future pharmacological agents that are more specific to the NF−κB signaling module may be evaluated in conjunction with mathematical modeling to alter temporal coding of NF−κB signaling, and thereby achieve specific inhibition of stimulus specific gene expression programs.

Table 5-1 Parameter Groupings - Biochemical, Pharmacological, and Genetic

		groupings			
Code	Description	biochem.	Pharm.	genetic	Reaction
a_c_an; a_n_an; a_c_2ain	Association IkB-NFkB	1			IkBan + NFkBn => NFkBnIkBa
d_c_an; d_n_an; d_c_2ain	Dissociation IkB-NFkB	2			IkBaNFkB => IkBa + NFkB
a_c_ai; a_c_2ani *	Association IKK-IkB	3			IkBa + IKK => IkBaIKK
d_c_ai; d_c_2ani *	Dissociation IKK-IkB	4			IkBaIKK => IkBa + IKK
ex_n	Export NFkB	5	LMB		NFkBn => NFkB
in_n	Import NFkB	6			NFkB => NFkBn
ex_2an *	Export IkB-NFkB	7	LMB		NFkBnIkBa => NFkBIkBa
in_2an *	Import IkB-NFkB	8			NFkBIkBa => NFkBnIkBa
ex_a *	Export IkB	9	LMB		IkBan => IkBa
in_a *	Import IkB	10			IkBa => IkBan
pd_c_a; pd_n_a *	Degradation IkB	11	MG132		IkBa =>
pd_c_2an; pd_n_2an *	Degradation IkB-NFkB	12	MG132		NFkBIkBa => NFkB
pd_c_2ai *	Degradation IKK-IkB	13	MG132		IkBaIKK => IKK
pd_c_3ain *	Deg. IKK-NFkB-IkB	14	MG132		NFkBIkBaIKK => NFkB + IKK
ps_c_a	IkB Protein synthesis	15	CHX		IkBat => IkBat + IkBa
ps_c_b		16	CHX		IkBbt => IkBbt + IkBb
ps_c_e		17	CHX		IkBet => IkBet + IkBe
rd_a	IkB RNA degradation	18			IkBat =>
rd_b		19			IkBbt =>
rd_e		20			IkBet =>
rsu_a	IkB RNA synthesis	21	TSA	ikba-/-	=> IkBat
rsu_b		22	TSA	ikbb-/-	=> IkBbt
rsu_e		23	TSA	ikbe-/-	=> IkBet
rsr_an	NF-kB responsive RNA synthesis	24	PDTC	ikba-/-	NFkB => IkBat +NF-kB
rsr_en		25	PDTC	ikbe-/-	NFkB => IkBet +NF-kB

Table 5-2 IKK Timecourses for Stimulus Specific Simulations

Min	TNFc	TNFp	LPS
0	1	1	1
5	59.38	59.38	2.45
10	100	100	6.95
15	64.57	64.57	2.44
20	50.15	50.15	4.05
25	35.73	35.73	5.66
30	30	21.3	7.27
35	30	19.66	12.43
40	30	18.03	17.59
45	30	16.39	22.74
50	30	14.16	23.50
55	30	11.93	24.25
60	30	9.7	25
65	30	8.25	24.46
70	30	6.8	23.91
75	30	5.35	23.37
80	30	3.9	22.82
85	30	2.45	22.28
90	30	1	21.74
95	30	1	21.38
100	30	1	21.03
105	30	1	20.68
110	30	1	20.33
115	30	1	19.98
120	30	1	19.62
125	30	1	19.62
130	30	1	19.62
135	30	1	19.62
140	30	1	19.62
145	30	1	19.62
150	30	1	19.62
155	30	1	19.62
160	30	1	19.62
165	30	1	19.62
170	30	1	19.62
175	30	1	19.62
180	30	1	19.62

Table 5-3 Pharmaceutical Abbreviations, Names, and Actions

Abb.	Name	Action
CHX	Cycloheximide	Inhibits translation
LMB	Leptomycin B	Inhibits nuclear export
MG132	Carbobenzoxy-L-leucyl-L-leucyl-L-leucinal	Inhibits protein degradation
PDTC	Pyrrolidine dithiocarbamate	Inhibits regulated transcription (NF–κB binding to DNA) (Malek, Chen et al. 2001)
TSA	Trichostatin A	Inhibits transcription (Histone Deacetylase inhibitor) (Adam, Quivy et al. 2003)

Table 5-4 Details of Treatments with Stimulus Specific Effects

	Drug	Dosage	Timing
1	MG132	x 0.65	Pre-treat
2	LMB	x 0.1	Post-treat
3	PDTC (low dose)	x 0.1	Co-treat
4	TSA	x 0.1	Co-treat
5	CHX	x 0.1	Co-treat
6	CHX	x 0.1	Pre-treat
7	PDTC (high dose)	X 0.01	Co-treat

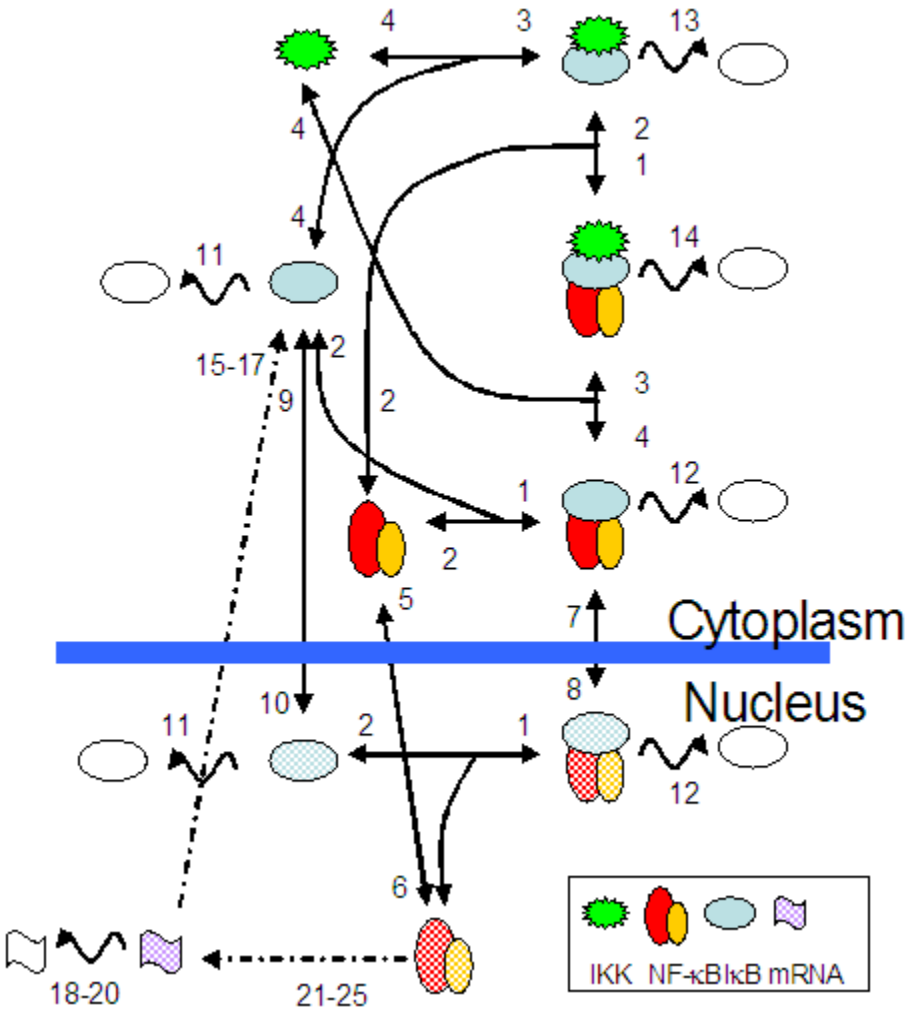

Figure 5-1 Illustration of Biochemical Groupings

Model parameters (and associated reactions) are grouped as shown. Group numbers correspond to entries in Table 5-1 Parameter Groupings - Biochemical, Pharmacological, and Genetic

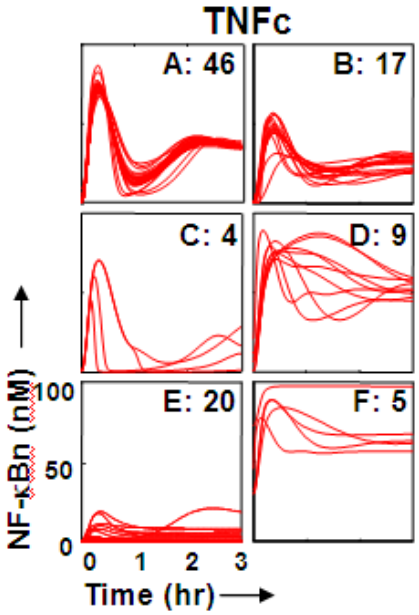

Figure 5-2 Clustering of NF–κB Profiles Resulting from TNF-chronic Input
NF-κB timecourses generated from 101 systems with parameters grouped and altered as explained in the text. Numbers indicate number of cluster members.

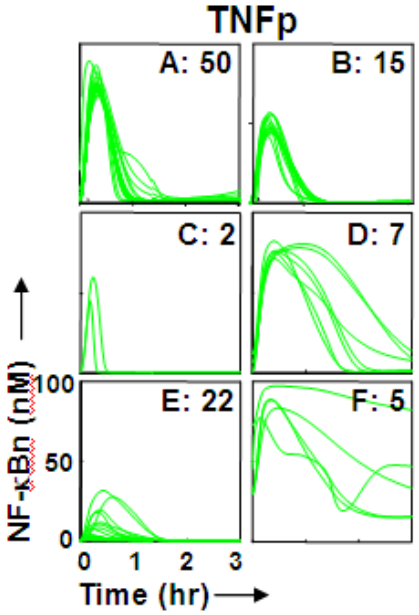

Figure 5-3 Clustering of NF–κB Profiles Resulting from TNF-pulse Input
NF-κB timecourses generated from 101 systems with parameters grouped and altered as explained in the text. Numbers indicate number of cluster members.

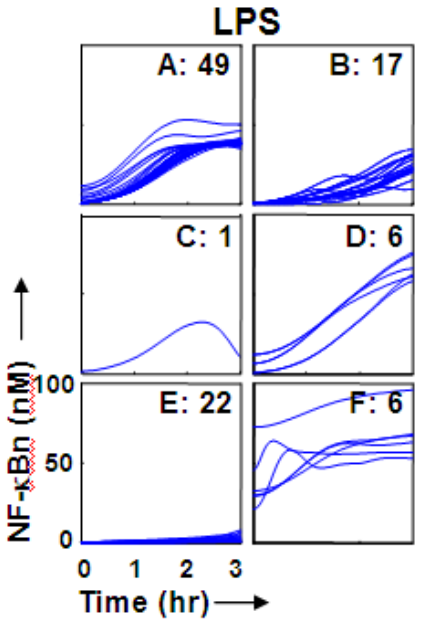

Figure 5-4 Clustering of NF–κB Profiles Resulting from LPS-pulse Input

NF-κB timecourses generated from 101 systems with parameters grouped and altered as explained in the text. Numbers indicate number of cluster members.

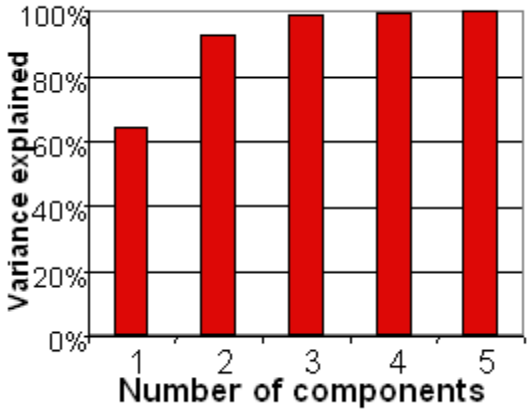

Figure 5-5 Variance Explained as a Function of Number of Principal Components

Variance explained by first five components of PCA calculation on 603 NF-κB timecourses.

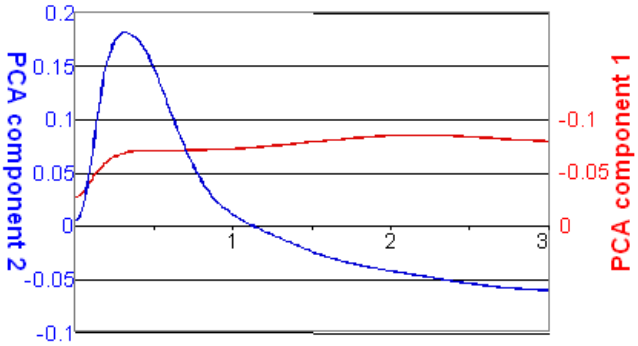

Figure 5-6 Weights for First Two PCA Components

Weights of first two components from PCA calculation on 603 NF-κB three hour timecourses. Red: PCA component 1; Blue: PCA component 2.

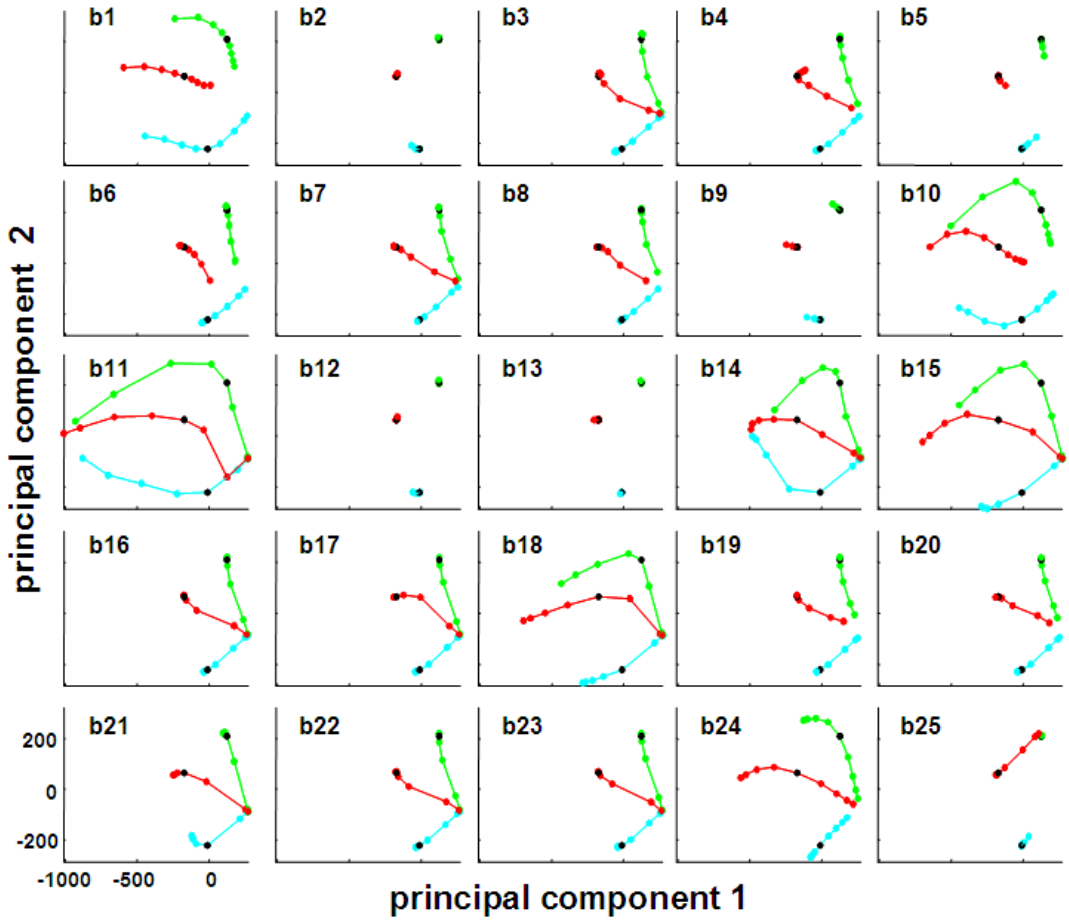

Figure 5-7 PCA for Biochemical Mechanisms With Stimulus Specific Effects

Plotted values for first two components resulting from PCA analysis. Groupings b1-b25: see Table 5-1. Red: TNFc. Green: TNFp. Blue: LPSp. Black: wild type.

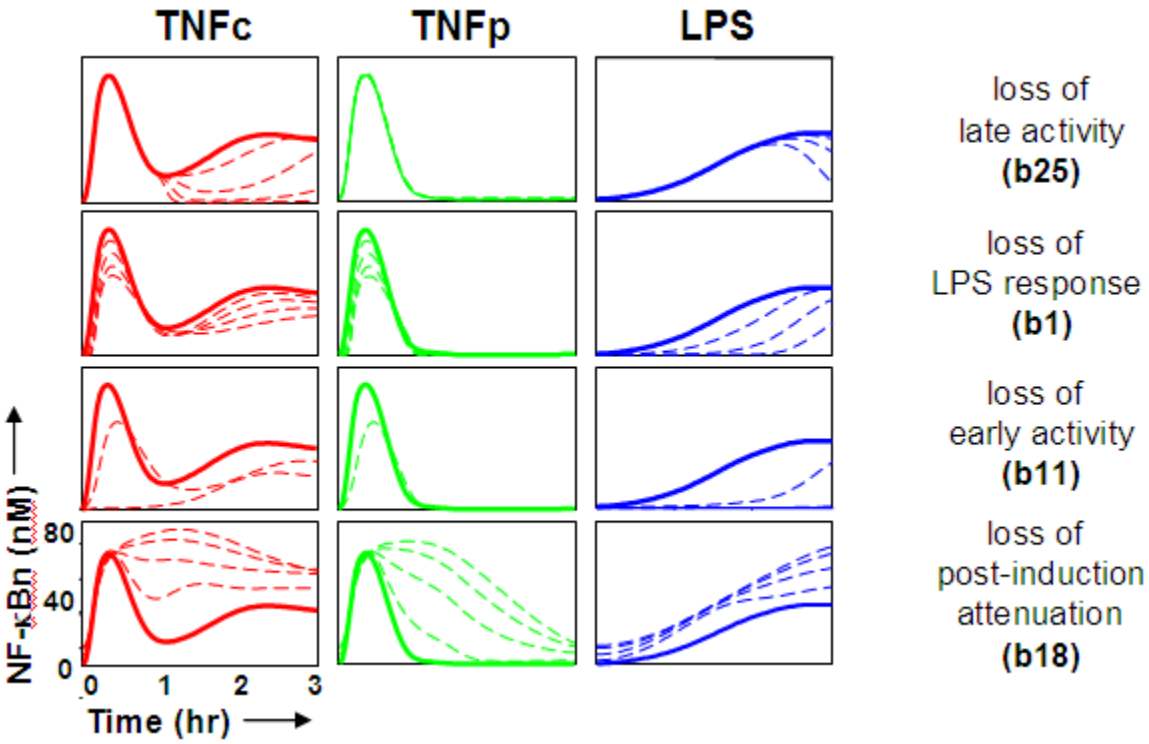

Figure 5-8 Examples of Signal Specificity in NF–κB Responses

Four examples of biochemical mechanisms that control dynamic NF-κB activity profiles in a stimulus specific manner. NF-κB activity produced in wild-type cells is shown as a continuous line, whereas dashed lines show successively more severe changes to the biochemical groupings indicated to the right.

One: loss of late activity [b25: NF-κB-responsive transcription of IκBε]
Two: loss of LPS response [b1: Association of NF-κB and IκB]
Three: Loss of early activity [b11: Degradation of free IκB protein]
Four: Loss of post-induction attenuation [b18: IκBα mRNA degradation]

In these figures, parameter values within biochemical groupings b1, b18 and b25 were successively increased; parameter values within grouping b11 were decreased. The complete set of curves is shown in .

Group b1: Association IκB-NFκB

Group b2: Dissociation IκB-NFκB

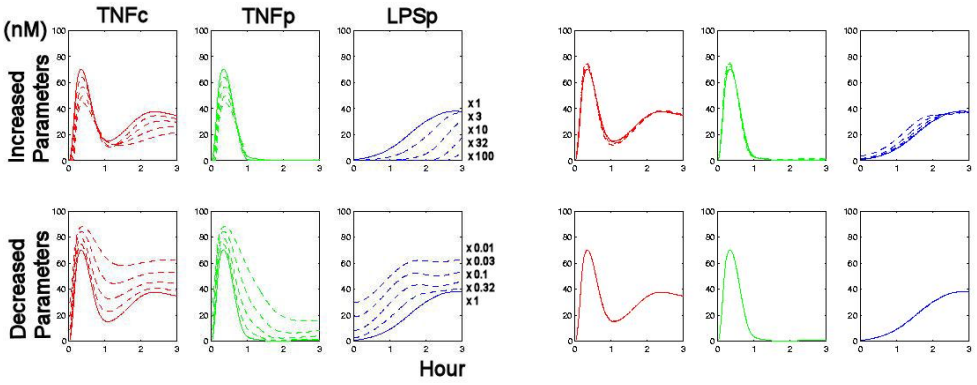

Group b3: Association IKK-IκB

Group b4: Dissociation IKK-IκB

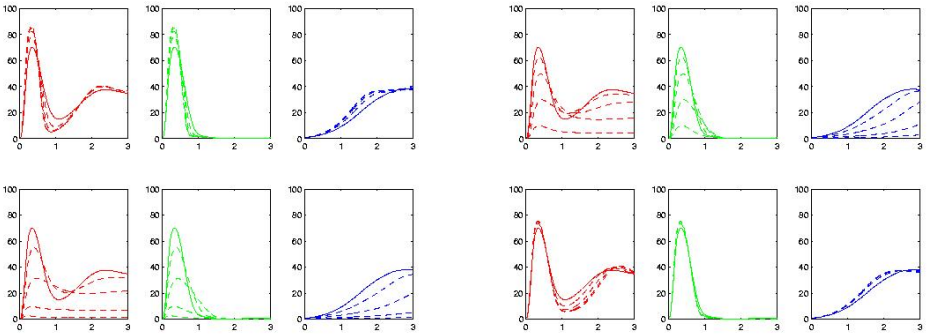

Group b5: Export NFκB

Group b6: Import NFκB

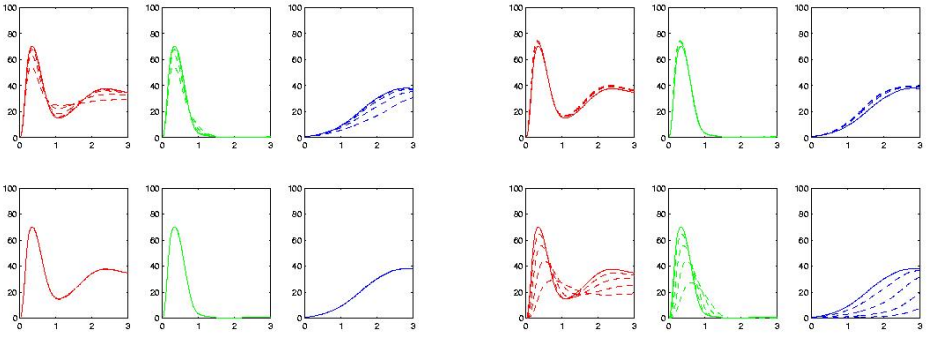

Figure 5-9 Detailed Effects of Simulated Biochemical Alterations

For each of 25 biochemical parameter groupings, six boxes are shown. Format is as Figure 5-8, with top three boxes for parameter increases, bottom three for decreases.

Group b7: Export IκB-NFκB

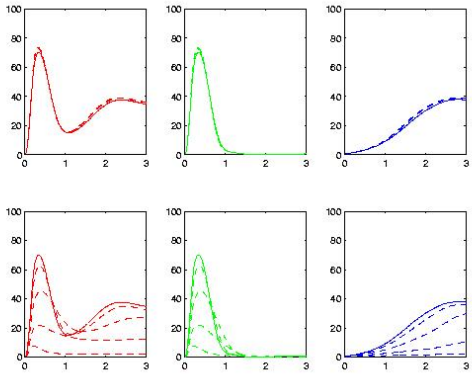

Group b8: Import IκB-NFκB

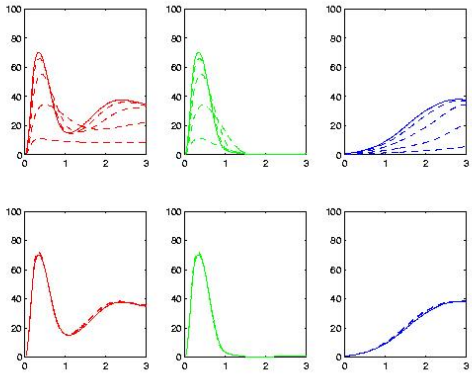

Group b9: Export IκB

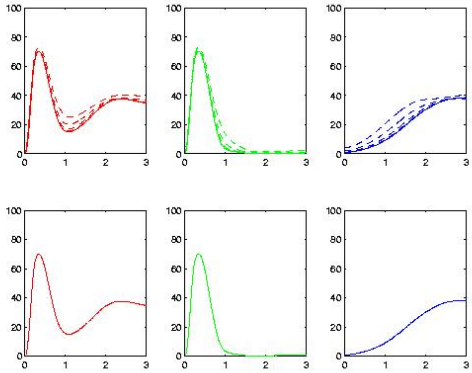

Group b10: Import IκB

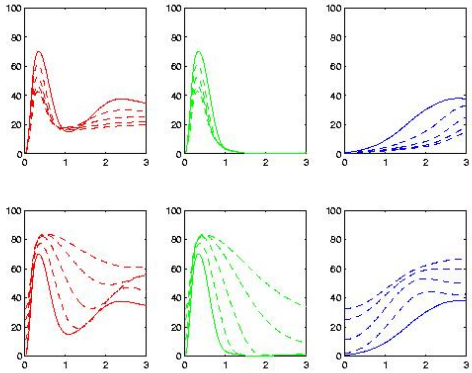

Group b11: Degradation IκB

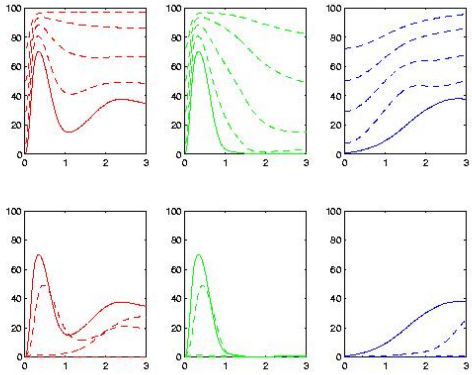

Group b12: Degradation IκB-NFκB

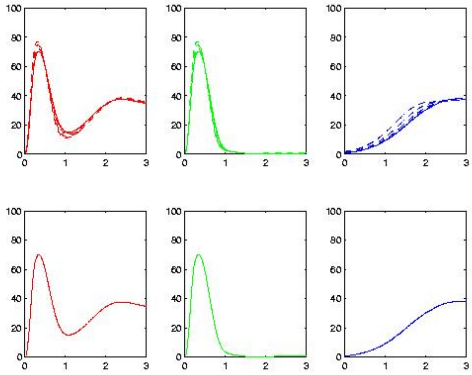

Figure 5-9 Continued

Group b13: Degradation IKK-IκB

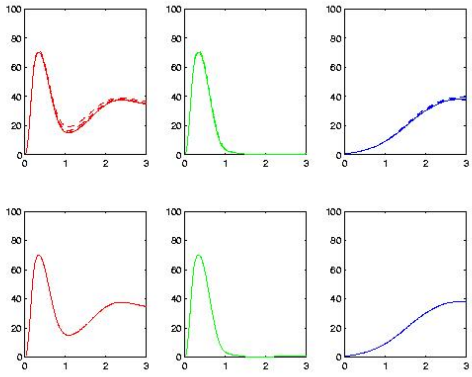

Group b14: Degradation IKK-NFκB-IκB

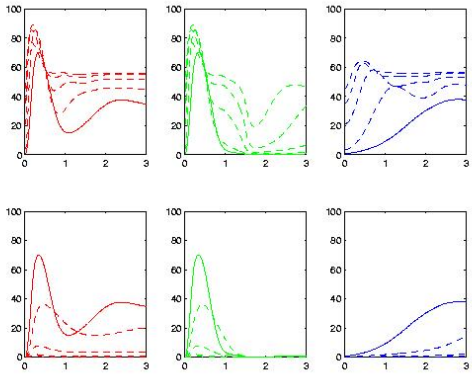

Group b15: Protein synthesis IκBα

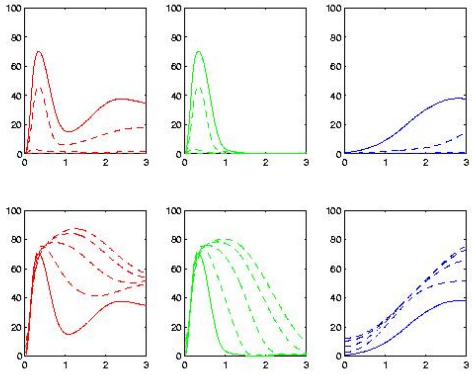

Group b16: Protein synthesis IκBβ

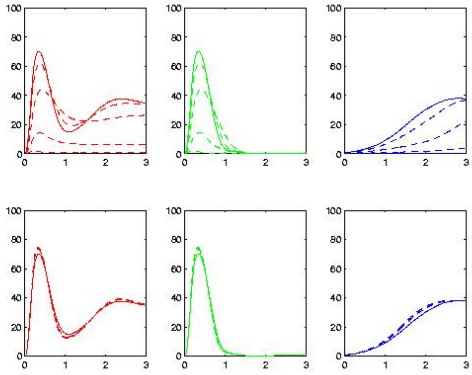

Group b17: Protein synthesis IκBε

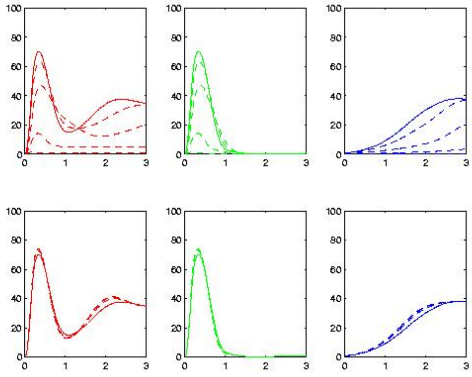

Group b18: RNA degradation IκBα

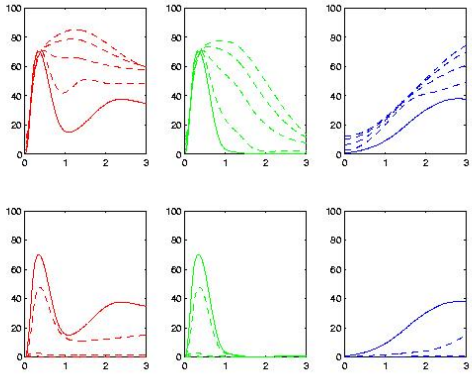

Figure 5-9 Continued

Group b19: RNA degradation IκBβ

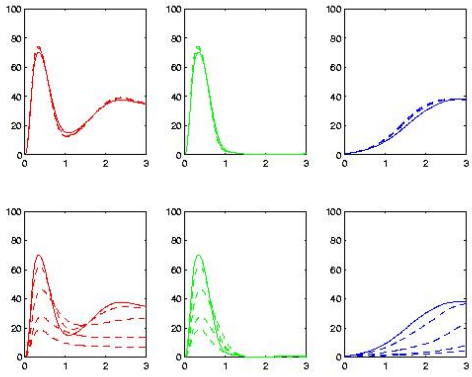

Group b20: RNA degradation IκBε

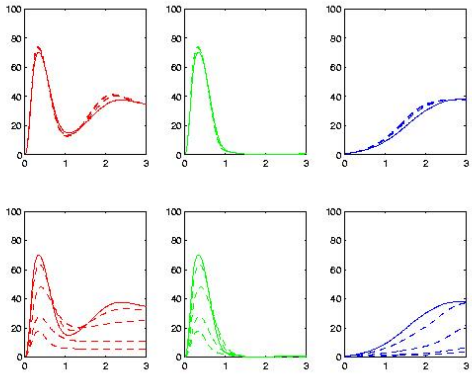

Group b21: RNA synthesis unregulated IκBα

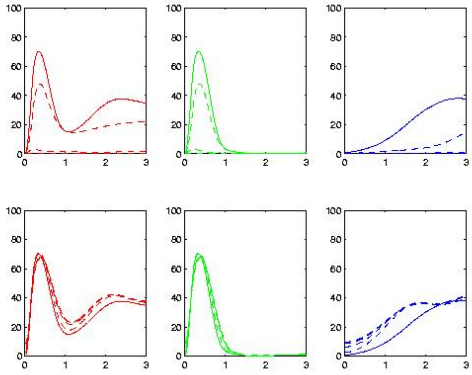

Group b22: RNA synthesis unregulated IκBβ

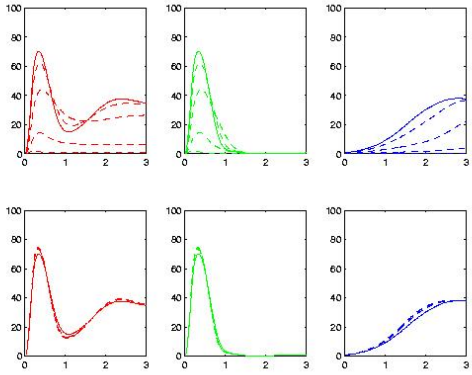

Group b23: RNA synthesis unregulated IκBε

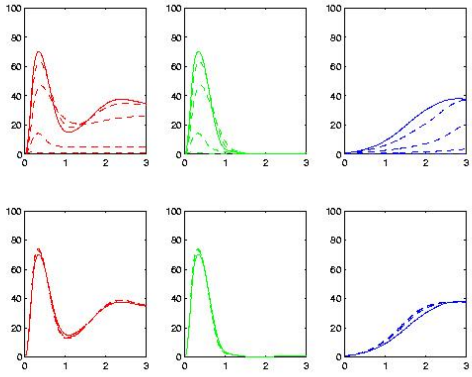

Group b24: RNA synthesis regulated IκBα

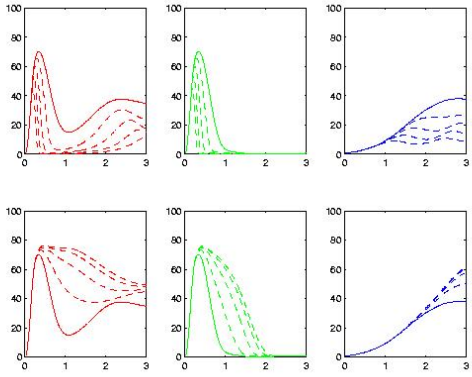

Figure 5-9 Continued

Group b25: RNA synthesis regulated IκBε

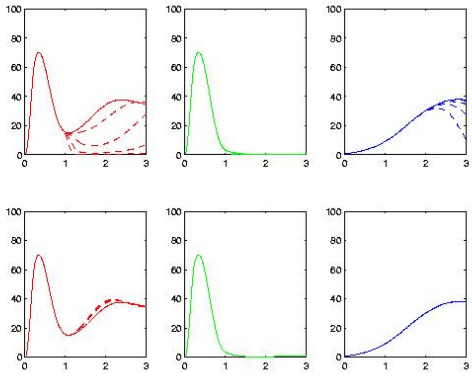

Figure 5-9 Continued

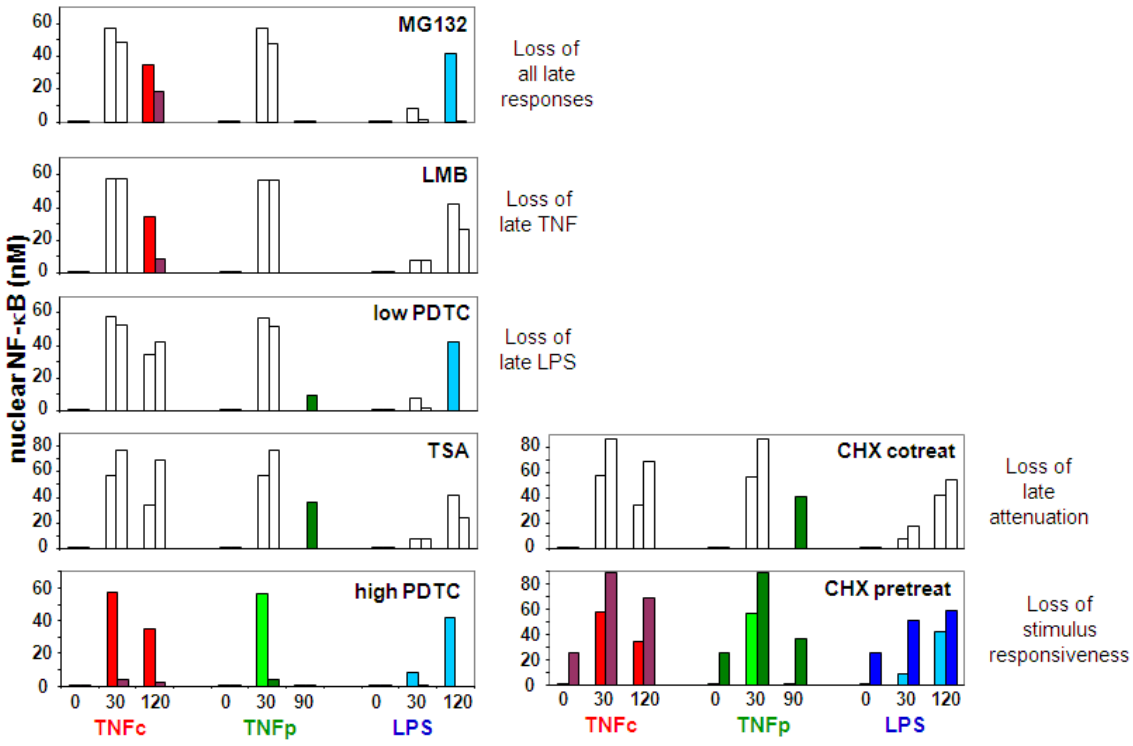

Figure 5-10 Pharmacological Agents with Stimulus Specific Effects

Stimulus specific effects of simulated treatments. For all pairs of bars, left bar (lighter shade) is wild type, right bar (darker shade) is treated. For underlying timecourses see

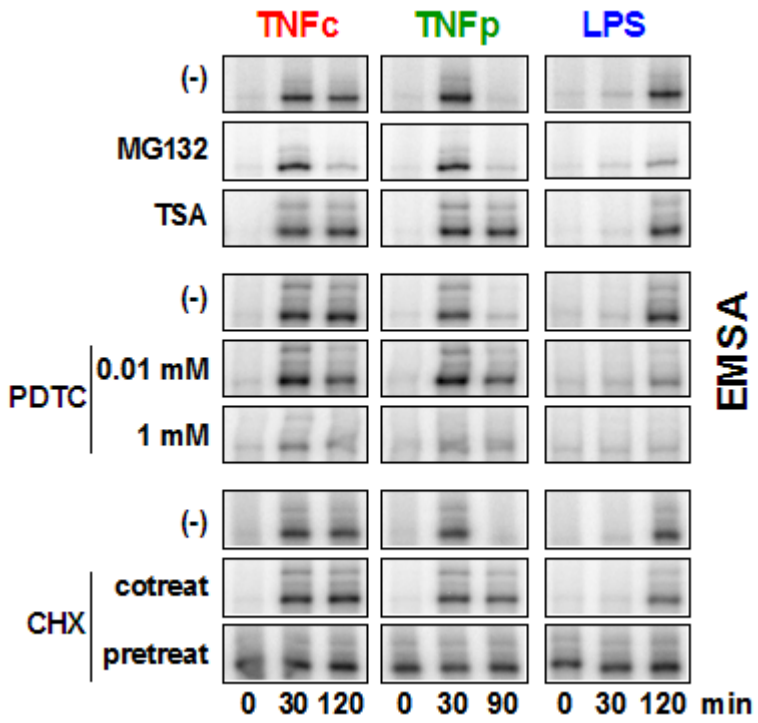

Figure 5-11 Experimental Validation of Stimulus Specific Effects

The effects of pharmacological inhibitors on stimulus-induced NF-κB DNA binding activity as revealed by EMSA. Extracts were prepared from cells at the indicated timepoints following TNFc, TNFp, or LPSp stimulus administration. Work of Shannon

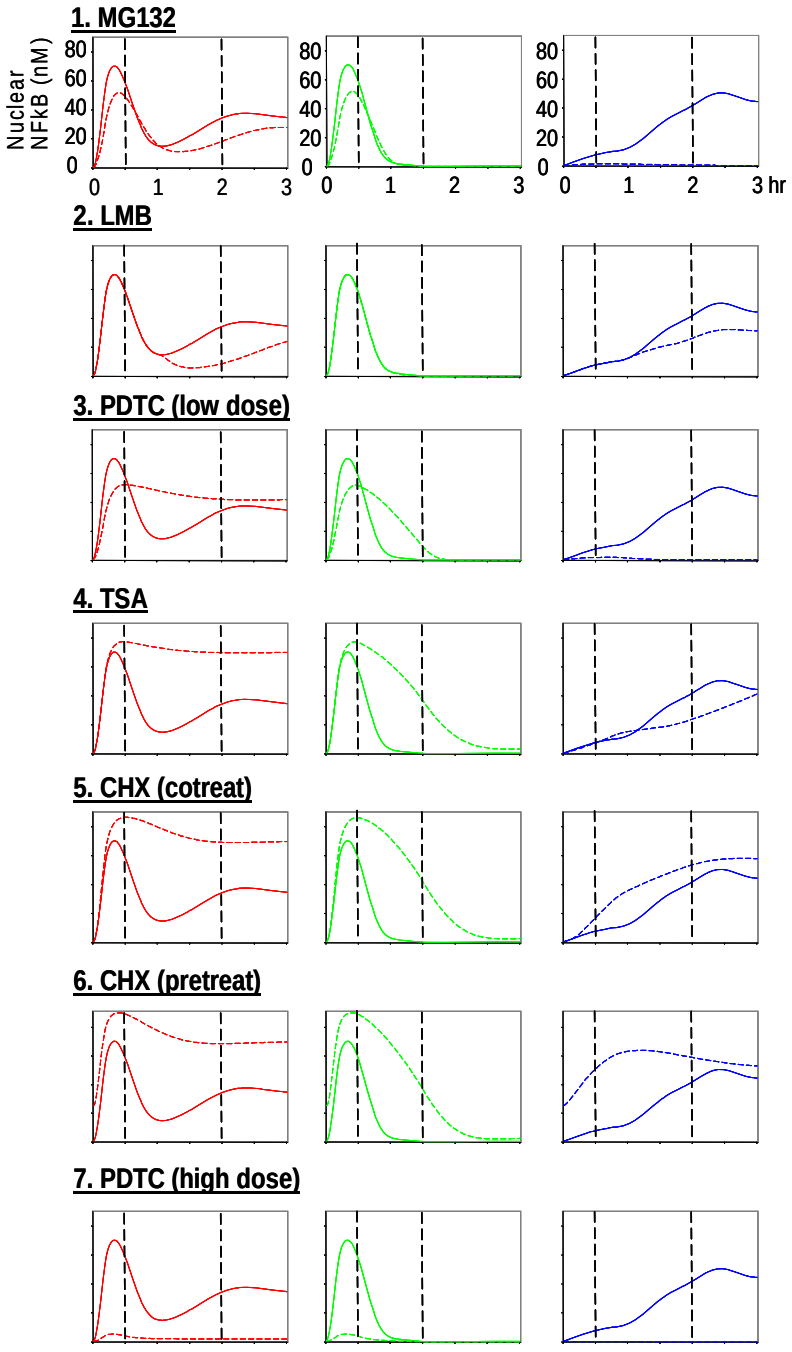

Figure 5-12 Predicted Effects of Pharmacological Inhibitors on NF-kB Activation

Timecourses showing effects of treatments that are stimulus specific. Solid line: no treatment. Dotted line: with treatment. Black lines: time points used for bar charts in Figure 5-10. For details of simulation conditions, see Table 5-4.

Chapter 6
Conclusions and Future Outlook

In this chapter, I broaden my discussion to discuss expected and speculative future developments in modeling of NF−κB, other cell signaling systems, and biological systems in general. This chapter contains three sections. In the first, I discuss future developments in modeling and understanding dynamic control, in encoding temporal profiles of IKK activity and decoding temporal profiles of NF−κB activity, with a focus on modeling feedback and feedforward signaling. In the second section, I discuss advances in modeling NF−κB dimers, proteolytic processing, modeling the noncanonical NF−κB pathway, and crosstalk with other signaling pathways. Finally, in section three, I conclude with a broader discussion of the context, relevance, and impact of the work presented in this thesis.

6.1 Extending our understanding of IKK encoding and NF−κB decoding

The modeling approach presented in this thesis has taken as its focus the system between IKK and NF−κB, and has focused on the importance of dynamic control of the activation profiles. As a result, it is interesting to consider how temporal and spatial patterns of ligand presentation on the cell surface are encoded into IKK activation profiles, and how NF−κB activation profiles are decoded into appropriate, sustained transcriptional cellular responses.

6.1.1 Mechanisms of encoding IKK temporal profiles

The work I have presented in previous chapters has focused on mechanistic details within the IKK-IκB-NF−κB signaling module. The mechanistic details of the ligands, receptors, and other intermediates signaling to IKK have been circumvented by measuring an IKK timecourse. However, the mechanisms that produce IKK timecourses are qualitatively understood – the last few years have seen significant progress in working out the details.

In particular, the IKK timecourse is influenced by a large number of upstream receptors (Hayden and Ghosh 2004) including the TNF superfamily, the TIR superfamily (TLR/IL1-R), and antigen receptors (TCR, BCR).

The best studied of these is the TNF receptor superfamily, which has at least 29 receptors (Aggarwal 2003). Some receptors, such as TNFR1, are known to signal through the canonical NF−κB pathway (Chen and Goeddel 2002), which others, such as LTβ-R, BAFF-R, and CD40 signal through the noncanonical pathway (Hayden and Ghosh 2004). In many cases, the intermediate adaptor proteins are well known, both from traditional molecular biology studies (Liu 2005) and from systems biology approaches using tandem affinity purification and liquid chromatography tandem mass spectrometry (Bouwmeester, Bauch et al. 2004). These studies suggest that possibility of explaining in mechanistic detail how the temporal (and even spatial (Guo and Levine 1999)) pattern of availability of ligands produces a temporal encoding of IKK and thus NF−κB.

Other receptor superfamilies are similarly being described in ever increasing detail. The TIR (Toll/Interleukin-1 Receptor) superfamily has at least 11 receptors in the TLR (Toll-Like Receptor) subgroup and at least ten receptors in the IL-1 subgroup (Liew, Xu et al. 2005). The mechanisms by which intermediate adaptor proteins form a signaling cascade to IKK have been detailed (Akira and Takeda 2004). In addition, signaling that emanates from antigen receptors (BCR and TCR) in lymphocytes (B-cells and T-cells) also drives the temporal dynamics of IKK and NF–κB (Weil and Israel 2004) through mechanisms that are now understood in some detail (Ruland and Mak 2003).

With all of these receptor families, there are multiple levels of potential regulation encoding temporal dynamics. The receptors themselves may be up- or downregulated metabolically or by localization and/or sequestration. The receptors and associated scaffolding proteins and second messengers may be capable of autophosphorylation and other kinds of post-translation modification. Negative feedback mechanisms (like A20) and positive autocrine loops (like TNF), or even paracrine/endocrine signaling, may influence the ultimate encoding of IKK.

With the details of these upstream systems increasingly known, not all signal cascade mechanisms will be equally interesting for modeling and/or experimental study. Instead, attention is likely to focus on certain phenomenon: negative and positive feedback and feedforward mechanisms, amplification, threshold activation mechanisms, and nonlinear responses.

Overall, the prodigious growth in mechanistic understanding upstream of IKK provides an opportunity to ask how these signaling cascades, individually and in combinations, encode a temporal pattern of IKK which ultimately has downstream consequences on gene expression, growth and apoptosis decision, and cell fate.

6.1.2 Mechanisms of decoding NF–κB temporal profiles

In this section I consider potential modeling work which may lead to greater understanding of the decoding of NF–κB temporal activity profiles. Downstream of NF–κB, the regulatory DNA elements (promoters, enhancers and others) may be thought of as highly effective scaffolds for integrating signals. I first consider modeling the interactions of NF–κB alone with these elements, then turn to adding the effects of interacting transcription factors. In both cases (NF–κB alone or in conjunction with other transcription factors), it is especially interesting to note the possibility of gene-by-gene modeling. Future models may model the interactions at individual genetic loci.

Beginning with NF–κB's interactions with DNA, there are two interesting possible additions: histone codes and dose/response curves. For histone codes, modeling may incorporate the interactions of NF–κB with chromatin (Natoli, Saccani et al. 2005). This is a complex topic due to the existence of noncanonical or degenerate NF–κB binding sites with different affinities. However, experimental techniques to study histone modifications have advanced in recent years and will continue to improve. Even without introducing additional (non NF–κB) transcription factors, it may be possible to model the

"state" of gene loci, and thus to model how NF−κB temporal profiles are decoded into gene expression.

Further, it is possible to model different dose-response behaviors via promoter (loci) specific Hill coefficients for the NF−κB induced transcription reactions. Previous work has noted the importance of these parameters (Nelson, Ihekwaba et al. 2004) – understanding the decoding of the NF−κB temporal code on a gene-specific basis may require an expanded understanding of this aspect of modeling transcription.

Next I turn to the role of other transcription factors in decoding NF−κB temporal profiles. Several other transcription factors are known to integrate with NF−κB in inducing gene expression. In one of the best characterized examples, at the human interferon-β gene enhancer, induced upon viral infection, NF−κB binds cooperatively with HMG-I, Jun, ATF2, and members of the IRF family (Ptashne and Gann 2002). Other examples include bZIP transcription factors, C/EBPβ, SP-1, and many others (Perkins 2007).

Given the importance of temporal regulation of NF−κB, it is natural to consider the potential for temporal regulation of its co-activators. It may be possible to dissect the sequence of events, which may occur, sequentially or in parallel, leading to activation. This would provide a richer model of how the temporal activity profile of NF−κB is decoded into temporal patterns of gene expression.

6.2 Extending our understanding of the IKK-IκB-NF−κB system details

Apart from IKK encoding and NF−κB decoding, the NF−κB system itself is ripe with possibilities for more advanced modeling. In this section, I discuss two primary avenues for improvement: first, models that incorporate dimers, proteolytic processing, and the noncanonical NF−κB pathway, and second, models that include crosstalk links to other signaling pathways.

6.2.1 Refining NF−κB modeling with dimers

Previous versions of the NF−κB model, as discussed in this thesis, have treated NF−κB as a single moiety, rather than a family of dimers, and have not modeled proteolytic processing of the family members. It is almost a certainty that work incorporating dimers into modeling is forthcoming. Such work is potentially significant in several ways.

First, it may address the question of whether dynamic control is dimer specific (Hoffmann and Baltimore 2006), since different dimers can be expected to have both different binding affinities to particular promoters, and different rate constants for their associations and dissociations with IκB inhibitor, their constitutive and induced expression and degradation rates, etc. (Hoffmann, Natoli et al. 2006).

In addition, modeling dimers will enable modeling of proteolytic processing, which will naturally lead to modeling a second NF−κB activation pathway, often called the non-canonical pathway. This pathway is thought to involve not inhibitor degradation but rather protein precursor processing of p100 (complexed to RelB) to form p52:RelB

transcriptionally active heterodimers (Pomerantz and Baltimore 2002). In addition, constitutive processing of p105 to p50 (Beinke and Ley 2004) within the canonical pathway may also be modeled.

Finally, many other modeling refinements can be expected, both from mechanisms that are currently known and mechanisms that are still to be elucidated. One likely example of the former is a feedforward mechanism provided by the role of IKK in the nucleus (Quivy and Van Lint 2004; Lawrence, Bebien et al. 2005; Gloire, Dejardin et al. 2006).

6.2.2 Refining NF−κB modeling with crosstalk

Looking beyond the immediate IKK-IκB-NF−κB system, there will be additional opportunities to mechanistically model temporal encoding in inflammation. There is a huge scope for explicitly modeling crosstalk, integrating other cell signaling pathways with IKK and NF−κB (Perkins 2007). The following three examples give the most likely avenues for modeling; they are by no means an exhaustive list.

The first example of crosstalk is the JNK pathway (Tang, Minemoto et al. 2001; Nakano, Nakajima et al. 2006; Papa, Bubici et al. 2006). Many cell stresses that activate the NF−κB pathway also induce JNK signaling.. However, a number of genes induced by NF−κB (MnSOD, GADD45β, XIAP) can counteract or suppress JNK activation.

The second example of crosstalk is the p53 pathway (Ryan, Ernst et al. 2000). NF−κB can increase p53 expression and stability (Aleyasin, Cregan et al. 2004; Fujioka,

Schmidt et al. 2004), and p53 can induce RSK1 activity, leading to the nuclear localization of NF−κB (Bohuslav, Chen et al. 2004).

The third example of crosstalk is nuclear receptors such as IRF3 and glucocorticoid receptor. These can function by direct interactions with NF−κB (Pascual and Glass 2006). There are also indirect mechanisms, such as competition for co-activators such as p300 and CBP (Sheppard, Phelps et al. 1998).

By modeling these pathways and their interactions with the IKK-IκB-NF−κB system at multiple levels, it may be possible to understand and predict a larger set of cellular behaviors and responses in inflammation and cell fate decisions.

6.3 Impact and conclusions

In this final section, I turn to the broader context and impact of my work. First, I discuss the potential for convergence between mechanistic modeling such as my work, and statistical, top-down, "systems biology" approaches. Second, summarize the relevance of my work to the broader goal of improved modeling and biological understanding of inflammation.

6.3.1 Convergence between mechanistic and statistical approaches

In contrast to the mechanistic modeling approach utilized in this thesis, other groups have studied NF−κB using 'statistical' or 'machine learning' top down methods (Aldridge, Burke et al. 2006; Janes and Yaffe 2006). In this section, I discuss two efforts: the work of Janes, Lauffenburger and coworkers, and the work of the Alliance for Cell Signaling.

For the former, the cue-signal-response analysis by partial least squares regression approach (Janes, Kelly et al. 2004) was pioneered by Janes and coworkers. This modeling approach is built on high-throughput experimental techniques (Janes, Albeck et al. 2003) and has been used to study cytokine induced apoptosis. (Janes, Albeck et al. 2005). This work encompasses combinations of TNF, EGF and insulin signaling, and measures 19 system variables, one of which is IKK activity.

Similarly, the Alliance for Cell Signaling has provided an even richer, broader set of signaling measurements (Natarajan, Lin et al. 2006; Pradervand, Maurya et al. 2006). The coverage and scope of this effort is dramatically greater than that presented in this thesis – it is an exemplar of systems biology, with multiple ligands, singly and in combination, in multiple cell types, and with a large number of cell state measurements. The resulting data has been successfully used to identify crosstalk (Lee, Sinkovits et al. 2006; Zhu, Chang et al. 2006).

These two efforts attempt to address a different but related set of questions. Looking to future work, it will be interesting to see whether mechanistic, bottom up approaches, such as the work presented in this thesis, and statistical, top down approaches, such as the work of Janes et. Al and the Alliance for Cell Signaling, will "meet in the middle". Over time, the mechanistic approaches will become broader, by, for example, incorporating crosstalk between multiple signaling systems. At the same time, the statistical, top down approaches will become more detailed, for example by increasing the number of internal measurements that drive the modeling. Since these two

approaches are studying the same systems with the same physiological behaviors of interest, their potential future convergence is a key test and a fascinating open question.

6.3.2 Closing

In this dissertation I have investigated the hypothesis that dynamic control of NF−κB is key to understanding the signal processing of the IKK-IκB-NF−κB system.

To study the existence, mechanisms, and implications of temporal coding in this system, I have taken an existing model of NF−κB signaling and improved it in a number of ways. I have extended its utility with additional computational techniques, and linked this computational work to experimental validation.

It is hoped that the knowledge, techniques and approaches developed by this work will be a contribution, not just to the extensive literature addressing NF-κB, but especially to the nascent but growing body of work which combines computational and experimental disciplines to further our understanding of cell signaling, in all its dazzling complexity.

Appendix A Model 1.1

nfkb_timecourse_1_1.m

nfkb_active.m
nfkb_active_1_1.m
nfkb_add_paths.m
nfkb_adjust_mets.m
nfkb_adjust_mets_1_1.m
nfkb_check_equilibrate.m
nfkb_clear_file.m
nfkb_core.m
nfkb_deltas.m
nfkb_deltas_1_1.m
nfkb_equilibrate.m
nfkb_fluxes.m
nfkb_fluxes_1_1.m
nfkb_main_2.m
nfkb_results_dir.m
nfkb_save_figures.m
nfkb_save_nfkbn_col.m
nfkb_set_params.m
nfkb_set_params_1_1.m
nfkb_sim_defaults.m
nfkb_simulate.m
nfkb_validate_output_type.m
nfkb_validate_version.m

File: nfkb_timecourse_1_1.m

```
%================================================
% NFKB_TIMECOURSE_1_1
%================================================

function nfkb_timecourse_1_1(filename)
  clear global;
  nfkb_add_paths();
  nfkb_results_dir();

  if not(exist('filename')); filename = 'results/holdout_timecourse_1_1.txt'; end;

  nfkb_clear_file(filename);

  sim_struct             = nfkb_sim_defaults();
  sim_struct.version     = '1_1';
  sim_struct.output_file = filename;
  sim_struct.equilibrate = 'none';
  nfkb_main2(sim_struct);
end
```

File: nfkb_active.m

```
%================================================
% NFKB_ACTIVE
%================================================

function active_nfkb = nfkb_active(results)

  global version;

  if     (strcmp(version, '1_0'))
    active_nfkb = nfkb_active_1_0(results);
  elseif (strcmp(version, '1_1'))
    active_nfkb = nfkb_active_1_1(results);
  elseif (strcmp(version, '1_2'))
    active_nfkb = nfkb_active_1_2(results);
  else
    error('Unknown version');
  end

end
```

File: nfkb_active_1_1.m

```
%================================================
% NFKB_ACTIVE_1_1
%================================================

function active_nfkb = nfkb_active_1_1(results)
  NFkBn     = results(:,2);
  active_nfkb = NFkBn;
end
```

File: nfkb_add_paths.m

```
%================================================
% NFKB_ADDPATHS
%================================================

function nfkb_addpaths()
  addpath('../lib');
  addpath('../lib/save');
  addpath('../lib/helpers');
  addpath('../lib/models/model_1_0');
  addpath('../lib/models/model_1_1');
  addpath('../lib/models/model_1_2');
end
```

File: nfkb_adjust_mets.m

```
%================================================
% NFKB_ADJUST_METS
%================================================

function mets = nfkb_adjust_mets(time, input_mets)
  global version;

  if (strcmp(version, '1_0'))
    mets = nfkb_adjust_mets_1_0(time, input_mets);
  elseif (strcmp(version, '1_1'))
    mets = nfkb_adjust_mets_1_1(time, input_mets);
  elseif (strcmp(version, '1_2'))
    mets = nfkb_adjust_mets_1_2(time, input_mets);
```

```
  else
    error('Unknown version');
  end
end
```

File: nfkb_adjust_mets_1_1.m

```
%================================================
% NFKB_ADJUST_METS_1_1
%================================================

function mets = nfkb_adjust_mets_1_1(time, input_mets)

  mets = input_mets;
  if (time == -1)
    mets(1,1)  = 0.1;    % NFkB
    mets(2,1)  = 0.001;  % NFkBn
    mets(6,1)  = 0.1;    % IkBa
    mets(18,1) = 0.001;  % IKK
  end
  if (time == 0)
    mets(18,1) = 0.1; % IKK
  end

end
```

File: nfkb_check_equilibrate.m

```
%================================================
% NFKB_CHECK_EQUILIBRATE
%================================================

function [time results] = nfkb_check_equilibrate()
  global equilibration_flag;

  equilibration_flag = 1;

  nfkb_set_params(-1);
  starting_mets = zeros(25,1);
  mets = nfkb_adjust_mets(-1, starting_mets);
  time = 0;

  before = mets;
  counter = 1;
  x(:,1) = before;
  while time < 1000000
    f = str2func('nfkb_core');
    [times results] = ode15s(f, [-1000 0],before,[]);
    after = transpose(results(end,:));
    time = time + 1000;
    counter = counter+1;
    x(:,counter) = after;
    if nfkb_check_equilibrium(before, after)
      break;
    else
      ttt = before;
      before = after;
    end
  end
  if time == 10000000
    error('Failed to equilibrate');
  end

  equilibration_flag = 0;
```

```
end

%================================================
% NFKB_CHECK_EQUILIBRIUM
%================================================

function flag = nfkb_check_equilibrium(before, after)
  diff = abs(after - before);
  biggest = max(diff);

  threshold = 100 * eps;  % previously: 0.001

  if (biggest < threshold)
    flag = 1;
  else
    flag = 0;
  end
end
```

File: nfkb_clear_file.m

```
%================================================
% NFKB_CLEAR_FILE
%================================================

function nfkb_clear_file(filename)
  fid = fopen(filename, 'w+');
  fclose(fid);
end
```

File: nfkb_core.m

```
%================================================
% NFKB_CORE
%================================================

function dxdt_nfkb = nfkb_core(t,mets)
  fluxes = nfkb_fluxes(mets, t);
  deltas = nfkb_deltas(fluxes, t);
  dxdt_nfkb = deltas';
end
```

File: nfkb_deltas.m

```
%================================================
% NFKB_DELTAS
%================================================

function deltas = nfkb_deltas(fluxes, t)
  global version;

  if     strcmp(version, '1_0')
    deltas = nfkb_deltas_1_0(fluxes,t);
  elseif strcmp(version, '1_1')
    deltas = nfkb_deltas_1_1(fluxes,t);
  elseif strcmp(version, '1_2')
    deltas = nfkb_deltas_1_2(fluxes,t);
  else
    error('Unknown version');
  end
end
```

File: nfkb_deltas_1_1.m

```
%=================================================
% NFKB_DELTAS_1_1
%=================================================

function deltas = nfkb_deltas_1_1(fluxes, t)

  global equilibration_flag;

  delta_NFkB        = 0;
  delta_NFkBn       = 0;
  delta_IkBat       = 0;
  delta_IkBbt       = 0;
  delta_IkBet       = 0;
  delta_IkBa        = 0;
  delta_IkBb        = 0;
  delta_IkBe        = 0;
  delta_IkBan       = 0;
  delta_IkBbn       = 0;
  delta_IkBen       = 0;
  delta_IkBaNFkB    = 0;
  delta_IkBbNFkB    = 0;
  delta_IkBeNFkB    = 0;
  delta_IkBaNFkBn   = 0;
  delta_IkBbNFkBn   = 0;
  delta_IkBeNFkBn   = 0;
  delta_IKK         = 0;
  delta_IKKIkBa     = 0;
  delta_IKKIkBb     = 0;
  delta_IKKIkBe     = 0;
  delta_IKKIkBaNFkB = 0;
  delta_IKKIkBbNFkB = 0;
  delta_IKKIkBeNFkB = 0;
  delta_FR          = 0;

  flux_a1_1     = fluxes(1);
  flux_a2_1     = fluxes(2);
  flux_a3_1     = fluxes(3);
  flux_a4_1     = fluxes(4);
  flux_a4_2     = fluxes(5);
  flux_a4_3     = fluxes(6);
  flux_a5_1     = fluxes(7);
  flux_a5_2     = fluxes(8);
  flux_a5_3     = fluxes(9);
  flux_a6_1     = fluxes(10);
  flux_a6_2     = fluxes(11);
  flux_a6_3     = fluxes(12);
  flux_a7_1     = fluxes(13);
  flux_a8_1     = fluxes(14);
  flux_a9_1     = fluxes(15);
  flux_d1_1     = fluxes(16);
  flux_d1_2     = fluxes(17);
  flux_d2_1     = fluxes(18);
  flux_d2_2     = fluxes(19);
  flux_d3_1     = fluxes(20);
  flux_d3_2     = fluxes(21);
  flux_d4_1     = fluxes(22);
  flux_d4_2     = fluxes(23);
  flux_d4_3     = fluxes(24);
  flux_d5_1     = fluxes(25);
  flux_d5_2     = fluxes(26);
  flux_d5_3     = fluxes(27);
  flux_d6_1     = fluxes(28);
  flux_d6_2     = fluxes(29);
  flux_d6_3     = fluxes(30);
```

```
flux_deg1_1   = fluxes(31);
flux_deg1_2   = fluxes(32);
flux_deg1_3   = fluxes(33);
flux_deg1_4   = fluxes(34);
flux_deg1_5   = fluxes(35);
flux_deg1_6   = fluxes(36);
flux_deg4_1   = fluxes(37);
flux_deg4_2   = fluxes(38);
flux_deg4_3   = fluxes(39);
flux_deg4_4   = fluxes(40);
flux_deg4_5   = fluxes(41);
flux_deg4_6   = fluxes(42);
flux_k01_1    = fluxes(43);
flux_k02_1    = fluxes(44);
flux_k1_1     = fluxes(45);
flux_k2_1     = fluxes(46);
flux_k2_2     = fluxes(47);
flux_k2_3     = fluxes(48);
flux_r1_1     = fluxes(49);
flux_r2_1     = fluxes(50);
flux_r3_1     = fluxes(51);
flux_r4_1     = fluxes(52);
flux_r5_1     = fluxes(53);
flux_r6_1     = fluxes(54);
flux_tp1_1    = fluxes(55);
flux_tp1_2    = fluxes(56);
flux_tp1_3    = fluxes(57);
flux_tp2_1    = fluxes(58);
flux_tp2_2    = fluxes(59);
flux_tp2_3    = fluxes(60);
flux_tr1_1    = fluxes(61);
flux_tr1_2    = fluxes(62);
flux_tr1_3    = fluxes(63);
flux_tr2_1    = fluxes(64);
flux_tr2a_1   = fluxes(65);
flux_tr2b_1   = fluxes(66);
flux_tr2e_1   = fluxes(67);
flux_tr3_1    = fluxes(68);
flux_tr3_2    = fluxes(69);
flux_tr3_3    = fluxes(70);

%%% === a1_1: IkBa + IKK => IkBaIKK
delta_IkBa    = delta_IkBa    - flux_a1_1;
delta_IKK     = delta_IKK     - flux_a1_1;
delta_IKKIkBa = delta_IKKIkBa + flux_a1_1;

%%% === a2_1: IkBb + IKK => IkBbIKK
delta_IkBb    = delta_IkBb    - flux_a2_1;
delta_IKK     = delta_IKK     - flux_a2_1;
delta_IKKIkBb = delta_IKKIkBb + flux_a2_1;

%%% === a3_1: IkBe + IKK => IkBeIKK
delta_IkBe    = delta_IkBe    - flux_a3_1;
delta_IKK     = delta_IKK     - flux_a3_1;
delta_IKKIkBe = delta_IKKIkBe + flux_a3_1;

%%% === a4_1: IkBa + NFkB => IkBaNFkB
delta_NFkB     = delta_NFkB     - flux_a4_1;
delta_IkBa     = delta_IkBa     - flux_a4_1;
delta_IkBaNFkB = delta_IkBaNFkB + flux_a4_1;

%%% === a4_2: IkBaIKK + NFkB => IkBaIKKNFkB
delta_NFkB        = delta_NFkB        - flux_a4_2;
delta_IKKIkBa     = delta_IKKIkBa     - flux_a4_2;
delta_IKKIkBaNFkB = delta_IKKIkBaNFkB + flux_a4_2;

%%% === a4_3: IkBan +NFkBn => IkBaNFkBn
```

```
delta_NFkBn     = delta_NFkBn     - flux_a4_3;
delta_IkBan     = delta_IkBan     - flux_a4_3;
delta_IkBaNFkBn = delta_IkBaNFkBn + flux_a4_3;

%%% === a5_1: IkBb + NFkB => IkBbNFkB
delta_NFkB     = delta_NFkB     - flux_a5_1;
delta_IkBb     = delta_IkBb     - flux_a5_1;
delta_IkBbNFkB = delta_IkBbNFkB + flux_a5_1;

%%% === a5_2: IkBbIKK + NFkB => IkBbIKKNFkB
delta_NFkB        = delta_NFkB        - flux_a5_2;
delta_IKKIkBb     = delta_IKKIkBb     - flux_a5_2;
delta_IKKIkBbNFkB = delta_IKKIkBbNFkB + flux_a5_2;

%%% === a5_3: IkBbn + NFkBn => IkBbNFkBn
delta_NFkBn        = delta_NFkBn     - flux_a5_3;
delta_IkBbn        = delta_IkBbn     - flux_a5_3;
delta_IkBbNFkBn    = delta_IkBbNFkBn + flux_a5_3;

%%% === a6_1: IkBe + NFkB => IkBeNFkB
delta_NFkB     = delta_NFkB     - flux_a6_1;
delta_IkBe     = delta_IkBe     - flux_a6_1;
delta_IkBeNFkB = delta_IkBeNFkB + flux_a6_1;

%%% === a6_2: IkBeIKK + NFkB => IkBeIKKNFkB
delta_NFkB        = delta_NFkB        - flux_a6_2;
delta_IKKIkBe     = delta_IKKIkBe     - flux_a6_2;
delta_IKKIkBeNFkB = delta_IKKIkBeNFkB + flux_a6_2;

%%% === a6_3: IkBen + NFkBn => IkBeNFkBn
delta_NFkBn     = delta_NFkBn     - flux_a6_3;
delta_IkBen     = delta_IkBen     - flux_a6_3;
delta_IkBeNFkBn = delta_IkBeNFkBn + flux_a6_3;

%%% === a7_1: IkBaNFkB + IKK => IkBaIKKNFkB
delta_IkBaNFkB    = delta_IkBaNFkB    - flux_a7_1;
delta_IKK         = delta_IKK         - flux_a7_1;
delta_IKKIkBaNFkB = delta_IKKIkBaNFkB + flux_a7_1;

%%% === a8_1: IkBbNFkB + IKK => IkBbIKKNFkB
delta_IkBbNFkB    = delta_IkBbNFkB    - flux_a8_1;
delta_IKK         = delta_IKK         - flux_a8_1;
delta_IKKIkBbNFkB = delta_IKKIkBbNFkB + flux_a8_1;

%%% === a9_1: IkBeNFkB + IKK => IkBeIKKNFkB
delta_IKK         = delta_IKK         - flux_a9_1;
delta_IkBeNFkB    = delta_IkBeNFkB    - flux_a9_1;
delta_IKKIkBeNFkB = delta_IKKIkBeNFkB + flux_a9_1;

%%% === d1_1: IkBaIKK => IkBa + IKK
delta_IKKIkBa = delta_IKKIkBa - flux_d1_1;
delta_IkBa    = delta_IkBa    + flux_d1_1;
delta_IKK     = delta_IKK     + flux_d1_1;

%%% === d1_2: IkBaIKKNFkB => IkBaNFkB + IKK
delta_IKKIkBaNFkB = delta_IKKIkBaNFkB - flux_d1_2;
delta_IkBaNFkB    = delta_IkBaNFkB    + flux_d1_2;
delta_IKK         = delta_IKK         + flux_d1_2;

%%% === d2_1: IkBbIKK => IkBb + IKK
delta_IKKIkBb = delta_IKKIkBb - flux_d2_1;
delta_IkBb    = delta_IkBb    + flux_d2_1;
delta_IKK     = delta_IKK     + flux_d2_1;

%%% === d2_2: IkBbIKKNFkB => IkBbNFkB + IKK
delta_IKKIkBbNFkB = delta_IKKIkBbNFkB - flux_d2_2;
delta_IkBbNFkB    = delta_IkBbNFkB    + flux_d2_2;
```

```
delta_IKK         = delta_IKK         + flux_d2_2;

%%% === d3_1: IkBeIKK => IkBe + IKK
delta_IKKIkBe = delta_IKKIkBe - flux_d3_1;
delta_IkBe    = delta_IkBe    + flux_d3_1;
delta_IKK     = delta_IKK     + flux_d3_1;

%%% === d3_2: IkBeIKKNFkB => IkBeNFkB + IKK
delta_IKKIkBeNFkB = delta_IKKIkBeNFkB - flux_d3_2;
delta_IkBeNFkB    = delta_IkBeNFkB    + flux_d3_2;
delta_IKK         = delta_IKK         + flux_d3_2;

%%% === d4_1: IkBaNFkB => IkBa + NFkB
delta_IkBaNFkB = delta_IkBaNFkB - flux_d4_1;
delta_NFkB     = delta_NFkB     + flux_d4_1;
delta_IkBa     = delta_IkBa     + flux_d4_1;

%%% === d4_2: IkBaNFkBn => IkBan + NFkBn
delta_IkBaNFkBn = delta_IkBaNFkBn - flux_d4_2;
delta_NFkBn     = delta_NFkBn     + flux_d4_2;
delta_IkBan     = delta_IkBan     + flux_d4_2;

%%% === d4_3: IkBaIKKNFkB => IkBaIKK + NFkB
delta_IKKIkBaNFkB = delta_IKKIkBaNFkB - flux_d4_3;
delta_NFkB        = delta_NFkB        + flux_d4_3;
delta_IKKIkBa     = delta_IKKIkBa     + flux_d4_3;

%%% === d5_1: IkBbNFkB => IkBb + NFkB
delta_IkBbNFkB = delta_IkBbNFkB - flux_d5_1;
delta_NFkB     = delta_NFkB     + flux_d5_1;
delta_IkBb     = delta_IkBb     + flux_d5_1;

%%% === d5_2: IkBbNFkBn => IkBbn + NFkBn
delta_IkBbNFkBn   = delta_IkBbNFkBn - flux_d5_2;
delta_NFkBn       = delta_NFkBn     + flux_d5_2;
delta_IkBbn       = delta_IkBbn     + flux_d5_2;

%%% === d5_3: IkBbIKKNFkB => IkBbIKK + NFkB
delta_IKKIkBbNFkB = delta_IKKIkBbNFkB - flux_d5_3;
delta_NFkB        = delta_NFkB        + flux_d5_3;
delta_IKKIkBb     = delta_IKKIkBb     + flux_d5_3;

%%% === d6_1: IkBeNFkB => IkBb + NFkB
delta_IkBeNFkB = delta_IkBeNFkB - flux_d6_1;
delta_NFkB     = delta_NFkB     + flux_d6_1;
delta_IkBe     = delta_IkBe     + flux_d6_1;

%%% === d6_2: IkBeNFkBn => IkBen + NFkBn
delta_IkBeNFkBn = delta_IkBeNFkBn - flux_d6_2;
delta_NFkBn     = delta_NFkBn     + flux_d6_2;
delta_IkBen     = delta_IkBen     + flux_d6_2;

%%% === d6_3: IkBeIKKNFkB => IkBeIKK + NFkB
delta_IKKIkBeNFkB = delta_IKKIkBeNFkB - flux_d6_3;
delta_NFkB        = delta_NFkB        + flux_d6_3;
delta_IKKIkBe     = delta_IKKIkBe     + flux_d6_3;

%%% === deg1_1: IkBa =>
delta_IkBa = delta_IkBa - flux_deg1_1;

%%% === deg1_2: IkBb =>
delta_IkBb = delta_IkBb - flux_deg1_2;

%%% === deg1_3: IkBe =>
delta_IkBe = delta_IkBe - flux_deg1_3;

%%% === deg1_4: IkBan =>
```

```
delta_IkBan = delta_IkBan - flux_deg1_4;

%%% === deg1_5: IkBbn =>
delta_IkBbn = delta_IkBbn - flux_deg1_5;

%%% === deg1_6: IkBen =>
delta_IkBen = delta_IkBen - flux_deg1_6;

%%% === deg4_1: IkBaNFkB => NFkB
delta_IkBaNFkB = delta_IkBaNFkB - flux_deg4_1;
delta_NFkB     = delta_NFkB     + flux_deg4_1;

%%% === deg4_2: IkBbNFkB => NFkB
delta_IkBbNFkB = delta_IkBbNFkB - flux_deg4_2;
delta_NFkB     = delta_NFkB     + flux_deg4_2;

%%% === deg4_3: IkBeNFkB => NFkB
delta_IkBeNFkB = delta_IkBeNFkB - flux_deg4_3;
delta_NFkB     = delta_NFkB     + flux_deg4_3;

%%% === deg4_4: IkBaNFkBn => NFkBn
delta_IkBaNFkBn = delta_IkBaNFkBn - flux_deg4_4;
delta_NFkBn     = delta_NFkBn     + flux_deg4_4;

%%% === deg4_5: IkBbNFkBn => NFkBn
delta_IkBbNFkBn = delta_IkBbNFkBn - flux_deg4_5;
delta_NFkBn     = delta_NFkBn     + flux_deg4_5;

%%% === deg4_6: IkBeNFkBn => NFkBn
delta_IkBeNFkBn = delta_IkBeNFkBn - flux_deg4_6;
delta_NFkBn     = delta_NFkBn     + flux_deg4_6;

%%% === k01_1: NFkBn => NFkB
delta_NFkBn = delta_NFkBn - flux_k01_1;
delta_NFkB  = delta_NFkB  + flux_k01_1;

%%% === k02_1: IKK =>
delta_IKK = delta_IKK - flux_k02_1;

%%% === k1_1: NFkB => NFkBn
delta_NFkB  = delta_NFkB  - flux_k1_1;
delta_NFkBn = delta_NFkBn + flux_k1_1;

%%% === k2_1: IkBaNFkBn => IkBaNFkB
delta_IkBaNFkBn = delta_IkBaNFkBn - flux_k2_1;
delta_IkBaNFkB  = delta_IkBaNFkB  + flux_k2_1;

%%% === k2_2: IkBbNFkBn => IkBbNFkB
delta_IkBbNFkBn = delta_IkBbNFkBn - flux_k2_2;
delta_IkBbNFkB  = delta_IkBbNFkB  + flux_k2_2;

%%% === k2_3: IkBeNFkBn => IkBeNFKB
delta_IkBeNFkBn = delta_IkBeNFkBn - flux_k2_3;
delta_IkBeNFkB  = delta_IkBeNFkB  + flux_k2_3;

%%% === r1_1: IkBaIKK => IKK
delta_IKKIkBa = delta_IKKIkBa - flux_r1_1;
delta_IKK     = delta_IKK     + flux_r1_1;

%%% === r2_1: IkBbIKK => IKK
delta_IKKIkBb = delta_IKKIkBb - flux_r2_1;
delta_IKK     = delta_IKK     + flux_r2_1;

%%% === r3_1: IkBeIKK => IKK
delta_IKKIkBe = delta_IKKIkBe - flux_r3_1;
delta_IKK     = delta_IKK     + flux_r3_1;
```

```
%%% === r4_1: IkBaIKKNFkB => IKK + NFkB
delta_IKKIkBaNFkB = delta_IKKIkBaNFkB - flux_r4_1;
delta_NFkB        = delta_NFkB        + flux_r4_1;
delta_IKK         = delta_IKK         + flux_r4_1;

%%% === r5_1: IkBbIKKNFkB => IKK + NFkB
delta_IKKIkBbNFkB = delta_IKKIkBbNFkB - flux_r5_1;
delta_NFkB        = delta_NFkB        + flux_r5_1;
delta_IKK         = delta_IKK         + flux_r5_1;

%%% === r6_1: IkBeIKKNFkB => IKK + NFkB
delta_IKKIkBeNFkB = delta_IKKIkBeNFkB - flux_r6_1;
delta_NFkB        = delta_NFkB        + flux_r6_1;
delta_IKK         = delta_IKK         + flux_r6_1;

%%% === tp1_1: IkBa => IkBaN
delta_IkBa  = delta_IkBa  - flux_tp1_1;
delta_IkBan = delta_IkBan + flux_tp1_1;

%%% === tp1_2: IkBb => IkBbN
delta_IkBb  = delta_IkBb  - flux_tp1_2;
delta_IkBbn = delta_IkBbn + flux_tp1_2;

%%% === tp1_3: IkBe => IkBen
delta_IkBe  = delta_IkBe  - flux_tp1_3;
delta_IkBen = delta_IkBen + flux_tp1_3;

%%% === tp2_1: IkBan => IkBa
delta_IkBan = delta_IkBan - flux_tp2_1;
delta_IkBa  = delta_IkBa  + flux_tp2_1;

%%% === tp2_2: IkBbn => IkBb
delta_IkBbn = delta_IkBbn - flux_tp2_2;
delta_IkBb  = delta_IkBb  + flux_tp2_2;

%%% === tp2_3: IkBen => IkBe
delta_IkBen = delta_IkBen - flux_tp2_3;
delta_IkBe  = delta_IkBe  + flux_tp2_3;

%%% === tr1_1: => IkBa
delta_IkBa = delta_IkBa + flux_tr1_1;

%%% === tr1_2: => IkBb
delta_IkBb = delta_IkBb + flux_tr1_2;

%%% === tr1_3: => IkBe
delta_IkBe = delta_IkBe + flux_tr1_3;

%%% === tr2_1: 2 NFkB => IkBat + 2 NFkB
delta_IkBat = delta_IkBat + flux_tr2_1;

%%% === tr2a_1: => IkBat
delta_IkBat = delta_IkBat + flux_tr2a_1;

%%% === tr2b_1: => IkBbt
delta_IkBbt = delta_IkBbt + flux_tr2b_1;

%%% === tr2e_1: IkBet
delta_IkBet = delta_IkBet + flux_tr2e_1;

%%% === tr3_1: IkBat =>
delta_IkBat = delta_IkBat - flux_tr3_1;

%%% === tr3_2: IkBbt =>
delta_IkBbt = delta_IkBbt - flux_tr3_2;

%%% === tr3_3: IkBet =>
```

```
  delta_IkBet = delta_IkBet - flux_tr3_3;

  % +-------------------------------------------------------------
  % | Special: FR decay
  % +-------------------------------------------------------------

  delta_FR = 0;

  deltas(1)  = delta_NFkB        ;
  deltas(2)  = delta_NFkBn       ;
  deltas(3)  = delta_IkBat       ;
  deltas(4)  = delta_IkBbt       ;
  deltas(5)  = delta_IkBet       ;
  deltas(6)  = delta_IkBa        ;
  deltas(7)  = delta_IkBb        ;
  deltas(8)  = delta_IkBe        ;
  deltas(9)  = delta_IkBan       ;
  deltas(10) = delta_IkBbn       ;
  deltas(11) = delta_IkBen       ;
  deltas(12) = delta_IkBaNFkB    ;
  deltas(13) = delta_IkBbNFkB    ;
  deltas(14) = delta_IkBeNFkB    ;
  deltas(15) = delta_IkBaNFkBn   ;
  deltas(16) = delta_IkBbNFkBn   ;
  deltas(17) = delta_IkBeNFkBn   ;
  deltas(18) = delta_IKK         ;
  deltas(19) = delta_IKKIkBa     ;
  deltas(20) = delta_IKKIkBb     ;
  deltas(21) = delta_IKKIkBe     ;
  deltas(22) = delta_IKKIkBaNFkB ;
  deltas(23) = delta_IKKIkBbNFkB ;
  deltas(24) = delta_IKKIkBeNFkB ;
  deltas(25) = delta_FR          ;

end
```

File: nfkb_equilibrate.m

```
%=================================================
% NFKB_EQUILIBRATE
%=================================================

function results = nfkb_equilibrate()
  global equilibration_flag;

  equilibration_flag = 1;

  nfkb_set_params(-1);
  starting_mets = zeros(25,1);
  mets = nfkb_adjust_mets(-1, starting_mets);

  f = str2func('nfkb_core');
  [times results] = ode15s(f, [-2000 0],mets,[]);

  equilibration_flag = 0;

end
```

File: nfkb_fluxes.m

```
%=================================================
% NFKB_FLUXES
%=================================================

function fluxes = nfkb_fluxes(x,t)
```

```
  global version;

  if     strcmp(version, '1_0')
    fluxes = nfkb_fluxes_1_0(x,t);
  elseif strcmp(version, '1_1')
    fluxes = nfkb_fluxes_1_1(x,t);
  elseif strcmp(version, '1_2')
    fluxes = nfkb_fluxes_1_2(x,t);
  else
    error('Unknown version');
  end
end
```

File: nfkb_fluxes_1_1.m

```
%=================================================
% NFKB_FLUXES_1_1
%=================================================

function fluxes = nfkb_fluxes_1_1(x,t)
  global equilibration_flag;

  params = nfkb_set_params(t);
  xparams = nfkb_expand_params(params);

  NFkB        = x(1);  % Free cytoplasmic NF-kB protein
  NFkBn       = x(2);  % Free nuclear NF-kB protein
  IkBat       = x(3);  % IkB mRNA transcript levels
  IkBbt       = x(4);  % IkB mRNA transcript levels
  IkBet       = x(5);  % IkB mRNA transcript levels
  IkBa        = x(6);  % Free cytoplasmic IkB proteins
  IkBb        = x(7);  % Free cytoplasmic IkB proteins
  IkBe        = x(8);  % Free cytoplasmic IkB proteins
  IkBan       = x(9);  % Free nuclear IkB proteins
  IkBbn       = x(10); % Free nuclear IkB proteins
  IkBen       = x(11); % Free nuclear IkB proteins
  IkBaNFkB    = x(12); % Cytoplasmic IkB-NFkB complexes
  IkBbNFkB    = x(13); % Cytoplasmic IkB-NFkB complexes
  IkBeNFkB    = x(14); % Cytoplasmic IkB-NFkB complexes
  IkBaNFkBn   = x(15); % Nuclear IkB-NFkB complexes
  IkBbNFkBn   = x(16); % Nuclear IkB-NFkB complexes
  IkBeNFkBn   = x(17); % Nuclear IkB-NFkB complexes
  IKK         = x(18); % Free cytoplasmic IKK protein
  IKKIkBa     = x(19); % Cytoplasmic IKK-IkB complexes
  IKKIkBb     = x(20); % Cytoplasmic IKK-IkB complexes
  IKKIkBe     = x(21); % Cytoplasmic IKK-IkB complexes
  IKKIkBaNFkB = x(22); % Cytoplasmic IKK-IkB-NFkB complexes
  IKKIkBbNFkB = x(23); % Cytoplasmic IKK-IkB-NFkB complexes
  IKKIkBeNFkB = x(24); % Cytoplasmic IKK-IkB-NFkB complexes
  fr          = x(25);

  a1_1   = xparams(1);
  a2_1   = xparams(2);
  a3_1   = xparams(3);
  a4_1   = xparams(4);
  a4_2   = xparams(5);
  a4_3   = xparams(6);
  a5_1   = xparams(7);
  a5_2   = xparams(8);
  a5_3   = xparams(9);
  a6_1   = xparams(10);
  a6_2   = xparams(11);
  a6_3   = xparams(12);
  a7_1   = xparams(13);
  a8_1   = xparams(14);
  a9_1   = xparams(15);
```

```
d1_1   = xparams(16);
d1_2   = xparams(17);
d2_1   = xparams(18);
d2_2   = xparams(19);
d3_1   = xparams(20);
d3_2   = xparams(21);
d4_1   = xparams(22);
d4_2   = xparams(23);
d4_3   = xparams(24);
d5_1   = xparams(25);
d5_2   = xparams(26);
d5_3   = xparams(27);
d6_1   = xparams(28);
d6_2   = xparams(29);
d6_3   = xparams(30);
deg1_1 = xparams(31);
deg1_2 = xparams(32);
deg1_3 = xparams(33);
deg1_4 = xparams(34);
deg1_5 = xparams(35);
deg1_6 = xparams(36);
deg4_1 = xparams(37);
deg4_2 = xparams(38);
deg4_3 = xparams(39);
deg4_4 = xparams(40);
deg4_5 = xparams(41);
deg4_6 = xparams(42);
k01_1  = xparams(43);
k02_1  = xparams(44);
k1_1   = xparams(45);
k2_1   = xparams(46);
k2_2   = xparams(47);
k2_3   = xparams(48);
r1_1   = xparams(49);
r2_1   = xparams(50);
r3_1   = xparams(51);
r4_1   = xparams(52);
r5_1   = xparams(53);
r6_1   = xparams(54);
tp1_1  = xparams(55);
tp1_2  = xparams(56);
tp1_3  = xparams(57);
tp2_1  = xparams(58);
tp2_2  = xparams(59);
tp2_3  = xparams(60);
tr1_1  = xparams(61);
tr1_2  = xparams(62);
tr1_3  = xparams(63);
tr2_1  = xparams(64);
tr2a_1 = xparams(65);
tr2b_1 = xparams(66);
tr2e_1 = xparams(67);
tr3_1  = xparams(68);
tr3_2  = xparams(69);
tr3_3  = xparams(70);

fluxes(1)  = a1_1    * IKK         * IkBa  ; % a1_1: IkBa + IKK => IkBaIKK
fluxes(2)  = a2_1    * IkBb        * IKK   ; % a2_1: IkBb + IKK => IkBbIKK
fluxes(3)  = a3_1    * IkBe        * IKK   ; % a3_1: IkBe + IKK => IkBeIKK
fluxes(4)  = a4_1    * NFkB * IkBa         ; % a4_1: IkBa + NFkB => IkBaNFkB
fluxes(5)  = a4_2    * NFkB * IKKIkBa      ; % a4_2: IkBaIKK + NFkB => IkBaIKKNFkB
fluxes(6)  = a4_3    * NFkBn       * IkBan ; % a4_3: IkBan +NFkBn => IkBaNFkBn
fluxes(7)  = a5_1    * NFkB * IkBb         ; % a5_1: IkBb + NFkB => IkBbNFkB
fluxes(8)  = a5_2    * NFkB * IKKIkBb      ; % a5_2: IkBbIKK + NFkB => IkBbIKKNFkB
fluxes(9)  = a5_3    * NFkBn       * IkBbn ; % a5_3: IkBbn + NFkBn => IkBbNFkBn
fluxes(10) = a6_1    * NFkB * IkBe         ; % a6_1: IkBe + NFkB => IkBeNFkB
fluxes(11) = a6_2    * NFkB * IKKIkBe      ; % a6_2: IkBeIKK + NFkB => IkBeIKKNFkB
```

```
  fluxes(12) = a6_3    * NFkBn       * IkBen ; % a6_3: IkBen + NFkBn => IkBeNFkBn
  fluxes(13) = a7_1    * IkBaNFkB    * IKK   ; % a7_1: IkBaNFkB + IKK => IkBaIKKNFkB
  fluxes(14) = a8_1    * IkBbNFkB    * IKK   ; % a8_1: IkBbNFkB + IKK => IkBbIKKNFkB
  fluxes(15) = a9_1    * IkBeNFkB    * IKK   ; % a9_1: IkBeNFkB + IKK => IkBeIKKNFkB
  fluxes(16) = d1_1    * IKKIkBa             ; % d1_1: IkBaIKK => IkBa + IKK
  fluxes(17) = d1_2    * IKKIkBaNFkB         ; % d1_2: IkBaIKKNFkB => IkBaNFkB + IKK
  fluxes(18) = d2_1    * IKKIkBb             ; % d2_1: IkBbIKK => IkBb + IKK
  fluxes(19) = d2_2    * IKKIkBbNFkB         ; % d2_2: IkBbIKKNFkB => IkBbNFkB + IKK
  fluxes(20) = d3_1    * IKKIkBe             ; % d3_1: IkBeIKK => IkBe + IKK
  fluxes(21) = d3_2    * IKKIkBeNFkB         ; % d3_2: IkBeIKKNFkB => IkBeNFkB + IKK
  fluxes(22) = d4_1    * IkBaNFkB            ; % d4_1: IkBaNFkB => IkBa + NFkB
  fluxes(23) = d4_2    * IkBaNFkBn           ; % d4_2: IkBaNFkBn => IkBan + NFkBn
  fluxes(24) = d4_3    * IKKIkBaNFkB         ; % d4_3: IkBaIKKNFkB => IkBaIKK + NFkB
  fluxes(25) = d5_1    * IkBbNFkB            ; % d5_1: IkBbNFkB => IkBb + NFkB
  fluxes(26) = d5_2    * IkBbNFkBn           ; % d5_2: IkBbNFkBn => IkBbn + NFkBn
  fluxes(27) = d5_3    * IKKIkBbNFkB         ; % d5_3: IkBbIKKNFkB => IkBbIKK + NFkB
  fluxes(28) = d6_1    * IkBeNFkB            ; % d6_1: IkBeNFkB => IkBb + NFkB
  fluxes(29) = d6_2    * IkBeNFkBn           ; % d6_2: IkBeNFkBn => IkBen + NFkBn
  fluxes(30) = d6_3    * IKKIkBeNFkB         ; % d6_3: IkBeIKKNFkB => IkBeIKK + NFkB
  fluxes(31) = deg1_1  * IkBa                ; % deg1_1: IkBa =>
  fluxes(32) = deg1_2  * IkBb                ; % deg1_2: IkBb =>
  fluxes(33) = deg1_3  * IkBe                ; % deg1_3: IkBe =>
  fluxes(34) = deg1_4  * IkBan               ; % deg1_4: IkBa =>
  fluxes(35) = deg1_5  * IkBbn               ; % deg1_5: IkBb =>
  fluxes(36) = deg1_6  * IkBen               ; % deg1_6: IkBe =>
  fluxes(37) = deg4_1  * IkBaNFkB            ; % deg4_1: IkBaNFkB => NFkB
  fluxes(38) = deg4_2  * IkBbNFkB            ; % deg4_2: IkBbNFkB => NFkB
  fluxes(39) = deg4_3  * IkBeNFkB            ; % deg4_3: IkBeNFkB => NFkB
  fluxes(40) = deg4_4  * IkBaNFkBn           ; % deg4_4: IkBaNFkB => NFkB
  fluxes(41) = deg4_5  * IkBbNFkBn           ; % deg4_5: IkBbNFkB => NFkB
  fluxes(42) = deg4_6  * IkBeNFkBn           ; % deg4_6: IkBeNFkB => NFkB
  fluxes(43) = k01_1   * NFkBn               ; % k01_1: NFkBn => NFkB
  fluxes(44) = k02_1   * IKK                 ; % k02_1: IKK =>
  fluxes(45) = k1_1    * NFkB                ; % k1_1: NFkB => NFkBn
  fluxes(46) = k2_1    * IkBaNFkBn           ; % k2_1: IkBaNFkBn => IkBaNFkB
  fluxes(47) = k2_2    * IkBbNFkBn           ; % k2_2: IkBbNFkBn => IkBbNFkB
  fluxes(48) = k2_3    * IkBeNFkBn           ; % k2_3: IkBeNFkBn => IkBeNFKB
  fluxes(49) = r1_1    * IKKIkBa             ; % r1_1: IkBaIKK => IKK
  fluxes(50) = r2_1    * IKKIkBb             ; % r2_1: IkBbIKK => IKK
  fluxes(51) = r3_1    * IKKIkBe             ; % r3_1: IkBeIKK => IKK
  fluxes(52) = r4_1    * IKKIkBaNFkB         ; % r4_1: IkBaIKKNFkB => IKK + NFkB
  fluxes(53) = r5_1    * IKKIkBbNFkB         ; % r5_1: IkBbIKKNFkB => IKK + NFkB
  fluxes(54) = r6_1    * IKKIkBeNFkB         ; % r6_1: IkBeIKKNFkB => IKK + NFkB
  fluxes(55) = tp1_1   * IkBa                ; % tp1_1: IkBa => IkBaN
  fluxes(56) = tp1_2   * IkBb                ; % tp1_2: IkBb => IkBbN
  fluxes(57) = tp1_3   * IkBe                ; % tp1_3: IkBe => IkBen
  fluxes(58) = tp2_1   * IkBan               ; % tp2_1: IkBan => IkBa
  fluxes(59) = tp2_2   * IkBbn               ; % tp2_2: IkBbn => IkBb
  fluxes(60) = tp2_3   * IkBen               ; % tp2_3: IkBen => IkBe
  fluxes(61) = tr1_1   * IkBat               ; % tr1_1: => IkBa
  fluxes(62) = tr1_2   * IkBbt               ; % tr1_2: => IkBb
  fluxes(63) = tr1_3   * IkBet               ; % tr1_3: => IkBe
  fluxes(64) = tr2_1   * NFkBn       * NFkBn ; % tr2_1: 2 NFkB => IkBat + 2 NFkB
  fluxes(65) = tr2a_1                        ; % tr2a_1: => IkBat
  fluxes(66) = tr2b_1                        ; % tr2b_1: => IkBbt
  fluxes(67) = tr2e_1                        ; % tr2e_1: IkBet
  fluxes(68) = tr3_1   * IkBat               ; % tr3_1: IkBat =>
  fluxes(69) = tr3_2   * IkBbt               ; % tr3_2: IkBbt =>
  fluxes(70) = tr3_3   * IkBet               ; % tr3_3: IkBet =>

end
```

File: nfkb_main_2.m

```
%================================================
% NFKB_MAIN2
```

```
%================================================
function nfkb_main2(sim_struct)
  if not(exist('sim_struct')); sim_struct = nfkb_sim_defaults(); end

  global version;
  global ko;

  version     = sim_struct.version;
  ko          = sim_struct.ko;
  output_file = sim_struct.output_file;
  output_type = sim_struct.output_type;
  total_time  = sim_struct.total_time;
  stim_time   = sim_struct.stim_time;
  equilibrate = sim_struct.equilibrate;

  nfkb_validate_version(version);
  nfkb_validate_output_type(output_type);

  if     (strcmp(equilibrate, 'none') == 1)
    results = nfkb_equilibrate();
    starting_mets = transpose(results(end,:));
  elseif (strcmp(equilibrate, 'time') == 1)
    [time results] = nfkb_check_equilibrate();
    starting_mets = transpose(results(end,:));
else
    error('equilibration strategy unknown');
  end

  [times,results] = nfkb_simulate(starting_mets, total_time, stim_time);
  nfkb_save_figures(output_file, output_type, times, results);
end
```

File: nfkb_results_dir.m

```
%================================================
% NFKB_RESULTS_DIR
%================================================

function nfkb_results_dir()
  status = exist('results');
  if (status ~= 7)
    mkdir('results');
  end
end
```

File: nfkb_save_figures.m

```
%================================================
% NFKB_SAVE
%================================================

function nfkb_save(output_file, output_type, times, results)

  fid = fopen(output_file, 'a');
  if strcmp(output_type, 'nfkbn_col')
    nfkb_save_nfkbn_col(fid, times, results);
  elseif strcmp(output_type, 'nfkbn_row')
    nfkb_save_nfkbn_row(fid, times, results);
  elseif strcmp(output_type, 'equilibrium_mets_row')
    nfkb_save_equilibrium_mets_row(fid, times, results);
  elseif strcmp(output_type, 'equilibrium_fluxes_row')
    nfkb_save_equilibrium_fluxes_row(fid, times, results);
  elseif strcmp(output_type, 'ikb_sums_row')
    nfkb_save_ikb_sums_row(fid, times, results);
  elseif strcmp(output_type, 'equilibrium_nfkbn')
```

```
    nfkb_save_equilibrium_nfkbn(fid, times, results);
  elseif strcmp(output_type, 'equilibrium_deg_fluxes_row')
    nfkb_save_equilibrium_deg_fluxes_row(fid, times, results);
  elseif strcmp(output_type, 'equilibrium_deltas_row')
    nfkb_save_equilibrium_deltas_row(fid, results);
  else
    error('output_type not recognized');
  end
  fclose(fid);

end
```

File: nfkb_save_nfkbn_col.m

```
%================================================
% NFKB_SAVE_NFKBN_COL
%================================================

function nfkb_save_nfkbn_col(fid, times, results)

  active_nfkb = 1000*nfkb_active(results);

  time_fixed = 0:1:360;
  nfkb_fixed = interp1(transpose(times), ...
                       transpose(active_nfkb), time_fixed);

  fprintf(fid,'%4.2f\n',  nfkb_fixed);

end
```

File: nfkb_set_params.m

```
%================================================
% NFKB_SET_PARAMS
%================================================
function params = nfkb_set_params(time)
  global version;
  if strcmp(version, '1_0')
    params = nfkb_set_params_1_0(time);
  elseif strcmp(version, '1_1')
    params = nfkb_set_params_1_1(time);
  elseif strcmp(version, '1_2')
    params = nfkb_set_params_1_2(time);
  else
    error('Unknown version');
  end
end
```

File: nfkb_set_params_1_1.m

```
%================================================
% NFKB_SET_PARAMS_1_1
%================================================

function params = nfkb_set_params_1_1(time)

  global equilibration_flag;
  global stim_time;
  global ko;
  global param_multipliers;

  params(1,1)  =    1.35       ;   % a1    Two component interaction
  params(2,1)  =    0.36       ;   % a2    Two component interaction
  params(3,1)  =    0.54       ;   % a3    Two component interaction
```

```
  params(4,1)  =   30.0        ;   % a4    Two component interaction
  params(5,1)  =   30.0        ;   % a5    Two component interaction
  params(6,1)  =   30.0        ;   % a6    Two component interaction
  params(7,1)  =   11.1        ;   % a7    Three component interactions
  params(8,1)  =    2.88       ;   % a8    Three component interactions
  params(9,1)  =    4.2        ;   % a9    Three component interactions
  params(10,1) =    0.075      ;   % d1    Two component interaction
  params(11,1) =    0.105      ;   % d2    Two component interaction
  params(12,1) =    0.105      ;   % d3    Two component interaction
  params(13,1) =    0.00006    ;   % DIFFERENT d4    Two component interaction
  params(14,1) =    0.00006    ;   % DIFFERENT d5    Two component interaction
  params(15,1) =    0.00006    ;   % DIFFERENT d6    Two component interaction
  params(16,1) =    0.12       ;   % DIFFERENT deg1  Synthesis and degradation
  params(17,1) =    0.00006    ;   % DIFFERENT deg4  Synthesis and degradation
  params(18,1) =    0.0048     ;   % k01   Nucleo-cytoplasmic transport
  params(19,1) =     0.0072      ;    % k02    % IKK adaptation (signal removal 0.18 see
below)
  params(20,1) =    5.4        ;   % k1    Nucleo-cytoplasmic transport
  params(21,1) =    0.828      ;   % k2    % Nucleo-cytoplasmic transport (1.38e-2?)

  params(22,1) =    0.072      ;   % DIFFERENT r1    Two component interaction
  params(23,1) =    0.024      ;   % DIFFERENT r2    Two component interaction
  params(24,1) =    0.036      ;   % DIFFERENT r3    Two component interaction

  params(25,1) =    0.36       ;   % DIFFERENT r4    Three component interactions
  params(26,1) =    0.12       ;   % DIFFERENT r5    Three component interactions
  params(27,1) =    0.18       ;   % DIFFERENT r6    Three component interactions

  params(28,1) =    0.018      ;   % tp1   Nucleo-cytoplasmic transport
  params(29,1) =    0.012      ;   % tp2   Nucleo-cytoplasmic transport
  params(30,1) =    0.2448     ;   % tr1   Synthesis and degradation

  params(31,1) =    1.98       ;   % DIFFERENT tr2   Synthesis and degradation
  params(32,1) =    0.0001848  ;   % DIFFERENT tr2a  Synthesis and degradation
  params(33,1) =    0.00004272 ;   % DIFFERENT tr2b  Synthesis and degradation
  params(34,1) =    0.00003048 ;   % DIFFERENT tr2e  Synthesis and degradation

  params(35,1) =    0.0168     ;   % tr3   Synthesis and degradation

  if (equilibration_flag == 1)
    params(19,1) =    0;           % k02   % IKK adaptation
  end

  if (equilibration_flag == 0)
    if (time > stim_time)
      params(19,1) =    0.18     ;   % k02   % IKK adaptation
    end
  end

  if (findstr(ko, 'a'))
    params(31,1) = 0; % tr2
    params(32,1) = 0; % tr2a
  end

  if (findstr(ko, 'b'))
    params(33,1) = 0; % tr2
  end

  if (findstr(ko, 'e'))
    params(34,1) = 0; % tr2
  end

end
```

File: nfkb_sim_defaults.m

```
%================================================
% NFKB_SIM_DEFAULTS
%================================================

function sim_struct = nfkb_sim_defaults()
  % equilibrate
  % - none
  % - time

  sim_struct             = struct();
  sim_struct.version     = '1_0';
  sim_struct.ko          = 'wt';
  sim_struct.output_file = 'holdout.txt';
  sim_struct.output_type = 'nfkbn_col';
  sim_struct.total_time  = 360;
  sim_struct.stim_time   = 360;
  sim_struct.equilibrate = 'time';

end
```

File: nfkb_simulate.m

```
%================================================
% NFKB_SIMULATE
%================================================

function [times, results] = nfkb_simulate(starting_mets, total_time, input_stim_time)

  global stim_time;

  stim_time = input_stim_time;
  mets = nfkb_adjust_mets(0, starting_mets);
  f = str2func('nfkb_core');
  [times results] = ode15s(f, [0 total_time],mets,[]);

end
```

File: nfkb_validate_output_type.m

```
%================================================
% NFKB_VALIDATE_OUTPUT_TYPE
%================================================

function nfkb_validate_output_type(output_type)
  types = {'nfkbn_col'                 ; ...
           'nfkbn_row'                 ; ...
           'equilibrium_mets_row'      ; ...
           'equilibrium_fluxes_row'    ; ...
           'ikb_sums_row'              ; ...
           'equilibrium_nfkbn '        ; ...
           'equilibrium_deg_fluxes_row' ; ...
           'equilibrium_deltas_row'    ; ...
          };
  index = strmatch(output_type, types);
  if (isempty(index)); error('output_type not recognized'); end
end
```

File: nfkb_validate_version.m

```
%================================================
% NFKB_VALIDATE_VERSION
%================================================

function nfkb_validate_version(version)
```

```
  versions = { '1_0'; ...
               '1_1'; ...
               '1_2'; ...
             };
  index = strmatch(version, versions);
  if (isempty(index)); error('version not recognized'); end
end
```

Appendix B Model 2.0

File: nfkb_run_2.m

```
%=========================================================
params(1,1) = 11.1;    % a_c_2ani
params(2,1) = 2.88;    % a_c_2bni
params(3,1) = 4.2;     % a_c_2eni
params(4,1) = 1.35;    % a_c_ai
params(5,1) = 30.0;    % a_c_an
params(6,1) = 0.36;    % a_c_bi
params(7,1) = 30.0;    % a_c_bn
params(8,1) = 0.54;    % a_c_ei
params(9,1) = 30.0;    % a_c_en
params(10,1) = 0.075;  % d_c_ai
params(11,1) = 0.00006;       % d_c_an
params(12,1) = 0.105;  % d_c_bi
params(13,1) = 0.00006;       % d_c_bn
params(14,1) = 0.105;  % d_c_ei
params(15,1) = 0.00006;       % d_c_en
params(16,1) = 0.828;  % ex_2an
params(17,1) = 0.012;  % ex_a
params(18,1) = 0.0048;        % ex_n
params(19,1) = 3.0;    % h_an
params(20,1) = 3.0;    % h_en
params(21,1) = 0.018;  % in_a
params(22,1) = 5.4;    % in_n
params(23,1) = 0.0018;        % pd_c_2ai
params(24,1) = 0.00006;       % pd_c_2an
params(25,1) = 0.0006;        % pd_c_2bi
params(26,1) = 0.0012;        % pd_c_2ei
params(27,1) = 0.36;   % pd_c_3ain
params(28,1) = 0.12;   % pd_c_3bin
params(29,1) = 0.18;   % pd_c_3ein
params(30,1) = 0.12;   % pd_c_a
params(31,1) = 0.2448;        % ps_c_a
params(32,1) = 0.0168;        % rd_a
params(33,1) = 1.98     * 4;   % rsr_an
params(34,1) = 0.2      * 4;   % rsr_en
params(35,1) = 0.0001848  * 1;        % rsu_a
params(36,1) = 0.00004272 * 1;        % rsu_b
params(37,1) = 0.00003048 * 1;        % rsu_e
%=========================================================
inputname = 'ikk_tnf.txt';
outputname = 'nfkb_tnf.dat';

fh2 = fopen(outputname, 'w+');
ikk = load(inputname);
fullikk   = interp1(0:5:120,ikk, 0:1:120);
nfkb_sim(fh2, params, fullikk);
fclose(fh2);
%=========================================================
inputname = 'ikk_lps.txt';
outputname = 'nfkb_lps.dat';

fh2 = fopen(outputname, 'w+');
ikk = load(inputname);
fullikk   = interp1(0:5:120,ikk, 0:1:120);
nfkb_sim(fh2, params, fullikk);
fclose(fh2);
%=========================================================
```

File: nfkb_sim.m

```
function nfkb_sim(fh2, params, ikk);
```

```
%=========================================================

initvalues = zeros(24,1);
initvalues(1,1)       = 0.0;   % IkBa
initvalues(2,1)       = 0.0;   % IkBaIKK
initvalues(3,1)       = 0.0;   % IkBaIKKNFkB
initvalues(4,1)       = 0.0;   % IkBan
initvalues(5,1)       = 0.07;  % IkBaNFkB
initvalues(6,1)       = 0.0;   % IkBaNFkBn
initvalues(7,1)       = 0.0;   % IkBat
initvalues(8,1)       = 0.0;   % IkBb
initvalues(9,1)       = 0.0;   % IkBbIKK
initvalues(10,1)      = 0.0;   % IkBbIKKNFkB
initvalues(11,1)      = 0.0;   % IkBbn
initvalues(12,1)      = 0.02;  % IkBbNFkB
initvalues(13,1)      = 0.0;   % IkBbNFkBn
initvalues(14,1)      = 0.0;   % IkBbt
initvalues(15,1)      = 0.0;   % IkBe
initvalues(16,1)      = 0.0;   % IkBeIKK
initvalues(17,1)      = 0.0;   % IkBeIKKNFkB
initvalues(18,1)      = 0.0;   % IkBen
initvalues(19,1)      = 0.01;  % IkBeNFkB
initvalues(20,1)      = 0.0;   % IkBeNFkBn
initvalues(21,1)      = 0.0;   % IkBet
initvalues(22,1)      = 0.001;        % IKK
initvalues(23,1)      = 0.0;   % NFkB
initvalues(24,1)      = 0.0;   % NFkBn
%=========================================================
a_c_2ani  = params(1,1);
a_c_2bni  = params(2,1);
a_c_2eni  = params(3,1);
a_c_ai    = params(4,1);
a_c_an    = params(5,1);
a_c_bi    = params(6,1);
a_c_bn    = params(7,1);
a_c_ei    = params(8,1);
a_c_en    = params(9,1);
d_c_ai    = params(10,1);
d_c_an    = params(11,1);
d_c_bi    = params(12,1);
d_c_bn    = params(13,1);
d_c_ei    = params(14,1);
d_c_en    = params(15,1);
ex_2an    = params(16,1);
ex_a      = params(17,1);
ex_n      = params(18,1);
h_an      = params(19,1);
h_en      = params(20,1);
in_a      = params(21,1);
in_n      = params(22,1);
pd_c_2ai  = params(23,1);
pd_c_2an  = params(24,1);
pd_c_2bi  = params(25,1);
pd_c_2ei  = params(26,1);
pd_c_3ain = params(27,1);
pd_c_3bin = params(28,1);
pd_c_3ein = params(29,1);
pd_c_a    = params(30,1);
ps_c_a    = params(31,1);
rd_a      = params(32,1);
rsr_an    = params(33,1);
rsr_en    = params(34,1);
rsu_a     = params(35,1);
rsu_b     = params(36,1);
rsu_e     = params(37,1);
%=========================================================
a_c_2ain = a_c_an;
```

```
a_c_2bin = a_c_bn;
a_c_2ein = a_c_en;
a_n_an = a_c_an;
a_n_bn = a_c_bn;
a_n_en = a_c_en;
d_c_2ain = d_c_an;
d_c_2ani = d_c_ai;
d_c_2bin = d_c_bn;
d_c_2bni = d_c_bi;
d_c_2ein = d_c_en;
d_c_2eni = d_c_ei;
d_n_an = d_c_an;
d_n_bn = d_c_bn;
d_n_en = d_c_en;
ex_2bn = ex_2an * 0.5;
ex_2en = ex_2an * 0.5;
ex_b = ex_a;
ex_e = ex_a;
in_b = in_a;
in_e = in_a;
pd_c_2bn = pd_c_2an;
pd_c_2en = pd_c_2an;
pd_c_b = pd_c_a * 1.5;
pd_c_e = pd_c_a * 1.5;
pd_n_2an = pd_c_2an;
pd_n_2bn = pd_c_2an;
pd_n_2en = pd_c_2an;
pd_n_a = pd_c_a;
pd_n_b = pd_c_a * 1.5;
pd_n_e = pd_c_a * 1.5;
ps_c_b = ps_c_a;
ps_c_e = ps_c_a;
rd_b = rd_a;
rd_e = rd_a;
%=============================================================
paramall = zeros(72,1);
paramall(1,1) = a_c_2ain;
paramall(2,1) = a_c_2ani;
paramall(3,1) = a_c_2bin;
paramall(4,1) = a_c_2bni;
paramall(5,1) = a_c_2ein;
paramall(6,1) = a_c_2eni;
paramall(7,1) = a_c_ai;
paramall(8,1) = a_c_an;
paramall(9,1) = a_c_bi;
paramall(10,1) = a_c_bn;
paramall(11,1) = a_c_ei;
paramall(12,1) = a_c_en;
paramall(13,1) = a_n_an;
paramall(14,1) = a_n_bn;
paramall(15,1) = a_n_en;
paramall(16,1) = d_c_2ain;
paramall(17,1) = d_c_2ani;
paramall(18,1) = d_c_2bin;
paramall(19,1) = d_c_2bni;
paramall(20,1) = d_c_2ein;
paramall(21,1) = d_c_2eni;
paramall(22,1) = d_c_ai;
paramall(23,1) = d_c_an;
paramall(24,1) = d_c_bi;
paramall(25,1) = d_c_bn;
paramall(26,1) = d_c_ei;
paramall(27,1) = d_c_en;
paramall(28,1) = d_n_an;
paramall(29,1) = d_n_bn;
paramall(30,1) = d_n_en;
paramall(31,1) = ex_2an;
```

```
paramall(32,1) = ex_2bn;
paramall(33,1) = ex_2en;
paramall(34,1) = ex_a;
paramall(35,1) = ex_b;
paramall(36,1) = ex_e;
paramall(37,1) = ex_n;
paramall(38,1) = h_an;
paramall(39,1) = h_en;
paramall(40,1) = in_a;
paramall(41,1) = in_b;
paramall(42,1) = in_e;
paramall(43,1) = in_n;
paramall(44,1) = pd_c_2ai;
paramall(45,1) = pd_c_2an;
paramall(46,1) = pd_c_2bi;
paramall(47,1) = pd_c_2bn;
paramall(48,1) = pd_c_2ei;
paramall(49,1) = pd_c_2en;
paramall(50,1) = pd_c_3ain;
paramall(51,1) = pd_c_3bin;
paramall(52,1) = pd_c_3ein;
paramall(53,1) = pd_c_a;
paramall(54,1) = pd_c_b;
paramall(55,1) = pd_c_e;
paramall(56,1) = pd_n_2an;
paramall(57,1) = pd_n_2bn;
paramall(58,1) = pd_n_2en;
paramall(59,1) = pd_n_a;
paramall(60,1) = pd_n_b;
paramall(61,1) = pd_n_e;
paramall(62,1) = ps_c_a;
paramall(63,1) = ps_c_b;
paramall(64,1) = ps_c_e;
paramall(65,1) = rd_a;
paramall(66,1) = rd_b;
paramall(67,1) = rd_e;
paramall(68,1) = rsr_an;
paramall(69,1) = rsr_en;
paramall(70,1) = rsu_a;
paramall(71,1) = rsu_b;
paramall(72,1) = rsu_e;
%=========================================================
[tsim1, results1] = ode15s('nfkb_ode', [-2000 0], initvalues, [], paramall, []);
%=========================================================
initvalues = results1(end,:)';
[tsim1, results1] = ode15s('nfkb_ode', [0 120], initvalues, [], paramall, ikk);
%=========================================================
cols = size(results1,2);
last_col = cols;
output = interp1(tsim1, results1(:,last_col),0:120);
fprintf(fh2, '%.8f\t', output);
fprintf(fh2, '\n');
```

File: nfkb_ode.m

```
function delta = nfkb_ode(t,x,flags, params, activeikk);
%============================================================
ikkcount = size(activeikk,2);
if ikkcount == 0;
  phase = 1;
else;
  phase = 2;
end;

IkBa           = x(1);
IkBaIKK        = x(2);
IkBaIKKNFkB    = x(3);
IkBan          = x(4);
IkBaNFkB       = x(5);
IkBaNFkBn      = x(6);
IkBat          = x(7);
IkBb           = x(8);
IkBbIKK        = x(9);
IkBbIKKNFkB    = x(10);
IkBbn          = x(11);
IkBbNFkB       = x(12);
IkBbNFkBn      = x(13);
IkBbt          = x(14);
IkBe           = x(15);
IkBeIKK        = x(16);
IkBeIKKNFkB    = x(17);
IkBen          = x(18);
IkBeNFkB       = x(19);
IkBeNFkBn      = x(20);
IkBet          = x(21);
IKK            = x(22);
NFkB           = x(23);
NFkBn          = x(24);
%============================================================
a_c_2ain       = params(1,1);
a_c_2ani       = params(2,1);
a_c_2bin       = params(3,1);
a_c_2bni       = params(4,1);
a_c_2ein       = params(5,1);
a_c_2eni       = params(6,1);
a_c_ai         = params(7,1);
a_c_an         = params(8,1);
a_c_bi         = params(9,1);
a_c_bn         = params(10,1);
a_c_ei         = params(11,1);
a_c_en         = params(12,1);
a_n_an         = params(13,1);
a_n_bn         = params(14,1);
a_n_en         = params(15,1);
d_c_2ain       = params(16,1);
d_c_2ani       = params(17,1);
d_c_2bin       = params(18,1);
d_c_2bni       = params(19,1);
d_c_2ein       = params(20,1);
d_c_2eni       = params(21,1);
d_c_ai         = params(22,1);
d_c_an         = params(23,1);
d_c_bi         = params(24,1);
d_c_bn         = params(25,1);
d_c_ei         = params(26,1);
d_c_en         = params(27,1);
d_n_an         = params(28,1);
d_n_bn         = params(29,1);
d_n_en         = params(30,1);
```

```
ex_2an         = params(31,1);
ex_2bn         = params(32,1);
ex_2en         = params(33,1);
ex_a           = params(34,1);
ex_b           = params(35,1);
ex_e           = params(36,1);
ex_n           = params(37,1);
h_an           = params(38,1);
h_en           = params(39,1);
in_a           = params(40,1);
in_b           = params(41,1);
in_e           = params(42,1);
in_n           = params(43,1);
pd_c_2ai       = params(44,1);
pd_c_2an       = params(45,1);
pd_c_2bi       = params(46,1);
pd_c_2bn       = params(47,1);
pd_c_2ei       = params(48,1);
pd_c_2en       = params(49,1);
pd_c_3ain      = params(50,1);
pd_c_3bin      = params(51,1);
pd_c_3ein      = params(52,1);
pd_c_a         = params(53,1);
pd_c_b         = params(54,1);
pd_c_e         = params(55,1);
pd_n_2an       = params(56,1);
pd_n_2bn       = params(57,1);
pd_n_2en       = params(58,1);
pd_n_a         = params(59,1);
pd_n_b         = params(60,1);
pd_n_e         = params(61,1);
ps_c_a         = params(62,1);
ps_c_b         = params(63,1);
ps_c_e         = params(64,1);
rd_a           = params(65,1);
rd_b           = params(66,1);
rd_e           = params(67,1);
rsr_an         = params(68,1);
rsr_en         = params(69,1);
rsu_a          = params(70,1);
rsu_b          = params(71,1);
rsu_e          = params(72,1);
%============================================================
flux_a_c_2ain  = a_c_2ain * IkBaIKK * NFkB;
flux_a_c_2ani  = a_c_2ani * IkBaNFkB * IKK;
flux_a_c_2bin  = a_c_2bin * IkBbIKK * NFkB;
flux_a_c_2bni  = a_c_2bni * IkBbNFkB * IKK;
flux_a_c_2ein  = a_c_2ein * IkBeIKK * NFkB;
flux_a_c_2eni  = a_c_2eni * IkBeNFkB * IKK;
flux_a_c_ai    = a_c_ai * IkBa * IKK;
flux_a_c_an    = a_c_an * IkBa * NFkB;
flux_a_c_bi    = a_c_bi * IkBb * IKK;
flux_a_c_bn    = a_c_bn * IkBb * NFkB;
flux_a_c_ei    = a_c_ei * IkBe * IKK;
flux_a_c_en    = a_c_en * IkBe * NFkB;
flux_a_n_an    = a_n_an * IkBan * NFkBn;
flux_a_n_bn    = a_n_bn * IkBbn * NFkBn;
flux_a_n_en    = a_n_en * IkBen * NFkBn;
flux_d_c_2ain  = d_c_2ain * IkBaIKKNFkB;
flux_d_c_2ani  = d_c_2ani * IkBaIKKNFkB;
flux_d_c_2bin  = d_c_2bin * IkBbIKKNFkB;
flux_d_c_2bni  = d_c_2bni * IkBbIKKNFkB;
flux_d_c_2ein  = d_c_2ein * IkBeIKKNFkB;
flux_d_c_2eni  = d_c_2eni * IkBeIKKNFkB;
flux_d_c_ai    = d_c_ai * IkBaIKK;
flux_d_c_an    = d_c_an * IkBaNFkB;
flux_d_c_bi    = d_c_bi * IkBbIKK;
```

```
flux_d_c_bn    = d_c_bn * IkBbNFkB;
flux_d_c_ei    = d_c_ei * IkBeIKK;
flux_d_c_en    = d_c_en * IkBeNFkB;
flux_d_n_an    = d_n_an * IkBaNFkBn;
flux_d_n_bn    = d_n_bn * IkBbNFkBn;
flux_d_n_en    = d_n_en * IkBeNFkBn;
flux_ex_2an    = ex_2an * IkBaNFkBn;
flux_ex_2bn    = ex_2bn * IkBbNFkBn;
flux_ex_2en    = ex_2en * IkBeNFkBn;
flux_ex_a      = ex_a * IkBan;
flux_ex_b      = ex_b * IkBbn;
flux_ex_e      = ex_e * IkBen;
flux_ex_n      = ex_n * NFkBn;
flux_in_a      = in_a * IkBa;
flux_in_b      = in_b * IkBb;
flux_in_e      = in_e * IkBe;
flux_in_n      = in_n * NFkB;
flux_pd_c_2ai  = pd_c_2ai * IkBaIKK;
flux_pd_c_2an  = pd_c_2an * IkBaNFkB;
flux_pd_c_2bi  = pd_c_2bi * IkBbIKK;
flux_pd_c_2bn  = pd_c_2bn * IkBbNFkB;
flux_pd_c_2ei  = pd_c_2ei * IkBeIKK;
flux_pd_c_2en  = pd_c_2en * IkBeNFkB;
flux_pd_c_3ain         = pd_c_3ain * IkBaIKKNFkB;
flux_pd_c_3bin         = pd_c_3bin * IkBbIKKNFkB;
flux_pd_c_3ein         = pd_c_3ein * IkBeIKKNFkB;
flux_pd_c_a    = pd_c_a * IkBa;
flux_pd_c_b    = pd_c_b * IkBb;
flux_pd_c_e    = pd_c_e * IkBe;
flux_pd_n_2an  = pd_n_2an * IkBaNFkBn;
flux_pd_n_2bn  = pd_n_2bn * IkBbNFkBn;
flux_pd_n_2en  = pd_n_2en * IkBeNFkBn;
flux_pd_n_a    = pd_n_a * IkBan;
flux_pd_n_b    = pd_n_b * IkBbn;
flux_pd_n_e    = pd_n_e * IkBen;
flux_ps_c_a    = ps_c_a * IkBat;
flux_ps_c_b    = ps_c_b * IkBbt;
flux_ps_c_e    = ps_c_e * IkBet;
flux_rd_a      = rd_a * IkBat;
flux_rd_b      = rd_b * IkBbt;
flux_rd_e      = rd_e * IkBet;
flux_rsr_an    = rsr_an * NFkBn^h_an;
flux_rsr_en    = rsr_en * NFkBn^h_en;
flux_rsu_a     = rsu_a * 1;
flux_rsu_b     = rsu_b * 1;
flux_rsu_e     = rsu_e * 1;
%============================================================
delta_IkBa             = 0;
delta_IkBaIKK          = 0;
delta_IkBaIKKNFkB      = 0;
delta_IkBan            = 0;
delta_IkBaNFkB         = 0;
delta_IkBaNFkBn        = 0;
delta_IkBat            = 0;
delta_IkBb             = 0;
delta_IkBbIKK          = 0;
delta_IkBbIKKNFkB      = 0;
delta_IkBbn            = 0;
delta_IkBbNFkB         = 0;
delta_IkBbNFkBn        = 0;
delta_IkBbt            = 0;
delta_IkBe             = 0;
delta_IkBeIKK          = 0;
delta_IkBeIKKNFkB      = 0;
delta_IkBen            = 0;
delta_IkBeNFkB         = 0;
delta_IkBeNFkBn        = 0;
```

```
delta_IkBet           = 0;
delta_IKK             = 0;
delta_NFkB            = 0;
delta_NFkBn           = 0;
%=======================================================
delta_IkBaIKK         = delta_IkBaIKK     - flux_a_c_2ain;
delta_NFkB            = delta_NFkB        - flux_a_c_2ain;
delta_IkBaIKKNFkB     = delta_IkBaIKKNFkB + flux_a_c_2ain;

delta_IkBaNFkB        = delta_IkBaNFkB    - flux_a_c_2ani;
delta_IKK             = delta_IKK         - flux_a_c_2ani;
delta_IkBaIKKNFkB     = delta_IkBaIKKNFkB + flux_a_c_2ani;

delta_IkBbIKK         = delta_IkBbIKK     - flux_a_c_2bin;
delta_NFkB            = delta_NFkB        - flux_a_c_2bin;
delta_IkBbIKKNFkB     = delta_IkBbIKKNFkB + flux_a_c_2bin;

delta_IkBbNFkB        = delta_IkBbNFkB    - flux_a_c_2bni;
delta_IKK             = delta_IKK         - flux_a_c_2bni;
delta_IkBbIKKNFkB     = delta_IkBbIKKNFkB + flux_a_c_2bni;

delta_IkBeIKK         = delta_IkBeIKK     - flux_a_c_2ein;
delta_NFkB            = delta_NFkB        - flux_a_c_2ein;
delta_IkBeIKKNFkB     = delta_IkBeIKKNFkB + flux_a_c_2ein;

delta_IkBeNFkB        = delta_IkBeNFkB    - flux_a_c_2eni;
delta_IKK             = delta_IKK         - flux_a_c_2eni;
delta_IkBeIKKNFkB     = delta_IkBeIKKNFkB + flux_a_c_2eni;

delta_IkBa            = delta_IkBa        - flux_a_c_ai;
delta_IKK             = delta_IKK         - flux_a_c_ai;
delta_IkBaIKK         = delta_IkBaIKK     + flux_a_c_ai;

delta_IkBa            = delta_IkBa        - flux_a_c_an;
delta_NFkB            = delta_NFkB        - flux_a_c_an;
delta_IkBaNFkB        = delta_IkBaNFkB    + flux_a_c_an;

delta_IkBb            = delta_IkBb        - flux_a_c_bi;
delta_IKK             = delta_IKK         - flux_a_c_bi;
delta_IkBbIKK         = delta_IkBbIKK     + flux_a_c_bi;

delta_IkBb            = delta_IkBb        - flux_a_c_bn;
delta_NFkB            = delta_NFkB        - flux_a_c_bn;
delta_IkBbNFkB        = delta_IkBbNFkB    + flux_a_c_bn;

delta_IkBe            = delta_IkBe        - flux_a_c_ei;
delta_IKK             = delta_IKK         - flux_a_c_ei;
delta_IkBeIKK         = delta_IkBeIKK     + flux_a_c_ei;

delta_IkBe            = delta_IkBe        - flux_a_c_en;
delta_NFkB            = delta_NFkB        - flux_a_c_en;
delta_IkBeNFkB        = delta_IkBeNFkB    + flux_a_c_en;

delta_IkBan           = delta_IkBan       - flux_a_n_an;
delta_NFkBn           = delta_NFkBn       - flux_a_n_an;
delta_IkBaNFkBn       = delta_IkBaNFkBn   + flux_a_n_an;

delta_IkBbn           = delta_IkBbn       - flux_a_n_bn;
delta_NFkBn           = delta_NFkBn       - flux_a_n_bn;
delta_IkBbNFkBn       = delta_IkBbNFkBn   + flux_a_n_bn;

delta_IkBen           = delta_IkBen       - flux_a_n_en;
delta_NFkBn           = delta_NFkBn       - flux_a_n_en;
delta_IkBeNFkBn       = delta_IkBeNFkBn   + flux_a_n_en;

delta_IkBaIKKNFkB     = delta_IkBaIKKNFkB - flux_d_c_2ain;
delta_IkBaIKK         = delta_IkBaIKK     + flux_d_c_2ain;
```

```
delta_NFkB            = delta_NFkB        + flux_d_c_2ain;

delta_IkBaIKKNFkB     = delta_IkBaIKKNFkB - flux_d_c_2ani;
delta_IkBaNFkB        = delta_IkBaNFkB    + flux_d_c_2ani;
delta_IKK             = delta_IKK         + flux_d_c_2ani;

delta_IkBbIKKNFkB     = delta_IkBbIKKNFkB - flux_d_c_2bin;
delta_IkBbIKK         = delta_IkBbIKK     + flux_d_c_2bin;
delta_NFkB            = delta_NFkB        + flux_d_c_2bin;

delta_IkBbIKKNFkB     = delta_IkBbIKKNFkB - flux_d_c_2bni;
delta_IkBbNFkB        = delta_IkBbNFkB    + flux_d_c_2bni;
delta_IKK             = delta_IKK         + flux_d_c_2bni;

delta_IkBeIKKNFkB     = delta_IkBeIKKNFkB - flux_d_c_2ein;
delta_IkBeIKK         = delta_IkBeIKK     + flux_d_c_2ein;
delta_NFkB            = delta_NFkB        + flux_d_c_2ein;

delta_IkBeIKKNFkB     = delta_IkBeIKKNFkB - flux_d_c_2eni;
delta_IkBeNFkB        = delta_IkBeNFkB    + flux_d_c_2eni;
delta_IKK             = delta_IKK         + flux_d_c_2eni;

delta_IkBaIKK         = delta_IkBaIKK     - flux_d_c_ai;
delta_IkBa            = delta_IkBa        + flux_d_c_ai;
delta_IKK             = delta_IKK         + flux_d_c_ai;

delta_IkBaNFkB        = delta_IkBaNFkB    - flux_d_c_an;
delta_IkBa            = delta_IkBa        + flux_d_c_an;
delta_NFkB            = delta_NFkB        + flux_d_c_an;

delta_IkBbIKK         = delta_IkBbIKK     - flux_d_c_bi;
delta_IkBb            = delta_IkBb        + flux_d_c_bi;
delta_IKK             = delta_IKK         + flux_d_c_bi;

delta_IkBbNFkB        = delta_IkBbNFkB    - flux_d_c_bn;
delta_IkBb            = delta_IkBb        + flux_d_c_bn;
delta_NFkB            = delta_NFkB        + flux_d_c_bn;

delta_IkBeIKK         = delta_IkBeIKK     - flux_d_c_ei;
delta_IkBe            = delta_IkBe        + flux_d_c_ei;
delta_IKK             = delta_IKK         + flux_d_c_ei;

delta_IkBeNFkB        = delta_IkBeNFkB    - flux_d_c_en;
delta_IkBe            = delta_IkBe        + flux_d_c_en;
delta_NFkB            = delta_NFkB        + flux_d_c_en;

delta_IkBaNFkBn       = delta_IkBaNFkBn   - flux_d_n_an;
delta_IkBan           = delta_IkBan       + flux_d_n_an;
delta_NFkBn           = delta_NFkBn       + flux_d_n_an;

delta_IkBbNFkBn       = delta_IkBbNFkBn   - flux_d_n_bn;
delta_IkBbn           = delta_IkBbn       + flux_d_n_bn;
delta_NFkBn           = delta_NFkBn       + flux_d_n_bn;

delta_IkBeNFkBn       = delta_IkBeNFkBn   - flux_d_n_en;
delta_IkBen           = delta_IkBen       + flux_d_n_en;
delta_NFkBn           = delta_NFkBn       + flux_d_n_en;

delta_IkBaNFkBn       = delta_IkBaNFkBn   - flux_ex_2an;
delta_IkBaNFkB        = delta_IkBaNFkB    + flux_ex_2an;

delta_IkBbNFkBn       = delta_IkBbNFkBn   - flux_ex_2bn;
delta_IkBbNFkB        = delta_IkBbNFkB    + flux_ex_2bn;

delta_IkBeNFkBn       = delta_IkBeNFkBn   - flux_ex_2en;
delta_IkBeNFkB        = delta_IkBeNFkB    + flux_ex_2en;
```

```
delta_IkBan           = delta_IkBan       - flux_ex_a;
delta_IkBa            = delta_IkBa        + flux_ex_a;

delta_IkBbn           = delta_IkBbn       - flux_ex_b;
delta_IkBb            = delta_IkBb        + flux_ex_b;

delta_IkBen           = delta_IkBen       - flux_ex_e;
delta_IkBe            = delta_IkBe        + flux_ex_e;

delta_NFkBn           = delta_NFkBn       - flux_ex_n;
delta_NFkB            = delta_NFkB        + flux_ex_n;

delta_IkBa            = delta_IkBa        - flux_in_a;
delta_IkBan           = delta_IkBan       + flux_in_a;

delta_IkBb            = delta_IkBb        - flux_in_b;
delta_IkBbn           = delta_IkBbn       + flux_in_b;

delta_IkBe            = delta_IkBe        - flux_in_e;
delta_IkBen           = delta_IkBen       + flux_in_e;

delta_NFkB            = delta_NFkB        - flux_in_n;
delta_NFkBn           = delta_NFkBn       + flux_in_n;

delta_IkBaIKK         = delta_IkBaIKK     - flux_pd_c_2ai;
delta_IKK             = delta_IKK         + flux_pd_c_2ai;

delta_IkBaNFkB        = delta_IkBaNFkB    - flux_pd_c_2an;
delta_NFkB            = delta_NFkB        + flux_pd_c_2an;

delta_IkBbIKK         = delta_IkBbIKK     - flux_pd_c_2bi;
delta_IKK             = delta_IKK         + flux_pd_c_2bi;

delta_IkBbNFkB        = delta_IkBbNFkB    - flux_pd_c_2bn;
delta_NFkB            = delta_NFkB        + flux_pd_c_2bn;

delta_IkBeIKK         = delta_IkBeIKK     - flux_pd_c_2ei;
delta_IKK             = delta_IKK         + flux_pd_c_2ei;

delta_IkBeNFkB        = delta_IkBeNFkB    - flux_pd_c_2en;
delta_NFkB            = delta_NFkB        + flux_pd_c_2en;

delta_IkBaIKKNFkB     = delta_IkBaIKKNFkB - flux_pd_c_3ain;
delta_IKK             = delta_IKK         + flux_pd_c_3ain;
delta_NFkB            = delta_NFkB        + flux_pd_c_3ain;

delta_IkBbIKKNFkB     = delta_IkBbIKKNFkB - flux_pd_c_3bin;
delta_IKK             = delta_IKK         + flux_pd_c_3bin;
delta_NFkB            = delta_NFkB        + flux_pd_c_3bin;

delta_IkBeIKKNFkB     = delta_IkBeIKKNFkB - flux_pd_c_3ein;
delta_IKK             = delta_IKK         + flux_pd_c_3ein;
delta_NFkB            = delta_NFkB        + flux_pd_c_3ein;

delta_IkBa            = delta_IkBa        - flux_pd_c_a;

delta_IkBb            = delta_IkBb        - flux_pd_c_b;

delta_IkBe            = delta_IkBe        - flux_pd_c_e;

delta_IkBaNFkBn       = delta_IkBaNFkBn   - flux_pd_n_2an;
delta_NFkBn           = delta_NFkBn       + flux_pd_n_2an;

delta_IkBbNFkBn       = delta_IkBbNFkBn   - flux_pd_n_2bn;
delta_NFkBn           = delta_NFkBn       + flux_pd_n_2bn;

delta_IkBeNFkBn       = delta_IkBeNFkBn   - flux_pd_n_2en;
```

```
delta_NFkBn           = delta_NFkBn       + flux_pd_n_2en;

delta_IkBan           = delta_IkBan       - flux_pd_n_a;

delta_IkBbn           = delta_IkBbn       - flux_pd_n_b;

delta_IkBen           = delta_IkBen       - flux_pd_n_e;

delta_IkBa            = delta_IkBa        + flux_ps_c_a;

delta_IkBb            = delta_IkBb        + flux_ps_c_b;

delta_IkBe            = delta_IkBe        + flux_ps_c_e;

delta_IkBat           = delta_IkBat       - flux_rd_a;

delta_IkBbt           = delta_IkBbt       - flux_rd_b;

delta_IkBet           = delta_IkBet       - flux_rd_e;

delta_IkBat           = delta_IkBat       + flux_rsr_an;

delta_IkBet           = delta_IkBet       + flux_rsr_en;

delta_IkBat           = delta_IkBat       + flux_rsu_a;

delta_IkBbt           = delta_IkBbt       + flux_rsu_b;

delta_IkBet           = delta_IkBet       + flux_rsu_e;

%=========================================================
if phase == 2
  if floor(t) < t;
    IKK_sum = IkBaIKK + IkBbIKK + IkBeIKK + IkBaIKKNFkB + IkBbIKKNFkB + IkBeIKKNFkB +
IKK;
    target_time = floor(t) + 1;
    target_ikk = activeikk(1,target_time+1);
    dx = target_time - t;
    dy = target_ikk - IKK_sum;
    ikk_change = dy / dx;
    if ikk_change > 0;
        delta_IKK         = delta_IKK         + ikk_change;
    else;
        percentAI  = IkBaIKK / IKK_sum;
        percentBI  = IkBbIKK / IKK_sum;
        percentEI  = IkBeIKK / IKK_sum;
        percentAIN = IkBaIKKNFkB / IKK_sum;
        percentBIN = IkBbIKKNFkB / IKK_sum;
        percentEIN = IkBeIKKNFkB / IKK_sum;
        percentI   = IKK / IKK_sum;
        delta_IkBaIKK     = delta_IkBaIKK     + (ikk_change * percentAI);
        delta_IkBa        = delta_IkBa        - (ikk_change * percentAI);

        delta_IkBbIKK     = delta_IkBbIKK     + (ikk_change * percentBI);
        delta_IkBb        = delta_IkBb        - (ikk_change * percentBI);

        delta_IkBeIKK     = delta_IkBeIKK     + (ikk_change * percentEI);
        delta_IkBe        = delta_IkBe        - (ikk_change * percentEI);

        delta_IkBaIKKNFkB = delta_IkBaIKKNFkB + (ikk_change * percentAIN);
        delta_IkBaNFkB    = delta_IkBaNFkB    - (ikk_change * percentAIN);

        delta_IkBbIKKNFkB = delta_IkBbIKKNFkB + (ikk_change * percentBIN);
        delta_IkBbNFkB    = delta_IkBbNFkB    - (ikk_change * percentBIN);

        delta_IkBeIKKNFkB = delta_IkBeIKKNFkB + (ikk_change * percentEIN);
        delta_IkBeNFkB    = delta_IkBeNFkB    - (ikk_change * percentEIN);
```

```
        delta_IKK         = delta_IKK         + (ikk_change * percentI);
    end;
  end;
end;
%============================================================
delta(1,1)     =delta_IkBa       ;
delta(2,1)     =delta_IkBaIKK    ;
delta(3,1)     =delta_IkBaIKKNFkB;
delta(4,1)     =delta_IkBan      ;
delta(5,1)     =delta_IkBaNFkB   ;
delta(6,1)     =delta_IkBaNFkBn  ;
delta(7,1)     =delta_IkBat      ;
delta(8,1)     =delta_IkBb       ;
delta(9,1)     =delta_IkBbIKK    ;
delta(10,1)    =delta_IkBbIKKNFkB;
delta(11,1)    =delta_IkBbn      ;
delta(12,1)    =delta_IkBbNFkB   ;
delta(13,1)    =delta_IkBbNFkBn  ;
delta(14,1)    =delta_IkBbt      ;
delta(15,1)    =delta_IkBe       ;
delta(16,1)    =delta_IkBeIKK    ;
delta(17,1)    =delta_IkBeIKKNFkB;
delta(18,1)    =delta_IkBen      ;
delta(19,1)    =delta_IkBeNFkB   ;
delta(20,1)    =delta_IkBeNFkBn  ;
delta(21,1)    =delta_IkBet      ;
delta(22,1)    =delta_IKK        ;
delta(23,1)    =delta_NFkB       ;
delta(24,1)    =delta_NFkBn      ;
%============================================================
```

Bibliography

Adam, E., V. Quivy, et al. (2003). "Potentiation of tumor necrosis factor-induced NF-kappa B activation by deacetylase inhibitors is associated with a delayed cytoplasmic reappearance of I kappa B alpha." Mol Cell Biol **23**(17): 6200-9.

Aggarwal, B. B. (2003). "Signalling pathways of the TNF superfamily: a double-edged sword." Nat Rev Immunol **3**(9): 745-56.

Akira, S. and K. Takeda (2004). "Toll-like receptor signalling." Nat Rev Immunol **4**(7): 499-511.

Akira, S., K. Takeda, et al. (2001). "Toll-like receptors: critical proteins linking innate and acquired immunity." Nat Immunol **2**(8): 675-80.

Aldridge, B. B., J. M. Burke, et al. (2006). "Physicochemical modelling of cell signalling pathways." Nat Cell Biol **8**(11): 1195-203.

Aleyasin, H., S. P. Cregan, et al. (2004). "Nuclear factor-(kappa)B modulates the p53 response in neurons exposed to DNA damage." J Neurosci **24**(12): 2963-73.

Arkan, M. C., A. L. Hevener, et al. (2005). "IKK-beta links inflammation to obesity-induced insulin resistance." Nat Med **11**(2): 191-8.

Arkin, A., J. Ross, et al. (1998). "Stochastic kinetic analysis of developmental pathway bifurcation in phage lambda-infected Escherichia coli cells." Genetics **149**(4): 1633-48.

Barken, D., C. J. Wang, et al. (2005). "Comment on "Oscillations in NF-kappaB signaling control the dynamics of gene expression"." Science **308**(5718): 52; author reply 52.

Barken, D., S. L. Werner, et al. (2007). "A temporal code for inflammatory signaling." (in preparation).

Barton, G. M. and R. Medzhitov (2003). "Toll-like receptor signaling pathways." Science **300**(5625): 1524-5.

Beinke, S. and S. C. Ley (2004). "Functions of NF-kappaB1 and NF-kappaB2 in immune cell biology." Biochem J **382**(Pt 2): 393-409.

Beutler, B. and V. Kruys (1995). "Lipopolysaccharide signal transduction, regulation of tumor necrosis factor biosynthesis, and signaling by tumor necrosis factor itself." J Cardiovasc Pharmacol **25 Suppl 2**: S1-8.

Beutler, B., I. W. Milsark, et al. (1985). "Passive immunization against cachectin/tumor necrosis factor protects mice from lethal effect of endotoxin." Science **229**(4716): 869-71.

Bhalla, U. S. (2004). "Models of cell signaling pathways." Curr Opin Genet Dev **14**(4): 375-81.

Bhalla, U. S., P. T. Ram, et al. (2002). "MAP kinase phosphatase as a locus of flexibility in a mitogen-activated protein kinase signaling network." Science **297**(5583): 1018-23.

Bohuslav, J., L. F. Chen, et al. (2004). "p53 induces NF-kappaB activation by an IkappaB kinase-independent mechanism involving phosphorylation of p65 by ribosomal S6 kinase 1." J Biol Chem **279**(25): 26115-25.

Bouwmeester, T., A. Bauch, et al. (2004). "A physical and functional map of the human TNF-alpha/NF-kappa B signal transduction pathway." Nat Cell Biol **6**(2): 97-105.

Bower, J. M. and H. Bolouri (2001). Computational modeling of genetic and biochemical networks. Cambridge, MA, MIT Press.

Brennan, P. and L. A. O'Neill (1996). "2-mercaptoethanol restores the ability of nuclear factor kappa B (NF kappa B) to bind DNA in nuclear extracts from interleukin 1-treated cells incubated with pyrollidine dithiocarbamate (PDTC). Evidence for oxidation of glutathione in the mechanism of inhibition of NF kappa B by PDTC." Biochem J **320 (Pt 3)**: 975-81.

Burke, J. R. (2003). "Targeting I kappa B kinase for the treatment of inflammatory and other disorders." Curr Opin Drug Discov Devel **6**(5): 720-8.

Chen, G. and D. V. Goeddel (2002). "TNF-R1 signaling: a beautiful pathway." Science **296**(5573): 1634-5.

Chen, L. F. and W. C. Greene (2004). "Shaping the nuclear action of NF-kappaB." Nat Rev Mol Cell Biol **5**(5): 392-401.

Cheong, R., A. Bergmann, et al. (2006). "Transient IkappaB kinase activity mediates temporal NF-kappaB dynamics in response to a wide range of tumor necrosis factor-alpha doses." J Biol Chem **281**(5): 2945-50.

Cho, K. H., S. Y. Shin, et al. (2003). "Experimental design in systems biology, based on parameter sensitivity analysis using a monte carlo method: a case study for the TNF-alpha-mediated NF-kappa-B signal transduction pathway." Simulation **79**(12): 726-39.

Cho, K. H., S. Y. Shin, et al. (2003). "Investigations into the analysis and modeling of the TNF alpha-mediated NF-kappa B-signaling pathway." Genome Res **13**(11): 2413-22.

Collado-Vides, J. and R. Hofestadt (2002). Gene regulation and metabolism. Cambridge, MA, MIT Press.

Collins, T. and M. I. Cybulsky (2001). "NF-kappaB: pivotal mediator or innocent bystander in atherogenesis?" J Clin Invest **107**(3): 255-64.

Cover, T. M. and J. A. Thomas (1991). Elements of Information Theory. New York, John Wiley and Sons.

Covert, M. W., T. H. Leung, et al. (2005). "Achieving stability of lipopolysaccharide-induced NF-kappaB activation." Science **309**(5742): 1854-7.

De Jong, H., J. L. Gouze, et al. (2004). "Qualitative simulation of genetic regulatory networks using piecewise-linear models." Bull Math Biol **66**(2): 301-40.

DeRisi, J. L., V. R. Iyer, et al. (1997). "Exploring the metabolic and genetic control of gene expression on a genomic scale." Science **278**(5338): 680-6.

Edelstein-Keshet, L. (1988). Mathematical Models in Biology. New York, Random House.

Edwards, J. S., R. U. Ibarra, et al. (2001). "In silico predictions of Escherichia coli metabolic capabilities are consistent with experimental data." Nat Biotechnol **19**(2): 125-30.

Eungdamrong, N. J. and R. Iyengar (2004). "Computational approaches for modeling regulatory cellular networks." Trends Cell Biol **14**(12): 661-9.

Fall, C. P., E. S. Marland, et al. (2002). Computational Cell Biology. New York, Springer.

Fall, C. P., E. S. Marland, et al. (2002). Computational cell biology. New York, Springer.
Field, M. J. (1999). A Practical Introduction to the Simulation of Molecular Systems. Cambridge, Cambridge University Press.
Fujioka, S., C. Schmidt, et al. (2004). "Stabilization of p53 is a novel mechanism for proapoptotic function of NF-kappaB." J Biol Chem **279**(26): 27549-59.
Garg, A. and B. B. Aggarwal (2002). "Nuclear transcription factor-kappaB as a target for cancer drug development." Leukemia **16**(6): 1053-68.
Gavin, A. C., M. Bosche, et al. (2002). "Functional organization of the yeast proteome by systematic analysis of protein complexes." Nature **415**(6868): 141-7.
Geva-Zatorsky, N., N. Rosenfeld, et al. (2006). "Oscillations and variability in the p53 system." Mol Syst Biol **2**: 2006 0033.
Ghosh, S. and M. Karin (2002). "Missing pieces in the NF-kappaB puzzle." Cell **109 Suppl**: S81-96.
Gilman, A. and A. P. Arkin (2002). "Genetic "code": representations and dynamical models of genetic components and networks." Annu Rev Genomics Hum Genet **3**: 341-69.
Gloire, G., E. Dejardin, et al. (2006). "Extending the nuclear roles of IkappaB kinase subunits." Biochem Pharmacol **72**(9): 1081-9.
Goldbeter, A. (1996). Biochemical Oscillations and Cellular Rhythms. Cambridge, Cambridge University Press.
Greten, F. R. and M. Karin (2004). "The IKK/NF-kappaB activation pathway-a target for prevention and treatment of cancer." Cancer Lett **206**(2): 193-9.
Guo, C. and H. Levine (1999). "A thermodynamic model for receptor clustering." Biophys J **77**(5): 2358-65.
Hasty, J., D. McMillen, et al. (2001). "Computational studies of gene regulatory networks: in numero molecular biology." Nat Rev Genet **2**(4): 268-79.
Hayden, M. S. and S. Ghosh (2004). "Signaling to NF-kappaB." Genes Dev **18**(18): 2195-224.
Heinrich, R. and S. Schuster (1996). The regulation of cellular systems. New York, Chapman & Hall.
Hiscott, J., H. Kwon, et al. (2001). "Hostile takeovers: viral appropriation of the NF-kappaB pathway." J Clin Invest **107**(2): 143-51.
Ho, Y., A. Gruhler, et al. (2002). "Systematic identification of protein complexes in Saccharomyces cerevisiae by mass spectrometry." Nature **415**(6868): 180-3.
Hoffmann, A. and D. Baltimore (2006). "Circuitry of nuclear factor kappaB signaling." Immunol Rev **210**: 171-86.
Hoffmann, A., A. Levchenko, et al. (2002). "The IkappaB-NF-kappaB signaling module: temporal control and selective gene activation." Science **298**(5596): 1241-5.
Hoffmann, A., G. Natoli, et al. (2006). "Transcriptional regulation via the NF-kappaB signaling module." Oncogene **25**(51): 6706-16.
Ideker, T., V. Thorsson, et al. (2001). "Integrated genomic and proteomic analyses of a systematically perturbed metabolic network." Science **292**(5518): 929-34.

Ihekwaba, A. E., D. S. Broomhead, et al. (2004). "Sensitivity analysis of parameters controlling oscillatory signalling in the NF-kappaB pathway: the roles of IKK and IkappaBalpha." Syst Biol (Stevenage) **1**(1): 93-103.

Ivan, M., K. Kondo, et al. (2001). "HIFalpha targeted for VHL-mediated destruction by proline hydroxylation: implications for O2 sensing." Science **292**(5516): 464-8.

Jaakkola, P., D. R. Mole, et al. (2001). "Targeting of HIF-alpha to the von Hippel-Lindau ubiquitylation complex by O2-regulated prolyl hydroxylation." Science **292**(5516): 468-72.

Janes, K. A., J. G. Albeck, et al. (2005). "A systems model of signaling identifies a molecular basis set for cytokine-induced apoptosis." Science **310**(5754): 1646-53.

Janes, K. A., J. G. Albeck, et al. (2003). "A high-throughput quantitative multiplex kinase assay for monitoring information flow in signaling networks: application to sepsis-apoptosis." Mol Cell Proteomics **2**(7): 463-73.

Janes, K. A., J. R. Kelly, et al. (2004). "Cue-signal-response analysis of TNF-induced apoptosis by partial least squares regression of dynamic multivariate data." J Comput Biol **11**(4): 544-61.

Janes, K. A. and M. B. Yaffe (2006). "Data-driven modelling of signal-transduction networks." Nat Rev Mol Cell Biol **7**(11): 820-8.

Karin, M. (2006). "Nuclear factor-kappaB in cancer development and progression." Nature **441**(7092): 431-6.

Karin, M. and Y. Ben-Neriah (2000). "Phosphorylation meets ubiquitination: the control of NF-[kappa]B activity." Annu Rev Immunol **18**: 621-63.

Karin, M., Y. Cao, et al. (2002). "NF-kappaB in cancer: from innocent bystander to major culprit." Nat Rev Cancer **2**(4): 301-10.

Karin, M., Y. Yamamoto, et al. (2004). "The IKK NF-kappa B system: a treasure trove for drug development." Nat Rev Drug Discov **3**(1): 17-26.

Kauffmann, S. A. (1993). The origins of order: self organization and selection in evolution. New York, Oxford University Press.

Kearns, J. D., S. Basak, et al. (2006). "IkappaBepsilon provides negative feedback to control NF-kappaB oscillations, signaling dynamics, and inflammatory gene expression." J Cell Biol **173**(5): 659-64.

Lawrence, T., M. Bebien, et al. (2005). "IKKalpha limits macrophage NF-kappaB activation and contributes to the resolution of inflammation." Nature **434**(7037): 1138-43.

Lee, E., A. Salic, et al. (2003). "The roles of APC and Axin derived from experimental and theoretical analysis of the Wnt pathway." PLoS Biol **1**(1): E10.

Lee, E. G., D. L. Boone, et al. (2000). "Failure to regulate TNF-induced NF-kappaB and cell death responses in A20-deficient mice." Science **289**(5488): 2350-4.

Lee, J. A., R. S. Sinkovits, et al. (2006). "Components of the antigen processing and presentation pathway revealed by gene expression microarray analysis following B cell antigen receptor (BCR) stimulation." BMC Bioinformatics **7**: 237.

Levchenko, A. (2003). "Dynamical and integrative cell signaling: challenges for the new biology." Biotechnol Bioeng **84**(7): 773-82.

Levine, S. (2003). KF-kB: a key signaling pathway in asthma. Signal transduction and human disease. T. Finkel. Hoboken, NJ, Wiley-Liss.

Liew, F. Y., D. Xu, et al. (2005). "Negative regulation of toll-like receptor-mediated immune responses." Nat Rev Immunol **5**(6): 446-58.

Lipniacki, T., P. Paszek, et al. (2004). "Mathematical model of NF-kappaB regulatory module." J Theor Biol **228**(2): 195-215.

Liu, Z. G. (2005). "Molecular mechanism of TNF signaling and beyond." Cell Res **15**(1): 24-7.

MacKay, D. J. C. (2003). Information Theory, Inference, and Learning Algorithms. Cambridge, Cambridge University Press.

Malek, S., Y. Chen, et al. (2001). "IkappaBbeta, but not IkappaBalpha, functions as a classical cytoplasmic inhibitor of NF-kappaB dimers by masking both NF-kappaB nuclear localization sequences in resting cells." J Biol Chem **276**(48): 45225-35.

Malek, S., T. Huxford, et al. (1998). "Ikappa Balpha functions through direct contacts with the nuclear localization signals and the DNA binding sequences of NF-kappaB." J Biol Chem **273**(39): 25427-35.

Mattson, M. P. and S. Camandola (2001). "NF-kappaB in neuronal plasticity and neurodegenerative disorders." J Clin Invest **107**(3): 247-54.

McAdams, H. H. and A. Arkin (1998). "Simulation of prokaryotic genetic circuits." Annu Rev Biophys Biomol Struct **27**: 199-224.

McAdams, H. H. and L. Shapiro (1995). "Circuit simulation of genetic networks." Science **269**(5224): 650-6.

Moon, R. (2005). "Wnt/beta-catenin pathway." Sci STKE **cm1**.

Nakano, H., A. Nakajima, et al. (2006). "Reactive oxygen species mediate crosstalk between NF-kappaB and JNK." Cell Death Differ **13**(5): 730-7.

Natarajan, M., K. M. Lin, et al. (2006). "A global analysis of cross-talk in a mammalian cellular signalling network." Nat Cell Biol **8**(6): 571-80.

Natoli, G., S. Saccani, et al. (2005). "Interactions of NF-kappaB with chromatin: the art of being at the right place at the right time." Nat Immunol **6**(5): 439-45.

Nelson, D. E., A. E. Ihekwaba, et al. (2004). "Oscillations in NF-kappaB signaling control the dynamics of gene expression." Science **306**(5696): 704-8.

O'Dea E, Barken D, et al. (2007). "A homeostatic model of IkB metabolism to control constitutive NF-kB activity." Molecular Systems Biology **submitted**.

Pando, M. P. and I. M. Verma (2000). "Signal-dependent and -independent degradation of free and NF-kappa B-bound IkappaBalpha." J Biol Chem **275**(28): 21278-86.

Papa, S., C. Bubici, et al. (2006). "The NF-kappaB-mediated control of the JNK cascade in the antagonism of programmed cell death in health and disease." Cell Death Differ **13**(5): 712-29.

Papin, J. and S. Subramaniam (2004). "Bioinformatics and cellular signaling." Curr Opin Biotechnol **15**(1): 78-81.

Papin, J. A. and B. O. Palsson (2004). "The JAK-STAT signaling network in the human B-cell: an extreme signaling pathway analysis." Biophys J **87**(1): 37-46.

Papin, J. A. and B. O. Palsson (2004). "Topological analysis of mass-balanced signaling networks: a framework to obtain network properties including crosstalk." J Theor Biol **227**(2): 283-97.

Pascual, G. and C. K. Glass (2006). "Nuclear receptors versus inflammation: mechanisms of transrepression." Trends Endocrinol Metab **17**(8): 321-7.

Paszek, P., T. Lipniacki, et al. (2005). "Stochastic effects of multiple regulators on expression profiles in eukaryotes." J Theor Biol **233**(3): 423-33.

Perkins, N. D. (2007). "Integrating cell-signalling pathways with NF-kappaB and IKK function." Nat Rev Mol Cell Biol **8**(1): 49-62.

Pomerantz, J. L. and D. Baltimore (2002). "Two pathways to NF-kappaB." Mol Cell **10**(4): 693-5.

Pradervand, S., M. R. Maurya, et al. (2006). "Identification of signaling components required for the prediction of cytokine release in RAW 264.7 macrophages." Genome Biol **7**(2): R11.

Ptashne, M. and A. Gann (2002). Genes & Signals. New York, Cold Spring Harbor Laboratory Press.

Quivy, V. and C. Van Lint (2004). "Regulation at multiple levels of NF-kappaB-mediated transactivation by protein acetylation." Biochem Pharmacol **68**(6): 1221-9.

Reddy, V. N., M. N. Liebman, et al. (1996). "Qualitative analysis of biochemical reaction systems." Comput Biol Med **26**(1): 9-24.

Reich, J. G. (1981). Energy metabolism of the cell. London, Academic Press.

Rice, N. R. and M. K. Ernst (1993). "In vivo control of NF-kappa B activation by I kappa B alpha." Embo J **12**(12): 4685-95.

Ruland, J. and T. W. Mak (2003). "From antigen to activation: specific signal transduction pathways linking antigen receptors to NF-kappaB." Semin Immunol **15**(3): 177-83.

Ryan, K. M., M. K. Ernst, et al. (2000). "Role of NF-kappaB in p53-mediated programmed cell death." Nature **404**(6780): 892-7.

Sachs, K., D. Gifford, et al. (2002). "Bayesian network approach to cell signaling pathway modeling." Sci STKE **2002**(148): PE38.

Sauro, H. M. and B. N. Kholodenko (2004). "Quantitative analysis of signaling networks." Prog Biophys Mol Biol **86**(1): 5-43.

Schaff, J. C., B. M. Slepchenko, et al. (2001). "Analysis of nonlinear dynamics on arbitrary geometries with the Virtual Cell." Chaos **11**(1): 115-131.

Schilling, C. H., J. S. Edwards, et al. (1999). "Toward metabolic phenomics: analysis of genomic data using flux balances." Biotechnol Prog **15**(3): 288-95.

Schoeberl, B., C. Eichler-Jonsson, et al. (2002). "Computational modeling of the dynamics of the MAP kinase cascade activated by surface and internalized EGF receptors." Nat Biotechnol **20**(4): 370-5.

Semmlow, J. (2005). Circuits, Signals, and Systems for Bioengineers: A Matlab Based Introduction, Elsevier Academic Press.

Shannon, C. E. (1948). "A Mathematical Theory of Communication (part 1)." Bell Systems Technical Journal **27**: 379-423

Shannon, C. E. (1948). "A Mathematical Theory of Communication (part 2)." Bell Systems Technical Journal **27**: 623-656.

Sheppard, K. A., K. M. Phelps, et al. (1998). "Nuclear integration of glucocorticoid receptor and nuclear factor-kappaB signaling by CREB-binding protein and steroid receptor coactivator-1." J Biol Chem **273**(45): 29291-4.

Shmulevich, I., E. R. Dougherty, et al. (2002). "Probabilistic Boolean Networks: a rule-based uncertainty model for gene regulatory networks." Bioinformatics **18**(2): 261-74.

Shvartsman, S. Y., H. S. Wiley, et al. (2001). "Spatial range of autocrine signaling: modeling and computational analysis." Biophys J **81**(4): 1854-67.

Smith, K. D. and H. Bolouri (2005). "Dissecting innate immune responses with the tools of systems biology." Curr Opin Immunol **17**(1): 49-54.

Stephanopoulos, G. N., A. A. Aristidou, et al. (1998). Metabolic engineering: principles and methodologies. San Diego, Academic Press.

Sung, M. H. and R. Simon (2004). "In silico simulation of inhibitor drug effects on nuclear factor-kappaB pathway dynamics." Mol Pharmacol **66**(1): 70-5.

Swameye, I., T. G. Muller, et al. (2003). "Identification of nucleocytoplasmic cycling as a remote sensor in cellular signaling by databased modeling." Proc Natl Acad Sci U S A **100**(3): 1028-33.

Tam, W. F., L. H. Lee, et al. (2000). "Cytoplasmic sequestration of rel proteins by IkappaBalpha requires CRM1-dependent nuclear export." Mol Cell Biol **20**(6): 2269-84.

Tang, G., Y. Minemoto, et al. (2001). "Inhibition of JNK activation through NF-kappaB target genes." Nature **414**(6861): 313-7.

Tyson, J. J., K. C. Chen, et al. (2003). "Sniffers, buzzers, toggles and blinkers: dynamics of regulatory and signaling pathways in the cell." Curr Opin Cell Biol **15**(2): 221-31.

Vayttaden, S. J., S. M. Ajay, et al. (2004). "A spectrum of models of signaling pathways." Chembiochem **5**(10): 1365-74.

Voit, E. O. (2000). Computational Analysis of Biochemical Systems. New York, Cambridge University Press.

von Dassow, G., E. Meir, et al. (2000). "The segment polarity network is a robust developmental module." Nature **406**(6792): 188-92.

Weil, R. and A. Israel (2004). "T-cell-receptor- and B-cell-receptor-mediated activation of NF-kappaB in lymphocytes." Curr Opin Immunol **16**(3): 374-81.

Werner, S. L., D. Barken, et al. (2005). "Stimulus specificity of gene expression programs determined by temporal control of IKK activity." Science **309**(5742): 1857-61.

Wertz, I. E., K. M. O'Rourke, et al. (2004). "De-ubiquitination and ubiquitin ligase domains of A20 downregulate NF-kappaB signalling." Nature **430**(7000): 694-9.

Yi, T. M., Y. Huang, et al. (2000). "Robust perfect adaptation in bacterial chemotaxis through integral feedback control." Proc Natl Acad Sci U S A **97**(9): 4649-53.

Zandi, E., Y. Chen, et al. (1998). "Direct phosphorylation of IkappaB by IKKalpha and IKKbeta: discrimination between free and NF-kappaB-bound substrate." Science **281**(5381): 1360-3.

Zhu, X., M. S. Chang, et al. (2006). "Dual ligand stimulation of RAW 264.7 cells uncovers feedback mechanisms that regulate TLR-mediated gene expression." J Immunol **177**(7): 4299-310.